NIST Special Publication 250-95

NIST Measurement Services
Photometric Calibrations

Yuqin Zong
Maria E. Nadal
Benjamin K. Tsai
C. Cameron Miller

This publication is available free of charge from:
https://doi.org/10.6028/NIST.SP.250-95

National Institute of
Standards and Technology
U.S. Department of Commerce

NIST Special Publication 250-95

NIST Measurement Services Photometric Calibrations

Yuqin Zong
Maria E. Nadal
Benjamin K. Tsai
C. Cameron Miller

Sensor Science Division
Physical Measurement Division
National Institute of Standards and Technology
100 Bureau Drive
Gaithersburg, MD 20899

This publication is available free of charge from:
https://doi.org/10.6028/NIST.SP.250-95

July 2018

U.S. Department of Commerce
Wilbur L. Ross, Jr., Secretary

National Institute of Standards and Technology
Walter G. Copan, NIST Director and Under Secretary of Commerce for Standards and Technology

National Institute of Standards and Technology Special Publication 250-95
Natl. Inst. Stand. Technol. Spec. Publ. 250-95, 147 pages (July 2018)
CODEN: NSPUE2

This publication is available free of charge from:
https://doi.org/10.6028/NIST.SP.250-95

Preface

The calibration and related measurement services of the National Institute of Standards and Technology (NIST) are intended to assist the makers and users of precision measuring instruments in achieving the highest possible levels of accuracy, quality, and productivity. NIST offers over 300 different calibrations, special tests, and measurement assurance services. These services allow customers to directly link their measurement systems to measurement systems and standards maintained by NIST. These services are offered to the public and private organizations alike. They are described in NIST Special Publication (SP) 250, NIST Calibration Services Users Guide.

The Users Guide is supplemented by a number of Special Publications (designated as the "SP250 Series") that provide detailed descriptions of the important features of specific NIST calibration services. These documents provide a description of the: (1) specifications for the services; (2) design philosophy and theory; (3) NIST measurement system; (4) NIST operational procedures; (5) assessment of the measurement uncertainty including an uncertainty budget; and (6) internal quality control procedures used by NIST. These documents will present more detail than can be given in NIST calibration reports, or than is generally allowed in articles in scientific journals. In the past, NIST has published such information in a variety of ways. This series will make this type of information more readily available to the user.

This document, SP250-95 (2017), NIST Photometric Calibrations, is a revision of SP250-37 (1997). It covers the calibration of standards of luminous intensity, luminous flux, illuminance, luminance, luminous exposure, and color temperature (test numbers 37010C–37070C and 37020S-37130S in SP250, NIST Calibration Services Users Guide). Inquiries concerning the technical content of this document or the specifications for these services should be directed to one of the authors or to one of the technical contacts cited in SP250.

NIST welcomes suggestions on how publications such as this might be made more useful. Suggestions are also welcome concerning the need for new calibrations services, special tests, and measurement assurance programs.

Gregory F. Strouse
Associate Director for Measurement Services

James K. Olthoff
Director
Physical Measurement Laboratory

Abstract

The National Institute of Standards and Technology provides calibration services for submitted artifacts for luminous intensity, illuminance, color temperature, total luminous flux, luminous exposure and luminance. Additionally, the National Institute of Standards and Technology issues calibrated standards of luminous intensity, luminance, and color temperature. The procedures, equipment, and techniques used to perform these calibrations are described. Detailed estimates and procedures for determining uncertainties of the reported values are also presented along with the internal quality control procedures.

Key words

Calibration; Candela; Color temperature; Illuminance; Lumen; Luminance; Luminous exposure; Luminous flux; Luminous intensity; Lux; Photometry; Standards; Total luminous flux.

Table of Contents

List of Tables

List of Figures

1. Introduction

This document supersedes the NIST Special Publication 250-37 (1997) and NBS Special Publication 250-15 (1987). In 1992, a new candela was realized based on an absolute cryogenic radiometer, and the old NIST gold-point blackbody-based unit [1] was replaced by the new detector-based unit [2]. A group of eight calibrated standard photometers based on the cryogenic radiometer maintains the capability to realize the NIST candela, and replaces the lamp-based standards formerly used. Further, the photometric calibration procedures have been revised to utilize the detector-based methods [3]. Since publication of the previous version (1997), the facilities for total luminous flux were improved significantly with the introduction of detector-based calibration procedures [4]. A new service for calibration of flash photometers was developed. There have been many improvements in other existing calibration facilities and procedures.

This document describes the updated photometric calibration procedures for luminous intensity (candela; cd), illuminance (lux; lx), total luminous flux (lumen; lm), luminance (cd/m^2), color temperature (Kelvin; K), and luminous exposure (lx·s, cd·s). Throughout this document, uncertainty statements follow the NIST policy given by Taylor and Kuyatt [5], which prescribes the use of an expanded uncertainty with a coverage factor $k = 2$ for uncertainties of all NIST calibrations.

Descriptions for the individual standards and calibrations available from NIST covered by this document, as of October 2017, are listed and explained in Section 2. Updated information about calibration services and prices are published periodically in the NIST Calibration Services Users Guide and Fee Schedule [6].

The material presented in this document describes photometric calibration facilities and procedures as they existed at the time of publication. Further improvement of photometric calibration facilities and procedures are underway. Additional documents will cover new photometric calibration procedures for average LED intensity (candela; cd), LED total luminous flux of LEDs (lumen; lm), colorimetry of LEDs, and spectrally integrated total radiant flux of LEDs (watt; W), along with total spectral radiant flux calibration procedures for incandescent light sources.

1.1. Photometry, physical photometry, and radiometry

The primary aim of photometry is to measure visible optical radiation, light, in such a way that the results correlate with what the visual sensation is to a normal human observer exposed to that radiation. Until about 1940, visual comparison techniques of measurements were predominant in photometry, whereby an observer was required to match the brightness of two visual fields viewed either simultaneously or sequentially. This method of photometry is so-called visual photometry and is seldom used today.

In modern photometric practice, measurements are made with photodetectors. This is referred to as physical photometry. In order to achieve the aim of photometry, one must take into account the characteristics of human vision. The relative spectral responsivity of the human vision system was first defined by the CIE (Commission Internationale de l'Éclairage) in 1924 [7], and redefined as part of colorimetric standard observers in 1931 [8]. It is called the spectral luminous efficiency function for photopic vision, or the $V(\lambda)$ function, defined in the domain from 360 nm to 830 nm, and is normalized to unity at its peak, 555 nm (Fig. 1) [9]. This model gained wide acceptance, was republished by CIE in 1983 [10] and was published by CIPM (Comité International des Poids et Mesures) in 1982 [11] to supplement the 1979 definition of candela. The tabulated values of the function at 1 nm increments are available in References [10-12]. In most cases, the region from 380 nm to 780 nm is used for calculation with negligible errors because the $V(\lambda)$ function falls below 10^{-4} outside this region. Thus, a photodetector having a spectral responsivity matched to the $V(\lambda)$ function replaced the role of human eyes in photometry.

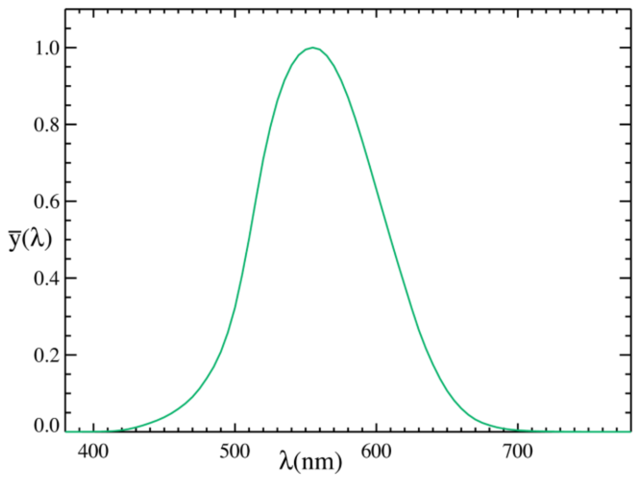

Fig. 1. CIE $V(\lambda)$ function.

Radiometry concerns physical measurement of optical radiation as a function of its wavelength. As specified in the definition of the candela by CGPM (Conférence Générale des Poids et Mesures) in 1979 [13] and CIPM in 1982 [11], a photometric quantity X_V is defined in relation to the corresponding radiometric quantity $X_{e,\lambda}$ by the equation,

$$X_v = K_m \int_{360\mathrm{nm}}^{830\mathrm{nm}} X_{e,\lambda} V(\lambda) d\lambda \ . \tag{1}$$

The constant, K_m, relates the photometric quantities and radiometric quantities, and is called the maximum spectral luminous efficacy (of radiation) for photopic vision. The value of K_m is given by the 1979 definition of candela, which defines the spectral luminous efficacy of light at the frequency 540×10^{12} Hz (at the wavelength 555.016 nm in standard air) to be 683 lm/W. Although the value of K_m is calculated as $683 \times V(555.000 \text{ nm})/V(555.016 \text{ nm}) =$ 683.002 lm/W [10], it is normally rounded to 683 lm/W with negligible errors [11]. Various photometric and radiometric quantities are described in the next section.

It should be noted that the $V(\lambda)$ function is based on the CIE standard photometric observer for photopic vision, which assumes additivity of sensation and a 2° field of view at relatively high luminance levels (higher than ≅1 cd/m^2). The human vision in this level is called photopic vision. The spectral responsivity of human vision deviates significantly at very low levels of luminance (less than ≅10^{-2} cd/m^2). This type of vision is called scotopic vision. Its spectral responsivity, peaking at 507 nm, is designated by the $V'(\lambda)$ function, which was defined by CIE in 1951 [14], recognized by CIPM in 1976 [15], and republished by CIPM in 1982 [11]. Human vision in the region between photopic vision and scotopic vision is called mesopic vision. While active research is being conducted [16, 17], there is no internationally accepted spectral luminous efficiency function for the mesopic region yet. In current practice, almost all photometric quantities are given in terms of photopic vision, even at low light levels, except for special measurements for research purposes. This document, therefore, does not deal with quantities specified in terms of scotopic or mesopic vision. Further details of definitions outlined in this section are given in Reference 10.

To better understand the international metrology system, it is useful to know the relationship among such organizations as CGPM (Conférence Générale des Poids et Mesures), CIPM (Comité international des poids et mesures), CCPR (Comité Consultatif de Photométrie et Radiométrie), BIPM (Bureau International des Poids et Mesures), and CIE (Commission Internationale de l´Eclairage). These abbreviations are based on their French names. In English, these organizations are: CGPM (General Conference of Weights and Measures), CIPM (International Committee for Weights and Measures), CCPR (Consultative Committee of Photometry and Radiometry), BIPM (International Bureau of Weights and Measures), and CIE (International Commission on Illumination). All SI units (Système international d'unités or International System of Units) are officially defined by the CGPM, which is the decision-making body for the Treaty of the Meter (Convention du Mètre), signed in 1875. The decisions of the CGPM legally govern the global metrology system among those countries signatory to the Treaty of the Meter or agreeing to its usage. The CIPM is a committee under the CGPM, charged with the management of the SI and related fundamental units, consisting of many subcommittees for each technical field. The CCPR is a subcommittee under the CIPM that discusses and recommends units in photometry and radiometry. It consists of representatives of interested national standardizing laboratories. The CCPR also holds international intercomparisons of photometric units and radiometric scales. The BIPM is a metrology laboratory under the supervision of the CIPM, with staff and facilities in Paris. The CIE, on the other hand, is originally an academic society in the field of lighting science and was organized to promote uniformity and quality in optical measurements. Many definitions developed by the CIE, such as the $V(\lambda)$ function, the color matching functions, and the standard illuminants, have been adopted by the CGPM and by the ISO (International Organization for Standardization) as international standards. The CIE has recently been recognized officially by the ISO as a standards-creating body in the field of optical radiation. The NIST staff actively participates in CCPR and CIE activities.

1.2. Photometric quantities and units

1.2.1. Photometric quantities

The base unit of all photometric quantities is the candela. The first realization of the candela was performed circa 1860 using candles made from sperm whale fat, known as spermacetti. In 1898, the candles were replaced by gas lamps that were wickless and used a mixture of pentane and air. In 1909, the first internationally recognized unit was established collaboratively between the National Bureau of Standards (currently NIST), the National Physical Laboratory in England, and the Laboratoire Central d'Electricité in France. The unit was based on the pentane lamp, but was maintained on carbon filament lamps. In 1948 the 'candle' became the candela and was defined by CGPM such that 'the magnitude of the candela is such that the luminance of a full radiator at the temperature of solidification of platinum is 60 candelas per square centimeter.' It became one of the base SI units when SI was established in 1960. Most recently, the candela was redefined by CGPM in 1979 as follows.

> "The candela is the luminous intensity, in a given direction, of a source that emits monochromatic radiation of frequency 540×10^{12} Hertz and that has a radiant intensity in that direction of (1/683) Watt per steradian [11]."

Table 1 lists photometric quantities and their corresponding radiometric quantities side by side, with units and symbols. The precise definition of each quantity is given by CCPR [12] and CIE [18].

Table 1. Quantities and units used in photometry and radiometry.

Photometric Quantity	Unit	Relationship to lumen	Radiometric Quantity	Unit
Luminous flux	lm (lumen)		Radiant flux	W (Watt)
Luminous intensity	cd (candela)	lm sr^{-1}	Radiant intensity	W sr^{-1}
Illuminance	lx (lux)	lm m^{-2}	Irradiance	W m^{-2}
Luminance	cd m^{-2}	lm sr^{-1} m^{-2}	Radiance	W sr^{-1} m^{-2}
Luminous exitance	lm m^{-2}		Radiant exitance	W m^{-2}
Luminous exposure	lx s	lm m^{-2} s	Radiant exposure	W m^{-2} s
Luminous energy	lm s		Radiant energy	J (Joule)
Color temperature	K (Kelvin)		Radiance temperature	K

Although the candela is defined as an SI base unit, luminous flux (lumen) is perhaps the most fundamental photometric quantity, as the four other photometric quantities are defined in terms of lumen with appropriate geometric factors. Luminous flux (Φ_{v}) is the time rate of flow of light as weighted by $V(\lambda)$. It is defined as

$$\Phi_{\mathrm{v}} = K_{\mathrm{m}} \int_{\lambda} \Phi_{\mathrm{e}.\lambda} V(\lambda) d\lambda \ , \qquad (2)$$

where $\Phi_{e,\lambda}$ is the spectral concentration of radiant flux in (W/nm) as a function of wavelength λ in nm.

Luminous intensity (I_v) is the luminous flux (from a point source) emitted per unit solid angle in a given direction. It is defined as

$$I_v = \frac{d\Phi_v}{d\Omega} \ , \tag{3}$$

where $d\Phi_v$ is the luminous flux leaving the source and propagating in an element of solid angle $d\Omega$ containing the given direction.

Illuminance (E_v) is the density of the luminous flux incident on a given point of a surface or a plane. It is defined as

$$E_v = \frac{d\Phi_v}{dA} \ , \tag{4}$$

where $d\Phi_V$ is the luminous flux incident on an element dA of the surface containing the point.

Luminance (L_V) is the luminous flux from an element of a surface surrounding a given point, emitted into a small solid angle containing the given direction, per unit area of the element projected on a plane perpendicular to that given direction. It is defined as

$$L_v = \lim_{\Delta\Omega \to 0, \Delta A \to 0} \frac{\Delta\Phi_v}{\Delta\Omega \Delta A \cos\theta} \ , \tag{5}$$

where $\Delta\Phi_V$ is the luminous flux emitted (reflected or transmitted) by an elementary beam passing through the given point and propagating in the solid angle $\Delta\Omega$ containing the given direction; ΔA is the area of a section of that beam containing the given point; θ is the angle between the normal to that section and the direction of the beam.

Luminance coefficient (q) is measured for opal glass and is defined as the ratio luminance to L_v illuminance E_v, as defined by

$$q = \frac{L_v}{E_v} \ . \tag{6}$$

Luminous exitance (M_V) is the density of luminous flux leaving a surface at a point. Eq. (6) is the same as Eq. (4), with dΦ_V meaning the luminous flux leaving a surface. This quantity is rarely used in the general practice of photometry. However, with the development and application of organic light emitting diodes, this quantity may become more popular.

Luminous exposure (H_V) is the time integral of illuminance $E_V(t)$ over a given duration Δt, as defined by

$$H_v = \int_{\Delta t} E_v(t) dt \ . \tag{7}$$

Luminous energy (Q_V) is the time integral of the luminous flux (Φ_V) over a given duration Δt, as defined by

$$Q_v = \int_{\Delta t} \Phi_v(t) dt \ \cdot \tag{8}$$

Color temperature (T_c) is the temperature of a Planckian radiator with radiation of the same chromaticity as that of the light source in question. However, the chromaticity coordinates of most lamps do not fall on the Planckian locus, and in actual lamp calibrations, either distribution temperature or correlated color temperature is used. “Color temperature” is often used informally for the correlated color temperature in the United States.

Distribution temperature (T_D) is the temperature of a blackbody with a spectral power distribution closest to that of the light source in question, and it is a useful concept for quasi-Planckian sources.

Correlated color temperature (T_{cp}) is a concept used for sources with a spectral power distribution significantly different from that of Planckian radiation, for example, discharge lamps. Correlated color temperature is the temperature of the Planckian radiator whose perceived color most closely resembles that of the light source in question.

General information (definitions, symbols, and expressions) on many other physical quantities and units including photometric and radiometric quantities are given in Reference 19.

1.2.2. Relationship between the SI units and English units

Under NIST policy [20], results of all NIST measurements are reported in SI units. However, the English units shown in Table 2 are still rather widely used. For all the photometric measurements and calculations, use of the SI units shown in Table 1 is recommended, and use of non-SI units is discouraged [21]. The definitions of the English units are described below for conversion purposes only.

Table 2. English units and definitions.

Unit	Quantity	Definition
foot candle (fc)	illuminance	lumen per square foot (lm ft^{-2})
foot-Lambert (fL)	luminance	$1/\pi$ candela per square foot (π^{-1} cd ft^{-2})

It should be noted that the definition of foot-Lambert is such that the luminance of a perfect diffuser is 1 fL when illuminated at 1 fc. In SI units, the luminance of a perfect diffuser would be $1/\pi$ (cd/m^2) when illuminated at 1 lx. For convenience of changing from English units to SI units, the conversion factors are listed in Table 3. For example, 1000 lx is the same illuminance as 92.9 fc, and 1000 cd/m^2 is the same luminance as 291.9 fL. Conversion factors to and from some other units are given in Reference 22.

Table 3. Conversion between English units and SI units.

To obtain value in	Multiply value by	By
lx from fc	fc	10.764
fc from lx	lx	0.09290
cd/m^2 from fL	fL	3.4263
fL from cd/m^2	cd m^{-2}	0.29186
m (meter) from feet	feet	0.30480
mm (millimeter) from inch	inch	25.400

1.3. NIST photometric units

1.3.1. Luminous intensity unit

Until 1991, the NIST luminous intensity unit was derived from the NIST spectral irradiance scale [23, 24], which was based on a gold-point blackbody, and therefore, was dependent on the temperature scale. In 1990, the international temperature scale was revised [25], thereby revising gold point temperature from 1337.58 K to 1337.33 K. Due to the change in the temperature scale, the NIST luminous intensity unit increased in magnitude by 0.35 %.

In 1992 at NIST, a new luminous intensity unit (candela) was realized based on the absolute responsivity of detectors (using 100 % Quantum Efficient silicon detectors [2] and subsequently a cryogenic electrical substitution radiometer [3]). The old luminous intensity unit was replaced with the new unit in 1992.

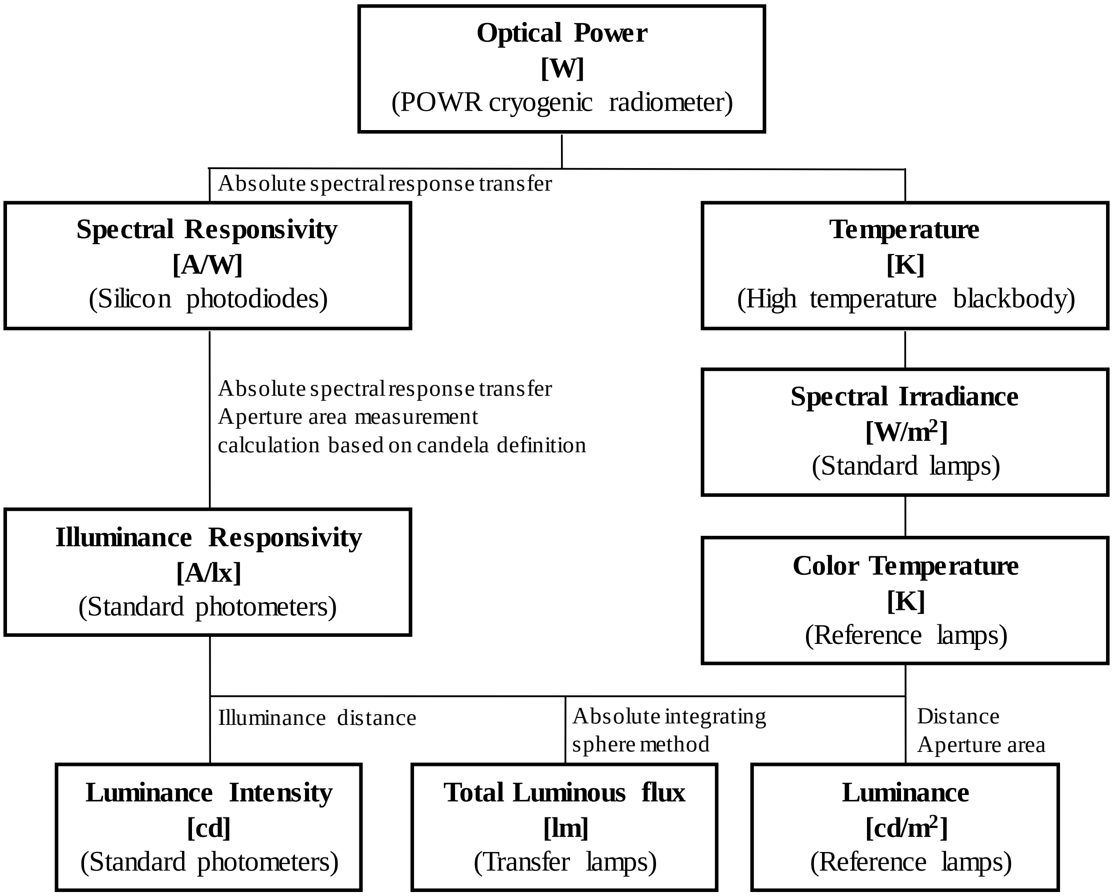

Fig. 2. Realization and maintenance of the NIST photometric units.

The new candela is realized and maintained on the NIST standard photometers (a group of eight photometers that are not temperature controlled) which are calibrated for illuminance responsivity in A/lx. These standard photometers also embody the NIST illuminance unit, and allow luminous intensity to be determined from measured illuminance and distance. The realization and maintenance of the photometric units at NIST are shown in Figure 2. A new NIST reference cryogenic radiometer, Primary Optical Watt Radiometer (POWR) [26], has been constructed and replaced the previous reference radiometer [27] in 2005. POWR realizes and maintains the optical power unit (watt, W), which serves as the basis for all radiometric and photometric units and scales realized at NIST. The POWR, including the detector module, has been completely designed by NIST. The radiometer is cooled by liquid helium to 5 K, and works on the principle of electrical substitution. The construction of the POWR is shown in Figure 3. Based on laser-beam power measurements with the POWR at several wavelengths, the NIST detector spectral responsivity scale is maintained on silicon photodiode light-trapping detectors. The new radiometer is designed to have the versatility to grow with NIST's needs, to embrace new technologies, and to be able to provide optical power measurements with expanded uncertainties of 0.02 % (k = 2), which has been verified by a recent intercomparison with two other cryogenic radiometer facilities at NIST [26].

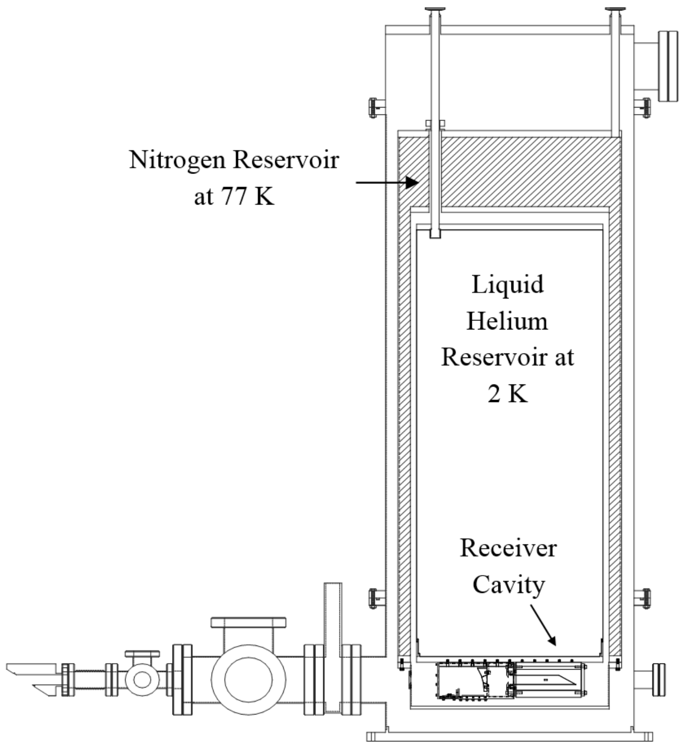

Fig. 3. Schematic of the NIST Primary Optical Watt Radiometer (POWR).

The spectral responsivity scale is transferred to other detectors using the Spectral Comparator Facility (SCF) [28], where the absolute spectral responsivity $s(\lambda)$ (A/W) of each of the NIST standard photometers is determined. The illuminance responsivity [A/lx] of each photometer is then calculated from $s(\lambda)$, the area of the aperture, and other correction factors. The relative expanded uncertainty of the illuminance responsivity determination is 0.39 % [2]. The standard photometers are recalibrated annually utilizing the detector spectral responsivity scale. The details of the candela realization are described in Section 3.1 and in Reference 2. As the result of the candela realization in 1992, the magnitude of the NIST luminous intensity unit increased by approximately 0.3 %. With the effect of the change of the international temperature scale in 1990 included, the magnitude of the NIST candela is larger (measured values are smaller) by approximately 0.6 % than that reported before 1990. At the latest CCPR international key comparison for luminous intensity (CCPR-K3.a) [29] in 1998, the NIST candela was 0.12 % smaller (measured values are larger) than the Key Comparison Reference Value (similar to what was called the world mean value). The 1998 intercomparison showed that the candela standards disseminated in different countries varied within about ± 1 %. The most recent status of the differences in the magnitude of photometric units for different countries in the world is published on the BIPM website http://www.bipm.org/.

1.3.2. Luminous flux unit

Until 1994, the NIST luminous flux unit was derived from the previous luminous intensity unit which was based on blackbody radiation. The previous luminous flux unit was last realized in 1985 by goniophotometric measurements [1], and was maintained on a group of six incandescent standard lamps. The unit was periodically transferred to groups of working standard lamps used for routine calibrations.

In 1995, a new NIST luminous flux unit was derived, based on the detector-based candela introduced in 1992, with a new method using an integrating sphere and an external source. The basic principle of this method (Absolute Integrating Sphere Method) is to measure the total flux of a lamp inside the sphere compared to a known amount of flux introduced into the sphere from a source outside the sphere.

This method was first studied theoretically using a computer simulation technique [30], then experimentally verified [31] using a 0.5 m integrating sphere. Utilizing this method with a 2 m integrating sphere, the new NIST luminous flux unit was established in 1995 [32, 33]. A new total luminous flux calibration facility using a 2.5 m sphere was developed at NIST [4, 34]. Primary standard lamps are calibrated periodically against the NIST illuminance unit in order to monitor the luminous flux unit. The 2.5 m absolute integrating sphere is used to provide routine calibrations. The details of the luminous flux unit realization are described in Section 4.1.

The realization of the 1995 luminous flux unit has resulted in a change (increase) of the magnitude of NIST luminous flux unit by approximately 1.1 % compared to older realizations. The measured lumen values reported by NIST are smaller by that percentage than those previously reported. The new luminous flux unit has been disseminated in NIST calibrations since January 1, 1996. At the latest CCPR international key comparison for total luminous flux (CCPR-K4) [29] in 1998, the NIST lumen was larger (measured value was smaller) by 0.21 % than the key comparison reference value. This intercomparison showed that the lumen standards disseminated in different countries varied within about ± 1 %.

1.3.3. Luminous exposure unit

The photometric measurement of flashing light is essential in the evaluation of various flashing-light sources used in many applications including photography and signaling in transportation. Among them, a need for accurate measurements of aircraft anticollision flashing lights is addressed by the Federal Aviation Administration [35]. The Federal Aviation Administration has specified the requirements for the intensity of anticollision flashing lights [36] and is enforcing the maintenance of the anticollision flashing lights on all commercial airplanes.

In the specification of aircraft anticollision flashing lights and other vehicle signals using flashing lights, the term effective intensity (unit: cd) is widely used. Effective intensity is the luminous intensity of a fixed (steady) light, of the same relative spectral distribution as the flashing light, which would have the same luminous intensity level as the flashing light under identical conditions of observation [37]. Effective intensity I_v is calculated from J_v, the time-integrated luminous intensity [cd·s], and a model based on visual perception. The variable, J_v $(= \int_0^T I_v(t)\,dt)$, is defined as the time integral of instantaneous luminous intensity $I_v(t)$ of a flash over the flash duration T.

Four effective intensity models are available: the Allard method [38], the Blondel-Rey equation [39], the Form Factor method [40], and the Modified Allard method [41]. The Blondel-Rey equation, developed in 1911, is most commonly used. The use of one single method has not been agreed upon internationally. All four methods give the same result for a very narrow, single pulse, as one emitted by a xenon flash tube. For such a very narrow single pulse, the effective intensity can be approximated to be five times the time-integrated luminous intensity. The integrated luminous intensity J_v $(= H_v \times d^2)$ can also be obtained by measuring the luminous exposure, H_v [lx·s] (see Eq. 7), and the photometer-to-source distance, d.

In order to calibrate photometers designed for measurement of the flashing lights, NIST established a luminous exposure scale in 1997 [42].

2. Outline of the calibration services

This section provides a list and brief description of the photometric calibration services currently available at NIST and covered in this SP250. In addition to the photometric calibration services in this SP250, additional documents will cover new photometric calibration procedures for average LED intensity (candela; cd), LED total luminous flux of LEDs (lumen; lm), colorimetry of LEDs, and spectrally integrated total radiant flux of LEDs (watt; W), along with new procedures for the total spectral radiant flux calibrations of incandescent light sources. For the updated information, please check the NIST photometry calibration service website https://www.nist.gov/calibrations/photometric-measurements-calibrations#37010C

All the calibration services listed here, including the Special Tests, are provided routinely. Fixed services (Test Numbers ending in the letter C) are those in which NIST issues calibrated artifacts to customers. Special Tests (Test Number ending with the letter S), on the other hand, are those in which NIST calibrates artifacts submitted by customers. The fees for the fixed services are listed in the NIST Calibration Services Users Guide (SP250) [6]. The fees for Special Tests depend on the type of artifacts, number of artifacts, measurement range requested, etc. Calibrations on Special Test items or under special conditions, other than listed, may be available after consultation as Special Photometric Tests 37100S. The details of the artifacts and measurement procedures for calibration are described in Sections 3 through 7.

***37010C** - Luminous Intensity and Correlated Color Temperature Standard Lamp*
NIST will issue to the customer a 1000 W modified FEL (a lamp-type designation, but not an acronym, of the American National Standards Institute or ANSI) quartz-halogen lamp calibrated for luminous intensity (candela) and correlated color temperature (Kelvin). This lamp has a double coil filament and a clear bulb, and is potted on a medium bipost base. The lamp is operated at approximately 7.3 A/85 V dc, at a correlated color temperature of 2856 K. The relative expanded uncertainty of the luminous intensity of this lamp is less than

0.6 % (k = 2) and the expanded uncertainty of the correlated color temperature is 8 K (k = 2) at 2856 K.

37020S *- Special Tests for Luminous Intensity and Correlated Color Temperature of Submitted Lamps*

NIST will calibrate the luminous intensity and correlated color temperature of incandescent lamps submitted by customers. The inside frosted lamps, the airway beacon lamps, and the 1000 W FEL lamps previously issued by NIST can be submitted for recalibration. Customers can specify either the lamp current or the correlated color temperature of the lamp (normally 2856 K) for calibration. The relative expanded uncertainty of the luminous intensity of these lamps is typically 0.6 % (k = 2) and the expanded uncertainty of the correlated color temperature is 8 K (k = 2) at 2856 K.

37030C *- Correlated Color Temperature Standard Lamp*

NIST will issue to the customer a 1000 W modified FEL quartz halogen lamp as described in 37010C calibrated for correlated color temperature. The lamp is usually calibrated for a correlated color temperature of 2856 K. The expanded uncertainty of the correlated color temperature of these lamps is 8 K (k = 2) at 2856 K.

37040C *- Each Additional Correlated Color Temperature for 37030C*

The correlated color temperature standard lamp issued for 37030C can be calibrated for additional correlated color temperature points in a range from 2000 K to 3200 K. The expanded uncertainty of this calibration is 5 K to 11 K (k = 2) in the range from 2000 K to 3200 K.

37050S *- Special Tests for Correlated Color Temperature of Submitted Lamps*

NIST will calibrate the correlated color temperature of incandescent lamps submitted by customers. The inside frosted lamps, the airway beacon lamps, and the 1000 W FEL lamps previously issued by NIST can be submitted for recalibration. The range of correlated color temperature points is from 2000 K to 3200 K. The expanded uncertainty of this calibration is 5 K to 11 K (k = 2) in the range from 2000 K to 3200 K.

37060S *- Special Tests for Total Luminous Flux of Submitted Incandescent and Fluorescent Lamps*

NIST will calibrate the total luminous flux (lumen) of incandescent lamps and fluorescent lamps submitted by customers. The standard lamps previously issued by NIST can be submitted for recalibration. Miniature lamps may also be accepted. Customers should contact NIST before submitting lamps. The relative expanded uncertainty of this calibration is typically 0.8 % (k = 2) for incandescent lamps and 2.0 % (k = 2) for fluorescent lamps, which depend upon the reproducibility of the test lamps.

37070C *- Opal Glass Luminance Coefficient Standards*

NIST will issue a flashed opal glass plate, 51 mm x 51 mm, calibrated for luminance coefficient (ratio of luminance/illuminance, unit: sr^{-1}) for CIE Illuminant A (2856 K source). The glass plate, masked with a circular aperture 25 mm in diameter, is calibrated for the luminance coefficient within a circular area of 1 cm in diameter in the center of the aperture. The relative expanded uncertainty of this calibration is 0.5 % (k = 2).

37080S *- Special Tests for Submitted Luminance Sources and Transmitting Diffusers*
NIST will calibrate luminance (cd/m^2) of submitted sources or the luminance coefficient (sr^{-1}) of submitted transmitting diffusers, including opal glass previously issued by NIST. Customers should contact NIST before sending sources or diffusers. The relative expanded uncertainty of luminance calibration is typically less than 0.8 % (k = 2).

37090S *- Special Tests for Submitted Photometers, Illuminance Meters, and Luminance Meters*
NIST is capable of calibrating photometers, illuminance meters, and luminance meters submitted by customers. Calibration is normally performed using a CIE Illuminant A source (2856 K incandescent source).

37091S *- Special Test for Submitted Illuminance Head or Illuminance Meter for Illuminance Responsivity*

NIST will calibrate illuminance photometers and illuminance meters submitted by customers for illuminance responsivities. Calibration is performed at illuminance levels from 0.1 lx to 3000 lx. Calibrations at higher illuminance levels (up to 100 klx) are also available under special arrangements. The relative expanded calibration uncertainty (k = 2) is typically 0.5 %, which may increase at low illuminance levels close to 0.1 lx or high illuminance levels close to 100 klx. As an option, NIST can also measure the spectral responsivity of a submitted illuminance photometer and calculate the spectral mismatch correction factor for a source with a known spectral power distribution.

37092S *- Special Test for Submitted Luminance Head or Luminance Meter for Luminance Responsivity*

NIST will calibrate luminance photometers and luminance meters submitted by customers for luminance responsivities. Calibration is performed at luminance levels from 0.1 cd/m^2 to 8000 cd/m^2. The relative expanded calibration uncertainty (k = 2) is typically 0.7 %, which may increase at low luminance levels close to 0.1 cd/m^2.

37100S *- Special Photometric Tests*
NIST can provide special tests for sources, detectors, and photometric instruments other than those stated above under limited conditions by special arrangements with NIST. Customers should contact NIST for consultation.

37110S *- Special Tests for Submitted Flash Photometers*
NIST will calibrate submitted flash photometers designed for measuring luminous exposure [lx•s] or effective intensity [cd]. Calibration is normally performed with white light (≅6500 K) from a Xenon strobe light in the range of 1 lx•s to 100 lx•s and with red light using an Aviation Red filter covering the Xenon strobe light. The relative expanded uncertainty of calibration is ≅1 % (k = 2) or larger depending on the performance of the flash photometer under test.

37130S *- Special Tests for Luminous Intensity and Luminous Flux of LEDs*
NIST is capable of calibrating various light emitting diodes (LEDs) submitted by customers including low-power, mid-power, and high-power LED packages, LED arrays or modules,

LED light engines, LED lamps, following measurement standards such as IES 79 and CIE S 025 for measurement of LED lamps and LED luminaires, IES 85, CIE 225:2017, and CIE 226-2017 for measurement of high-power LED packages at a specified junction temperature, and CIE 127:2007 for measurement of low power LED packages.

37131S *- Special Test for Submitted LEDs for Luminous and/or Radiant Intensity and Color (Optional)*

NIST can calibrate submitted LEDs for Averaged LED Intensity under the CIE Standard Conditions A and B (defined in CIE 127:2007), true luminous/radiant intensity as defined in CIE 225:2017, and color characteristics. The relative expanded uncertainty ($k = 2$) for an intensity calibration varies from 0.5 % to 2 % depending on the test LED, and less than 0.001 in chromaticity for a color characteristic calibration.

37132S *- Special Test for Submitted LEDs for total Luminous Flux and/or Total Radiant Flux and Color (Optional)*

NIST will calibrate submitted LEDs for total luminous flux (lm), total radiant flux (W), and color characteristics using the detector-based 2.5 m absolute integrating sphere. The relative expanded uncertainty ($k = 2$) for a total flux calibration varies from 0.5 % to 1.5 % depending on the test LED, and less than 0.001 in chromaticity for a color characteristic calibration.

3. Luminous intensity and illuminance responsivity calibrations

3.1. Photometry, physical photometry, and radiometry

As stated in Section 1.3, the NIST candela is realized and maintained on a group of eight NIST standard photometers. The illuminance responsivity (A/lx) of the photometers is calibrated annually utilizing the NIST spectral responsivity scale. The principles of the calibration of the photometers are described below.

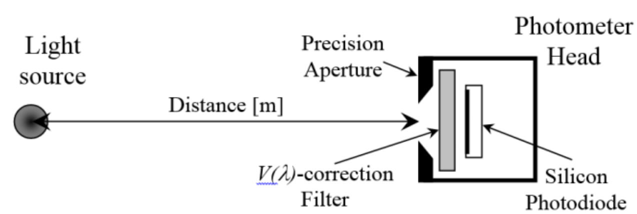

Fig. 4. Geometry for the detector-based candela realization.

A standard photometer basically consists of a silicon photodiode, a $V(\lambda)$-matching filter, and a precision aperture, as shown in Figure 4. When the absolute spectral responsivity $s(\lambda)$ (A/W) of the photometer is measured, the luminous flux responsivity $s_{v,f}$ (A/lm) of the photometer within the aperture is given by

$$s_{\mathrm{v,f}} = \frac{\int_\lambda S_\mathrm{t}(\lambda)s(\lambda)\mathrm{d}\lambda}{K_\mathrm{m}\int_\lambda S_\mathrm{t}(\lambda)V(\lambda)\mathrm{d}\lambda}, \tag{9}$$

where $S_\mathrm{t}(\lambda)$ is the spectral power distribution of the lamp to measure, $V(\lambda)$ is the spectral luminous efficiency function, and K_m is the maximum spectral efficacy (683 lm/W). Usually a Planckian radiator at 2856 K (CIE Illuminant A) [43] is used to provide the light flux $S_\mathrm{A}(\lambda)$, but a different source distribution may be chosen. If the area, A (m^2) of the aperture is known and the responsivity $s_{\mathrm{v,f}}$ is uniform over the aperture, the illuminance responsivity $s_{\mathrm{v,i}}$ (A/lx) of the photometer is given by

$$s_{\mathrm{v,i}} = A \cdot s_{\mathrm{v,f}} \; . \tag{10}$$

When a photometer calibrated for $s_{\mathrm{v,i}}$ is used to measure the illuminance from a point source, the luminous intensity I_v (cd) of the source is given by

$$I_\mathrm{v} = d^2 \cdot y / s_{\mathrm{v,i}} \; , \tag{11}$$

where d is the distance (m) from the light source to the aperture surface of the photometer and y is the output current (A) of the photometer. In practice, d must be larger than the minimum distance where the deviation from the inverse square law of the light source is negligibly small.

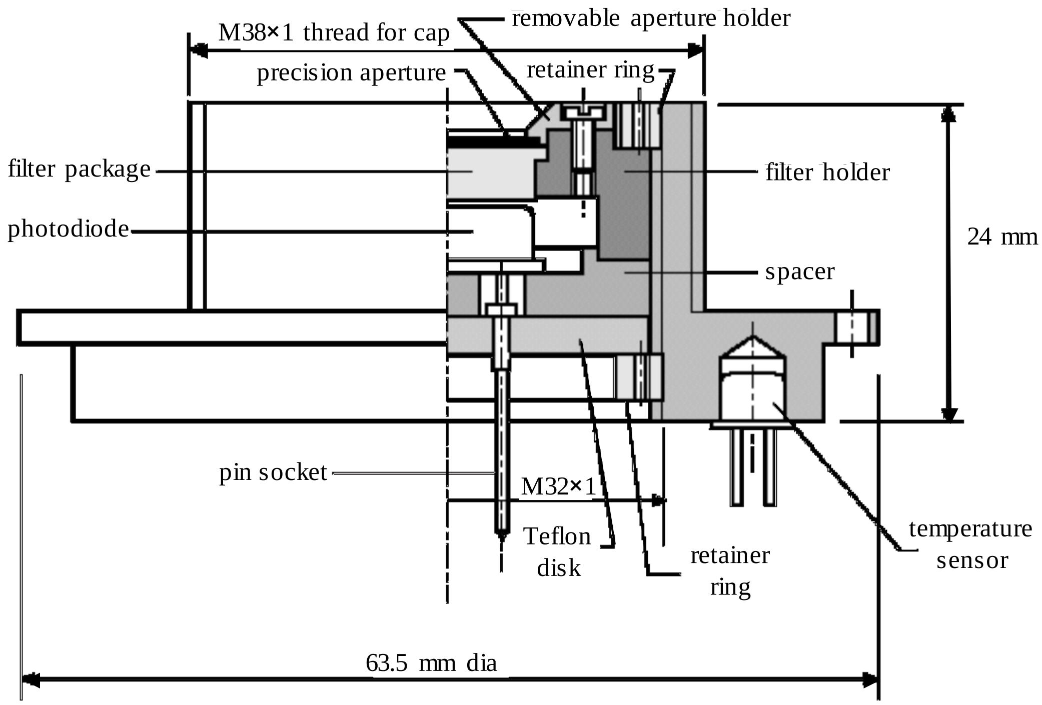

Fig. 5. Design of the NIST standard photometer.

3.2. Design of the NIST standard photometers

Figure 5 shows the design of the NIST standard photometers. A silicon photodiode, a $V(\lambda)$-matching filter, and a precision aperture are mounted in a cylindrical housing. The photodiode is plugged into a socket with a Teflon base of low electrical conductivity. The $V(\lambda)$-matching filter is made of several layers of glass filters, and affixed to the photodiode. On the front side of the filter, the precision aperture is glued to a holder which is carefully machined so that its front surface (the reference surface of the photometer) is 3.0 mm from the plane of the aperture knife edge. The precision aperture was electroformed out of nickel-clad copper and given a black nickel finish. Two of the photometers have precision apertures with nominal areas of 0.5 cm^2. The remaining photometers have precision apertures with nominal areas of 0.1 cm^2. These areas were measured and certified by the Aperture Area Facility in the Sensor Science Division at NIST [44]. An electronic assembly containing a current-to-voltage converter circuit having a high sensitivity and a wide dynamic range [45] is mounted directly behind the photodiode to minimize noise. The circuit has a manual switchable gain setting from 10^4 V/A to 10^{10} V/A (10^{11} V/A for two of the photometers). An input equivalent noise of ≅1 fA is achieved at the gain setting of 10^{11} V/A with an integration time of 1.67 s, and a bandwidth of 0.3 Hz. This high sensitivity feature allows precise measurement of $s(\lambda)$ even in the wings of the $V(\lambda)$ curve. Since the characteristics of the filter and photodiode can change with temperature, a temperature sensor is installed in the front piece of the housing to monitor the photometer temperature [46].

3.3. Realization of the NIST illuminance responsivity unit

3.3.1. Calibration of the NIST standard photometers

The spectral responsivity $s(\lambda)$ [A/W] of the photometers is measured with the NIST SCF at 5 nm intervals. The photometer aperture is underfilled with a beam of 1 mm diameter from the monochromator positioned at the center of the aperture. The SCF has a triangular bandpass with a bandwidth of 4 nm at full width half maximum (FWHM). The error due to the bandpass is corrected using the Stearns and Stearns method [47], but it is negligible. The magnitude of the bandpass correction in $s_{v,f}$ is ≅0.1 %, and the residual standard uncertainty is estimated to be 0.02 %. The responsivity of the photometer is then mapped over the entire area of the precision aperture at several wavelengths. From the mapping data, the ratio of the average responsivity over the aperture to the responsivity at the center of the aperture is calculated and applied in the responsivity calculation. The illuminance responsivity of NIST photometers, $s_{v,i}$ [A/lx], is calculated for Planckian radiation at 2856 K (CIE Illuminant A) according to Eqs. (9) and (10). The f_1' values of the eight photometers range from 1.8 % to 7 %. The f_1' is a term defined by CIE [48] to indicate the degree of spectral mismatch of a photometer to the $V(\lambda)$ function.

The expanded uncertainty of the spectral power responsivity $s(\lambda)$ measured by the SCF is stated to be 0.22 % (k = 2) in the visible region [28], thus an uncertainty contribution of 0.11 %, which is the value for typical photodiodes whose spectral responsivity curve is fairly linear in the visible region. For measurement of photometers by the SCF, additional uncertainty components are considered due to the sharply changing spectral responsivity curve and fairly thick $V(\lambda)$-matching filter (≅ 4 mm) used in the photometer. These are the uncertainty contributions due to the wavelength scale uncertainty (0.05 %), bandpass correction (0.02 %), and the effect of the converging beam with f/9 numerical aperture (0.05 %).

To determine the illuminance responsivity, there are additional corrections and uncertainties related to the characteristics of photometers themselves, as discussed in the following sections.

3.3.2. Correction for the photometer temperature

The NIST photometers are temperature monitored not controlled, and $V(\lambda)$-matching filters typically have a temperature dependence on the order of -0.1 %/°C. The temperature coefficients of the illuminance responsivity of the photometers, measured in a temperature-controlled chamber, are shown in Figure 6. The figure shows the data for three different photometers in the group. The temperature coefficients, c_p, for the eight photometers range from -0.049 %/°C to -0.088 %/°C. Whenever the photometers are used, the temperature correction factor, c_T, as given by.

$$c_T = 1 - (T_p - 25°)c_p \ , \tag{12}$$

is calculated, which is multiplied to the photometer output signal. Using this correction, the photometer signals are always converted to signals at 25 °C. When the photometers are calibrated at the SCF, the determined photometric responsivity is given at 25 °C. The standard uncertainty introduced by the temperature correction factor during the SCF calibration is 0.07 %.

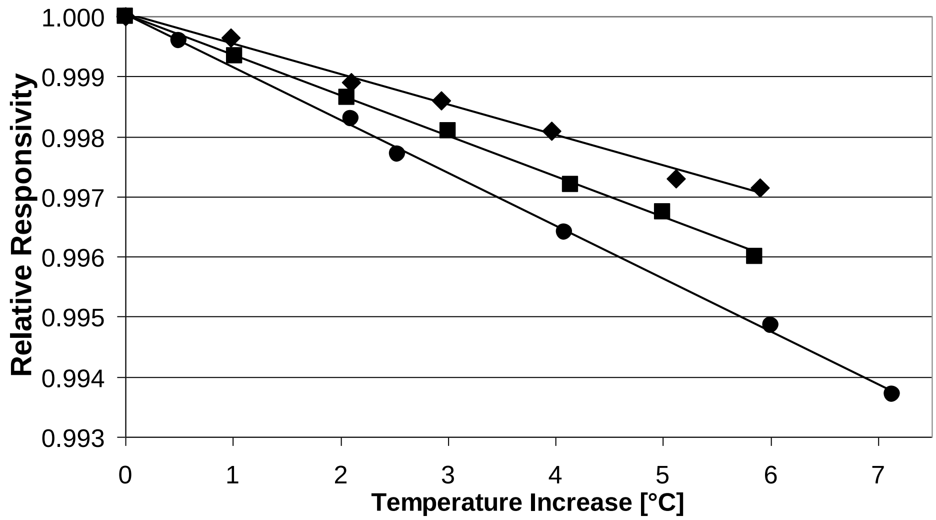

Fig. 6. Temperature dependence of the photometers' illuminance responsivity.

3.3.3. Correction for illuminance responsivity geometry

To convert from luminous flux responsivity $s_{v,f}$ to illuminance responsivity $s_{v,i}$, several uncertainty components are added. The standard uncertainty of the aperture area, which is critical for the conversion, is 0.05 %. As stated in the calibration of the NIST standard photometers in the SCF, the photometer aperture is underfilled with a beam of light 1 mm diameter. The responsivity of the photometer is mapped over the entire area of the precision aperture at several wavelengths. From the mapping data, the ratio of the average responsivity over the aperture to the responsivity at the center of the aperture, c_A, is calculated and applied in the responsivity calculation. The magnitude of c_A is close to unity (typically 0.98 to 1.02) and the standard uncertainty of this ratio is estimated to be 0.10 % from the effects of beam size, aperture edge effects, etc. This is large because the SCF calibrates the detectors in an underfilled geometry, but the photometers are used in an overfilled geometry. Not all of the geometrical considerations can be corrected and these are accounted for in this uncertainty statement.

3.3.4. Linearity of the NIST standard photometers

The linearity of the photometers was measured using a beam conjoiner instrument [49], which is a ratio-and-additive beam device designed to test the linearity of photodetectors. These data indicate that the photometer is linear over an output current range of 10^{-10} A to 10^{-4} A, corresponding to an illuminance range of 10^{-2} lx to 10^{4} lx. If the integration time for the signal is longer, the photometer can be used for even lower illuminance levels [50]. The linearity data also assures negligible non-linearity error in the spectral responsivity measurements.

Each NIST standard photometer is equipped with a built in transimpedance amplifier. The data presented in Figure 7 was measured at gain settings of 10^4 V/A to 10^{10} V/A combined. The ratios of transimpedance gains between different ranges were determined by measuring the same input current from a calibration quality current source at two neighboring ranges (e.g., 0.8 V and 8.0 V output). Gain correction factors, c_G. were defined for each range relative to the 10^7 V/A range. Correction factors are less than 0.02 % at range 10^8 V/A or smaller, and increase up to 0.4 % at a range of 10^{10} V/A. The NIST standard photometers are calibrated at the SCF using a gain setting of 10^7 V/A.

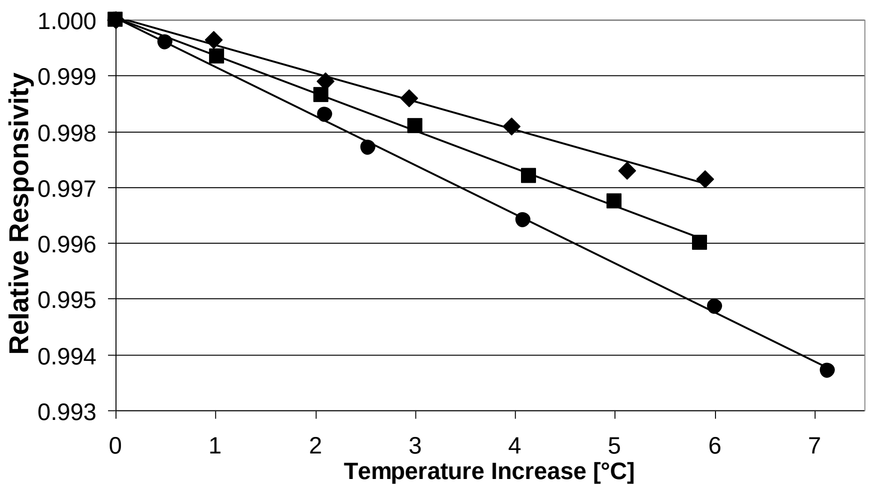

Fig. 7. Linearity of one transimpedance amplifier for NIST standard photometers.

3.3.5. Uncertainty budget for NIST illuminance responsivity unit

To determine the uncertainty of a measurement, the procedures outlined in the Guide to the Expression of Uncertainty in Measurement (GUM) are followed [51]. The analysis of the uncertainty begins with a model or measurement equation for a measurand that describes the calibration in terms of a mathematical function. The following equation describes the scale realization of the NIST illuminance responsivity unit,

$$s_{v,i} = s_{v,f} \cdot A \cdot c_f \ , \qquad (13)$$

where $s_{v,f}$ is the photometric responsivity (A/lm) of the photometer within the aperture, which is based on the spectral power responsivity measurements with the NIST SCF, and A is the area of the aperture. The remaining terms, combined into c_f, are correction factors that relate to the illuminance responsivity (A/lx) calibration of the photometers as described in the earlier sections.

According to GUM, the general equation for combining uncertainties is

$$u_c(y)^2 = \sum_{i=1}^{N}\left[\frac{\partial f}{\partial x_i}\right]^2 u^2(x_i) + 2\sum_{i=1}^{N-1}\sum_{j=i+1}^{N}\frac{\partial f}{\partial x_i}\frac{\partial f}{\partial x_j}u(x_i)u(x_j)r(x_i,x_j) \quad . \tag{14}$$

The degree of correlation between x_i and x_j is characterized by the estimated correlation coefficient, $r(x_i, x_j)$. For the NIST illuminance responsivity unit realization the components are uncorrelated, $r = 0$; therefore, the combined standard uncertainty reduces to the positive square root of the sum of the squares of the sensitivity coefficients multiplied by the squares of the uncertainty contributions. Applying Eq. (14) to Eq. (13), the combined standard uncertainty for the illuminance responsivity is given by

$$u_c^2(s_{\mathrm{v,i}}) = \left(\frac{\partial s_{\mathrm{v,i}}}{\partial s_{\mathrm{v,f}}}\right)^2 u(s_{\mathrm{v,f}})^2 + \left(\frac{\partial s_{\mathrm{v,i}}}{\partial A}\right)^2 u(A)^2 + \left(\frac{\partial s_{\mathrm{v,i}}}{\partial c_{\mathrm{f}}}\right)^2 u(c_{\mathrm{f}})^2 \quad . \tag{15}$$

Converting this to relative uncertainty gives

$$\frac{u_c^2(s_{\mathrm{v,i}})}{s_{\mathrm{v,i}}{}^2} = \left(\frac{\partial s_{\mathrm{v,i}}}{\partial s_{\mathrm{v,f}}}\right)^2 \frac{u(s_{\mathrm{v,f}})^2}{s_{\mathrm{v,i}}{}^2} + \left(\frac{\partial s_{\mathrm{v,i}}}{\partial A}\right)^2 \frac{u(A)^2}{s_{\mathrm{v,i}}{}^2} + \left(\frac{\partial s_{\mathrm{v,i}}}{\partial c_{\mathrm{f}}}\right)^2 \frac{u(c_{\mathrm{f}})^2}{s_{\mathrm{v,i}}{}^2} \quad , \tag{16}$$

For this measurement equation, the sensitivity coefficients reduce to the illuminance responsivity divided by the uncertainty component, such that

$$\frac{u_{\mathrm{c}}^2(s_{\mathrm{v,i}})}{s_{\mathrm{v,i}}{}^2} = \frac{u(s_{\mathrm{v,f}})^2}{s_{\mathrm{v,f}}{}^2} + \frac{u(A)^2}{A^2} + \frac{u(c_{\mathrm{f}})^2}{c_{\mathrm{f}}{}^2} \quad , \tag{17}$$

and thus,

$$u_{\mathrm{c,rel}}^2(s_{\mathrm{v,i}}) = u_{\mathrm{rel}}^2(s_{\mathrm{v,f}})^2 + u_{\mathrm{rel}}^2(A) + u_{\mathrm{rel}}^2(c_{\mathrm{f}})^2 \quad . \tag{18}$$

Table 4 summarizes all of the uncertainty components required to analyze the uncertainty for NIST illuminance responsivity unit which is modeled by Eq. (13). Type A evaluation is based on statistical analysis of a series of observations. Type B evaluation is based on means other than statistical analysis; that is, scientific judgment using all relevant information, including previous measurement data, previous experience, manufacturers' specifications, and data in calibration reports.

Table 4. Uncertainty budget for NIST illuminance responsivity unit.

Symbol	Uncertainty component	Type	Relative Unc. Contribution (%)
$u_{rel}(s_{v,f})$	Spectral responsivity scale and measurement at SCF	B	0.11
	Wavelength scale uncertainty of SCF	B	0.04
	Bandpass correction of SCF	B	0.02
	Numerical aperture of SCF output beam	B	0.05
$u_{rel}(A)$	Aperture area	B	0.05
$u_{rel}(c_f)$	Photometer temperature correction, c_T	B	0.07
	Illuminance responsivity geometry correction, c_A	B	0.10
	Photometer transimpedance gain amplifier correction, c_G	B	0.02
$u_{rel}(s_{v,i})$	Rel. combined standard uncertainty for illuminance responsivity		0.19
Relative expanded uncertainty for illuminance responsivity (*k* = 2)			0.37 %

In this case, $u_{rel}(s_{v,f})$ includes four uncertainty components that are uncorrelated which are fundamental uncertainty of SCF, wavelength scale uncertainty of SCF, bandwidth correction of SCF, and f/9 numerical aperture of SCF. The three uncertainty components that make up the combined uncertainty of the illuminance responsivity of the photometer within the aperture are listed separately in the table.

The relative expanded uncertainty is based on the effective degree of freedom for the measurement. The degree of freedom describes the number of values in the calculation of the quantity that are free to vary. For a Type A determination such as the statistical deviation of a random sample, if the number of values measured is given by n, the degree of freedom is given by (n-1). While there will be n deviations from the mean, only (n-1) of them are free to assume any value. For Type B determinations the degree of freedom is infinite because it is described by a probability distribution, where it is implicitly assumed that the value of the standard deviation resulting from such a determination is exactly known. The effective degrees of freedom for the NIST photometry measurements is extremely large; therefore, the conversion for combined standard uncertainty to expanded uncertainty is simply found by multiplication with a coverage factor $k = 2$. The relative expanded uncertainty for the NIST illuminance responsivity unit is 0.37 % ($k = 2$)

3.4. Realization of the NIST candela and luminous intensity unit

The NIST illuminance unit and NIST candela unit are realized from the NIST illuminance responsivity scale maintained on the NIST standard photometers and knowledge of the spectral distribution of the light source. The details including the facilities, the correction factors to non-ideal situations and the uncertainty analysis are described in the following sections.

3.4.1. Photometry bench

The photometry bench shown in Figure 8 is used for luminous intensity and illuminance calibrations. The base of the bench consists of three 1.8 m long steel optical tables arranged side by side in a linear fashion. A 5 m long rail system with movable carriages is mounted on the table. The optical bench is covered by a light-tight box, the inside of which is covered with black velvet. There are two baffles with variable aperture diaphragms and a shutter mounted along the optical axis. The stray light, checked with various arrangements, is consistently less than 0.05 %, most of which is reflection from the edges of variable aperture diaphragms between the compartments of the photometric bench. Besides the shutter, a $V(\lambda)$-corrected monitor detector is mounted to monitor the stability of the lamp during calibration of photometers. This monitor detector gives a consistent signal independent of the shutter position and regardless of whether the photometer is mounted or not on the carriage.

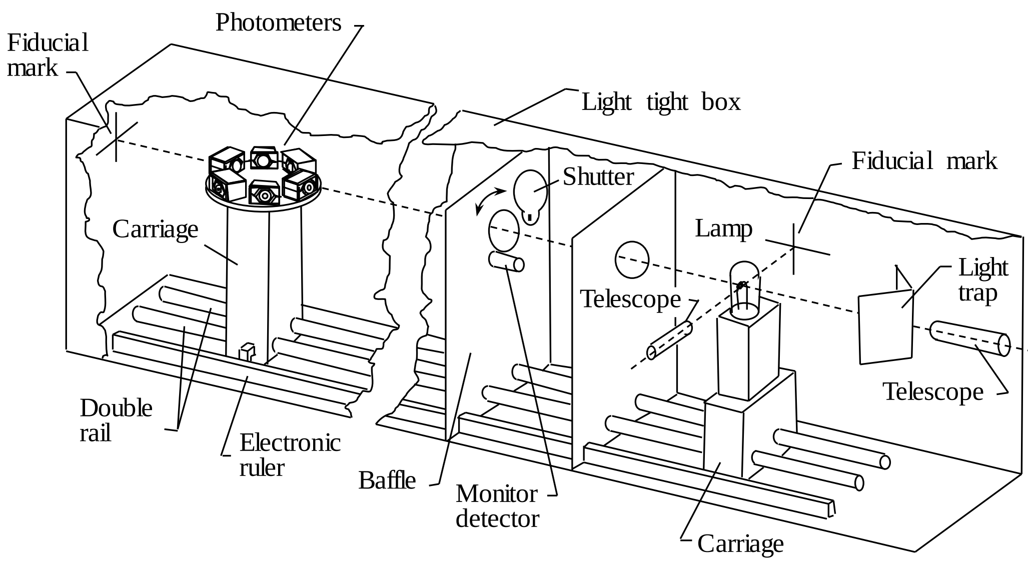

Fig. 8. Schematic of the NIST photometric bench.

The luminous intensity (of a point source) is the density of luminous flux in a given direction. Therefore, setting the location of the emitting element and the direction of the emittance with respect to the optical axis of the NIST photometric bench is critical. Each test lamp is mounted on a photometry bench in the base-down position, and with the identifying number facing the direction opposite to the photometer. For lamps with bi-post bases, the lamp orientation is accomplished, as shown in Figure 9, by aligning the lamp socket so that the lamp posts are held vertically and the plane formed by the axes of the posts is perpendicular to the optical axis of the photometer. An alignment jig (a mirror mounted on a bi-post base to be parallel to the plane formed by the axes of the posts) is used in combination with a laser. The laser is placed in the photometer's position and the beam is autocollimated.

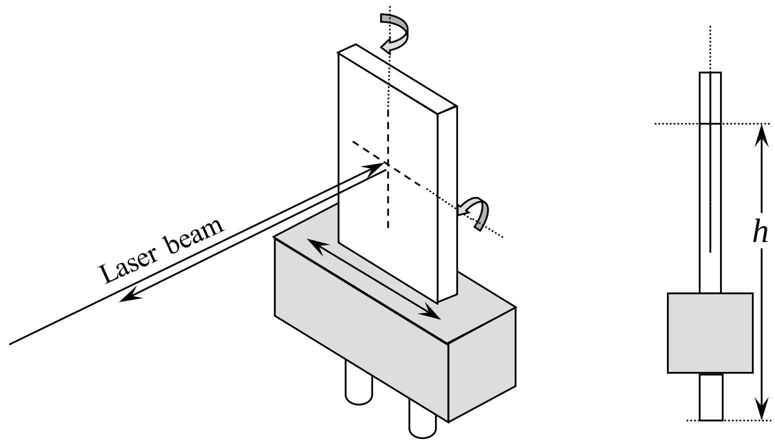

Fig. 9. Alignment of the bi-post base socket using a jig.

The alignment of the distance origin and the height of the lamps is performed using a side viewing telescope. For a lamp with a clear bulb, the center of the posts of the jig is adjusted to the distance origin, and the height of the lamp is aligned so that the optical axis goes through the lamp filament. For a lamp with a frosted bulb, the height of the lamp is set a fixed distance independent of the filament. It should be noted that, although the FEL type lamp is the same type as used for spectral irradiance calibrations [24], the distance origin of the lamp for luminous intensity is different from that for the spectral irradiance calibration. For spectral irradiance calibrations, the front surface of the jig plate is used, which is 3 mm off from the center of the posts. For lamps with a screw-base (E27 and E40) and with a clear bulb, alignment is performed by viewing the filament with the telescope. The distance origin of lamps with a screw base is aligned to the center of the lamp filament, and the height of the lamp is aligned so that the filament center is on the optical axis

The distance from the reference plane of the standard photometers to the reference plane of the lamp is determined by the following equation,

$$d = d_{\mathrm{B}} + d_{\mathrm{P}} + d_{\mathrm{L}} \ , \tag{19}$$

where dB is the distance between the photometry bench origin to the reference plane of the photometer carriage measured by the electronic linear encoder, d_{P} is the distance offset from the photometer carriage reference plane to the standard photometer reference plane, and d_{L} is the distance offset from the photometry bench origin to the lamp reference plane. Six photometers can be mounted on the carousel. The photometers are aligned against the front surface of the mounts fixed on the carousel. The position of the carriage on the rails is monitored by a computer-readable, linear encoder that provides an absolute position with a resolution of 0.01 mm. The encoder reading was verified by comparison with a 2.75 m NIST-calibrated Vernier caliper with a standard uncertainty of 0.36 mm. The standard uncertainty of d_P is 0.1 mm and d_L is 1.0 mm. Applying Eq. (14) to Eq. (19) and since all three components are uncorrelated, the combined uncertainty of distance d is

$$u_c^2(d) = \left(\frac{\partial d}{\partial d_{\mathrm{b}}}\right)^2 u(d_{\mathrm{b}})^2 + \left(\frac{\partial d}{\partial d_{\mathrm{P}}}\right)^2 u(d_{\mathrm{P}})^2 + \left(\frac{\partial d}{\partial d_{\mathrm{L}}}\right)^2 u(d_{\mathrm{L}})^2 \ . \tag{20}$$

The sensitivity coefficients are the partial derivatives of the measurement equation with respect to the different contributions to the measurement equation evaluated at the given value. The sensitivity coefficient describes how the output of the measurement equation varies with changes in the values of the different contributions. The sensitivity coefficients are one for all the components. Thus, the combined standard uncertainty, $u_c(d)$, which is the square root of the sum of the squares of the uncertainty components, is 1.1 mm for a measured distance of 3.65 m

3.4.2. Alignment of the NIST standard photometers

The NIST standard photometers are mounted in a specially designed carousel and are aligned to within 0.5° of the optical axis. The response of the NIST standard photometers follows a cosine response over a small angular interval. The magnitude of the photometer alignment correction factor is unity. The standard uncertainty is determined by the following equation,

$$u(c_\gamma) = \frac{a^2}{\sqrt{20}} \ , \tag{21}$$

where a is the alignment interval and equals 0.5° or 0.00873 radians. The relative standard uncertainty of the photometer alignment correction factor is 0.0017 %

3.4.3. Spectral mismatch correction factor (SMCF)

When the photometers measure light sources whose spectral distribution is different from the calibration source (2856 K Planckian source in this case), an error occurs due to the spectral mismatch of the photometers (section 3.3.3). This error is corrected by a SMCF which removes the CIE illuminant A calibration factor and applies a correction factor based on the spectral power distribution of the test lamp. The SMCF, F^*, is given by

$$F^{*}\left(s_{\mathrm{t}}(\lambda)\right)=\left.\frac{\int_{\lambda} s_{\mathrm{A}}(\lambda) s_{\mathrm{rel}}(\lambda) \mathrm{d} \lambda}{\int_{\lambda} s_{\mathrm{A}}(\lambda) V(\lambda) \mathrm{d} \lambda} \middle/ \frac{\int_{\lambda} s_{\mathrm{t}}(\lambda) s_{\mathrm{rel}}(\lambda) \mathrm{d} \lambda}{\int_{\lambda} s_{\mathrm{t}}(\lambda) V(\lambda) \mathrm{d} \lambda}\right., \tag{22}$$

where $s_{\mathrm{t}}(\lambda)$ is the spectral power distribution of the test lamp, $s_{\mathrm{A}}(\lambda)$ is the spectral data of the CIE Illuminant A, and $s_{\mathrm{rel}}(\lambda)$ is the relative spectral responsivity of the photometer. Using this equation, the SMCF can be obtained for any light source with known spectral power distribution.

For convenience in measuring incandescent lamps, F^* is expressed as a function of the color temperature, T_{c}, of the lamp to be measured. The $F^*(s_{\mathrm{t}})$ is calculated for Planckian radiation of four temperatures, and then the correction factors are fit to a polynomial function. The $F^*(T_{\mathrm{c}})$ is then given by

$$F^{*}(T_{\mathrm{c}})=\sum_{j=0}^{3} a_{j} T_{\mathrm{c}}^{j}\ , \tag{23}$$

The polynomial constants are obtained for each of the NIST standard photometers. An example is shown in Figure 10. The SMCFs for incandescent lamps of known color temperature are automatically calculated using this polynomial. The output signal of the photometer is multiplied by this correction factor. The uncertainty of the SMCF has three components. The first component is the uncertainty in the data points calculated from Eq. (22). The data points calculated for the polynomial fit are determined from ideal Planckian radiators; therefore, Eq. (23) is only appropriate for incandescent lamps or sphere sources that have a light output close to Planckian. Thus, the only quantity in Eq. (22) with an uncertainty is the relative spectral responsivity of the photometer from the SCF. The relative standard uncertainty for each data point is 0.02 %. The second component is the uncertainty caused by fitting a polynomial to the calculated points. A prediction band analysis, which shows the region within which random samples from that model plus random errors are expected to fall, is used to determine the standard uncertainty caused by the fit. The standard uncertainty for the prediction band is 0.02 %. The third component is the uncertainty in the lamp color temperature used to calculate the SMCF. The standard uncertainty for the lamp color temperature is 4 K; however, the sensitivity coefficient calculated from the derivative of the polynomial is extremely small, resulting in an uncertainty of 0.02%, which is negligible. The relative standard uncertainty of the SMCF is the square root of the sum of the squares of the two other components, which is 0.03 %

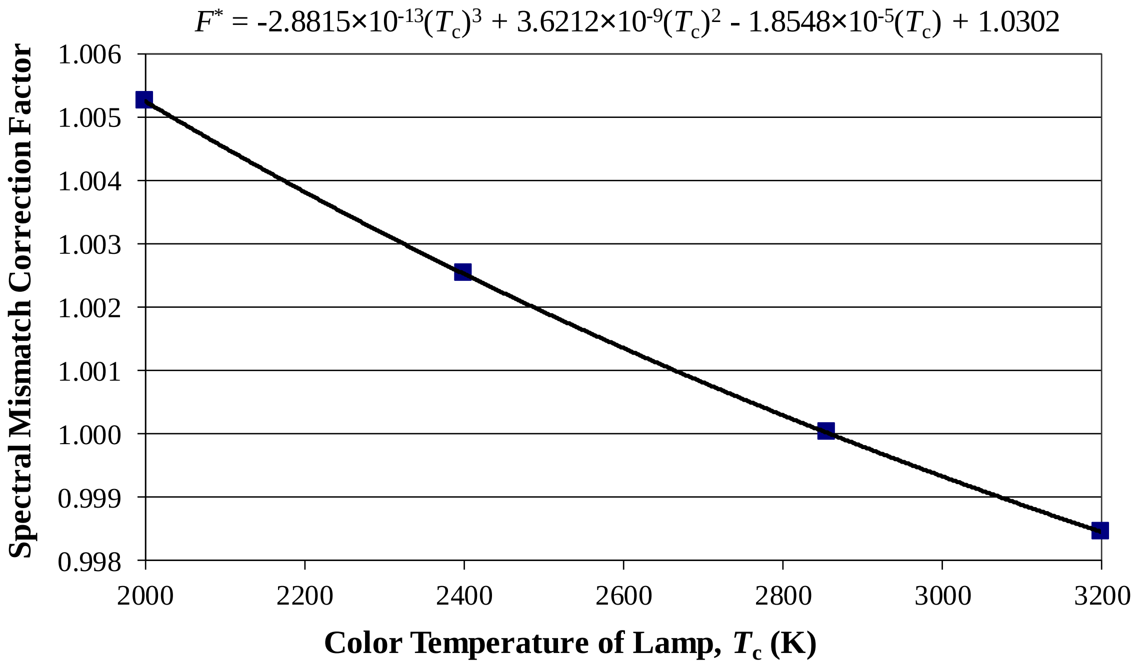

Fig. 10. Polynomial fit for the SMCFs.

3.4.4. Uncertainty budget for NIST illuminance unit

The uncertainty budget in Section 3.3.5 was for the illuminance responsivity of the standard photometers for CIE Illuminant A (theoretical source) and did not include uncertainties associated with measurement of real lamps. The illuminance unit is realized by measuring a working standard lamp of known spectral distribution and uncertainty with the NIST standard photometers. The measurement equation is

$$E_\mathrm{v} = \frac{(y - y_d)}{s_{\mathrm{v,i}}} \cdot c_\mathrm{f} \quad , \tag{24}$$

where E_v is the measured illuminance (lx), y is the signal from the photometer (A), y_d is the dark output voltage typically from unbalanced offset voltage of the transimpedance operational amplifier measured by closing the shutter between lamp and photometer, and $s_{\mathrm{v,i}}$ the illuminance responsivity (A/lx) of the photometer. In practice, the photocurrent from the photometer is converted to a voltage by the transimpedance gain amplifier, which is measured by a digital voltmeter that has a calibration uncertainty. Several uncorrelated components of uncertainty have been combined in one factor, c_f. A list of these uncertainty components and relative standard uncertainty are summarized in Table 5.

Table 5. Uncertainty components as correction factors for NIST illuminance unit.

Symbol	Uncertainty component	Type	Relative Unc. Contribution (%)
c_T	Photometer temperature correction	B	0.05
c_G	Photometer transimpedance gain amplifier correction	B	0.02
c_y	Digital voltmeter calibration	B	0.004
F^*	SMCF	B	0.03
c_S	Spatial stray light	B	0.05
c_γ	Photometer alignment	B	0.002
$\boldsymbol{c_f}$	**NIST illuminance unit correction factor**		**0.079**

The uncertainty budget for the NIST illuminance unit is summarized in Table 6 based on the model Eq. (24). The relative standard uncertainty for the average signal voltage, y, is 0.01 %. The relative expanded uncertainty for the NIST illuminance unit is 0.40 % (k = 2)

Table 6. Uncertainty budget for NIST illuminance unit.

Symbol	Component	Value x_i	Standard Uncertainty $u(x_i)$	Unit	Type	Sensitivity Coefficient c_i	Unc. Contribution $u_i(y)$
y	Photometer signal	1.819×10^{-6}	2.42×10^{-10}	A	A	9.88×10^{7}	0.024
y_d	Photometer dark signal	-5.0×10^{-10}	6.10×10^{-12}	A	A	-9.88×10^{7}	-0.001
$s_{v,i}$	Illuminance responsivity	1.0118×10^{-8}	1.88×10^{-11}	A/lx	B	-1.78×10^{10}	-0.334
c_f	Correction factor	1.000	7.90×10^{-4}		B	179.8	0.142
$\boldsymbol{E_v}$	NIST illuminance unit	**179.83**		**lx**			**0.364**
Relative expanded uncertainty for NIST illuminance unit (*k* = 2)							**0.41 %**

The relative standard uncertainty was not used in Table 6 because the subtraction of the dark signal complicates the calculus; therefore, it is simpler to use Eq. (15). The contribution to the overall uncertainty, $u_i(y)$, is defined as the standard uncertainty multiplied by the sensitivity coefficient. The uncertainty contribution column is very useful in quickly determining which contributions contribute the most uncertainty to the measurement.

Because the components are uncorrelated, the combine standard uncertainty (displayed in the lower right cell) is the sum of the squares of the uncertainty contribution.

3.4.5. Uncertainty budget for NIST candela unit

With the illuminance unit realized as described in the previous section, the candela is realized by the standard photometer and a test lamp of known spectral distribution measured at a known distance *d*. The measurement equation is

$$I_{\mathrm{v}} = E_{\mathrm{v}} \cdot d^{2} , \qquad (25)$$

with E_{v} and *d* uncorrelated, the uncertainty in measured luminous intensity is given by

$$u^{2}(I_{\mathrm{v}}) = \left(\frac{\partial I_{\mathrm{v}}}{\partial E_{\mathrm{v}}}\right)^{2} u^{2}(E_{\mathrm{v}}) + \left(\frac{\partial I_{\mathrm{v}}}{\partial d}\right)^{2} u^{2}(d) . \qquad (26)$$

Reducing this to a relative form,

$$u_{\mathrm{rel}}^{2}(I_{\mathrm{v}}) = u_{\mathrm{rel}}^{2}(E_{\mathrm{v}}) + 4 \cdot u_{\mathrm{rel}}^{2}(d) . \qquad (27)$$

See section 3.4.1 for the analysis of uncertainty of distance *d*. While real lamps are not exactly point sources, the NIST candela is realized and maintained at a fix distance, and thus, the inverse-square law error is not included in this budget. The uncertainty budget for the NIST candela unit is summarized in Table 7 based on the model Eq. (25). The relative expanded uncertainty for the NIST candela unit is 0.41 % (k = 2).

Table 7. Uncertainty budget for NIST candela unit.

Symbol	Uncertainty component	Type	Relative Unc. Contribution (%)
E_{v}	NIST illuminance unit	B	0.202
d	Photometric distance	B	0.030
$\boldsymbol{I_{\mathrm{v}}}$	**NIST candela unit**		**0.204**
Relative expanded uncertainty for NIST candela unit (*k* = 2)			**0.41 %**

3.5. Luminous intensity calibrations

3.5.1. Lamp standards for luminous intensity

For many years, NIST issued gas-filled, inside-frosted, GE Airway Beacon type lamps (100 W, 500 W, and 1000 W) as luminous intensity transfer standards of approximately 150 cd, 700 cd, and 1400 cd, respectively. These lamps are still accepted for recalibration by NIST. The 100 W and 500 W lamps have T-20 bulbs, and the 1000 W lamps have T-24 bulbs. They all have medium bi-post bases and C-13B filaments. The lamp designation number is etched on the bulb. Figure 11 (left) shows the appearance of this type of lamp and the electrical polarity applied during calibration by NIST. The designation number on the bulb always faces opposite to the direction of calibration. For inside-frosted Airway Beacon type lamps, the center of the posts of the jig is adjusted to the distance origin, and the height of the lamp, *h*, is aligned so that the optical axis is 12.7 cm (5 in) for 100 W and 500 W lamps and 11.4 cm (4.5 in) for 1000 W lamps, from the bottom of the posts.

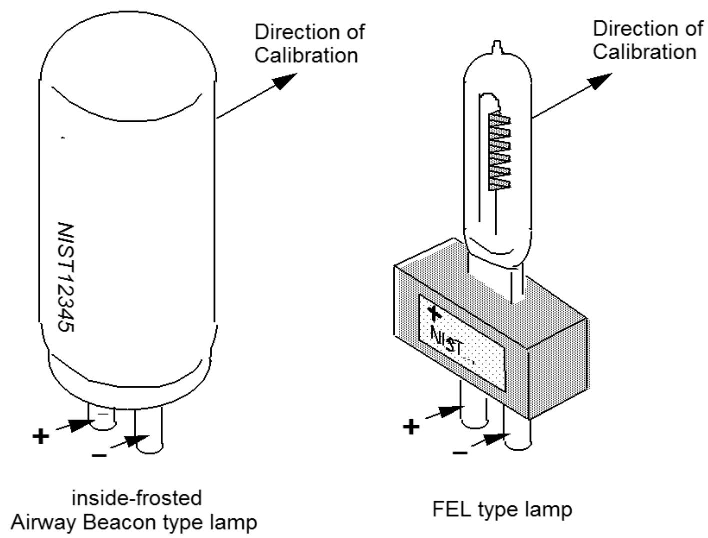

Fig. 11. Appearance of luminous intensity standard lamps and their electrical polarity.

Figure 12 shows the aging characteristics (the change in the luminous intensity of the lamp as a function of operating time) of a typical Airway Beacon type lamp at 2856 K. The lamp needs to be recalibrated after a certain operation time depending on the user's uncertainty requirements, and the aging characteristics of the individual lamp should be taken into account in the uncertainty budget. It is generally recommended that this type of lamp be recalibrated after 25 h of operating time.

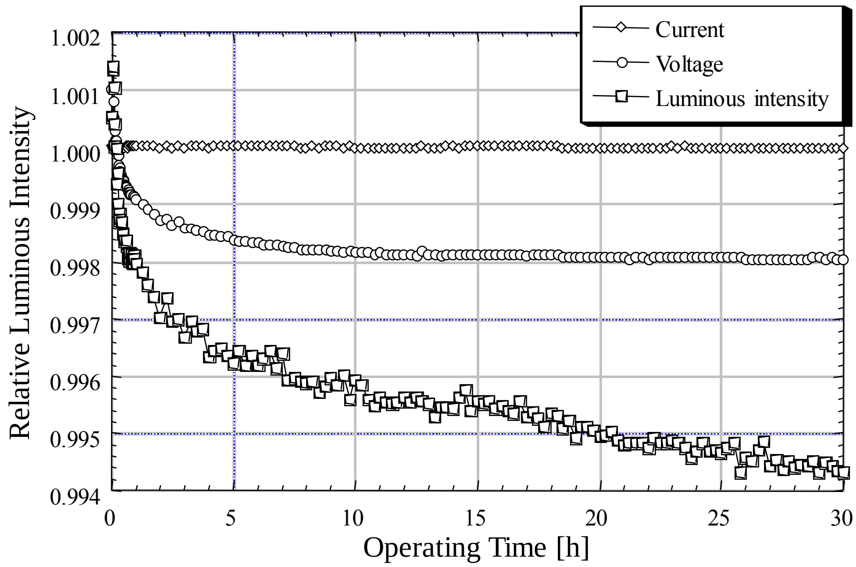

Fig. 12. Aging characteristics of a typical Airway Beacon type lamp at 2856 K.

NIST issues standard lamps calibrated for luminous intensity and color temperature. The type of lamp issued by NIST is a 1000 W, FEL type, quartz halogen lamp with a coiled-coil tungsten filament, as shown in Figure 11 (right). The lamps, manufactured by Osram-Sylvania Inc., are potted on a medium bi-post base, and seasoned with DC power for 48 h at 8.4 A and then for 72 h at 7.2 A. The luminous intensity of an FEL lamp can change by 20 % during the seasoning. Lamps are operated and calibrated at a color temperature of 2856 K with an operating current of ≅7.2 A and voltage of ≅85 V. The lamp designation numbers and the electrical polarity are engraved on an identification plate affixed to the base.

Figure 13 shows the aging characteristics of a typical selected FEL type lamp at 2856 K. The luminous intensity lamps issued by NIST are screened to obtain a luminous intensity drift of smaller than 0.3 % during a continuous 24 h period of operation. It can be assumed that the lamp changes at a similar rate in ensuing hours of operation. Further details of the characteristics of these FEL type lamps are described in Reference 44.

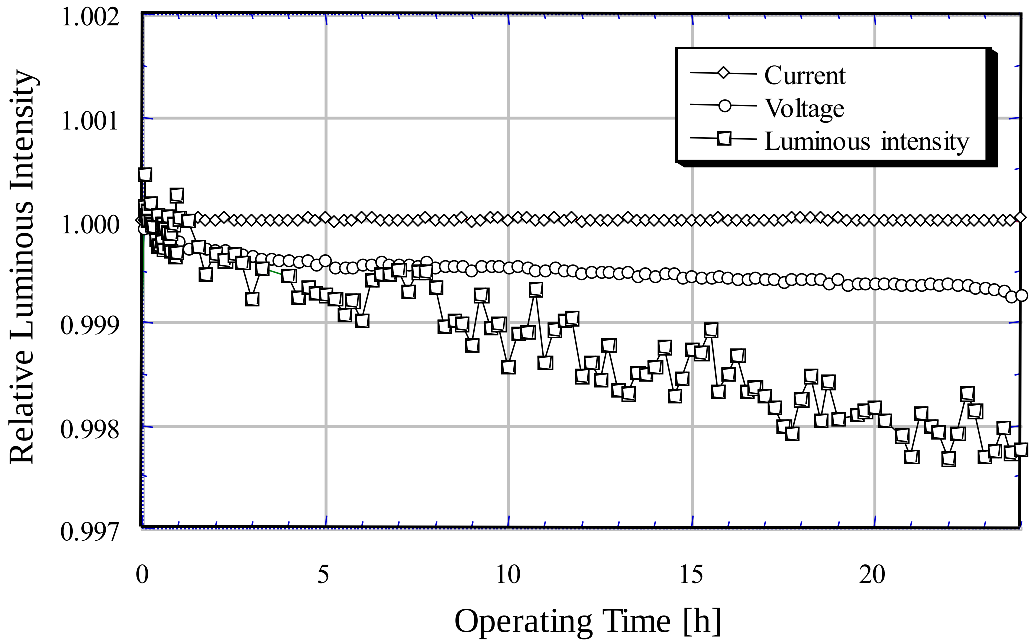

Fig. 13. Aging characteristics of a selected FEL type lamp at 2856 K.

The FEL type lamps issued by NIST are also screened for angular uniformity of luminous intensity. Figure 14 shows the data of a typical selected FEL type lamp. If the filament is tilted from the perpendicular of the optical axis, the angular uniformity is degraded. The lamps are selected for the variation of luminous intensity not to exceed ± 0.5 % in a ± 1° rectangular region around the optical axis. It should be noted that, even though the lamps are selected as mentioned above, the angular alignment of the FEL type lamps with a clear bulb is more critical than with the frosted lamps previously issued by NIST. The angular alignment of the lamp correction factor, γ_L, has a magnitude of one. The standard uncertainty of the lamp angular alignment correction factor is determined by mapping the uncertainty of the tip and tilt angle or vertical angle and the rotation angle or horizontal angle onto the spatial non-uniformity plot in Figure 14. The relative standard uncertainty for a typical FEL lamp is 0.05 %.

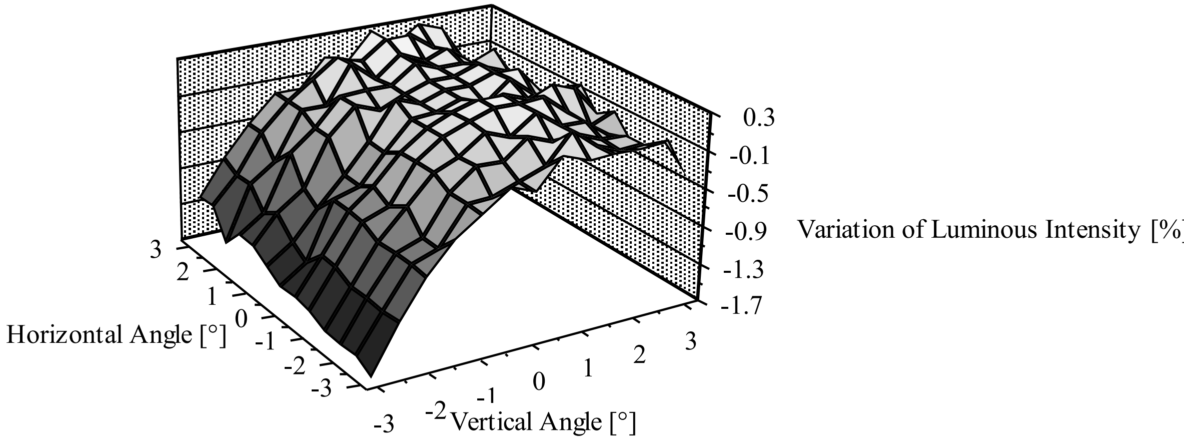

Fig. 14. Spatial non-uniformity of a typical FEL type lamp.

The lamps should be handled very carefully to avoid mechanical shocks to the filament. The bulb of any lamp should not be touched with bare hands. Before operation, the bulb of the lamp should be cleaned with a soft, lint-free cloth to remove any dust accumulation from the packing material. Lamps are best kept in a container when not used. Special attention should be paid to quartz halogen lamps (FEL lamps) to avoid moisture on the envelope. Water droplets on the bulb can cause a white spot on the quartz envelope after burning the lamp, and can result in a permanent damage to the lamp. If a quartz halogen lamp is accidentally touched with a bare hand, the bulb should be cleaned using ethyl alcohol.

3.5.2. Long-term stability of NIST standard photometers

The NIST standard photometers are calibrated on an annual basis at the NIST SCF [25] utilizing the spectral responsivity scale. The drift of the illuminance responsivity of the NIST standard photometers over a 15 year period is shown in Figure 15. Note that these results include the uncertainty of the illuminance unit realization (0.39 %). Photometers 1, 2, and 3, which showed larger drift than the rest, employ $V(\lambda)$-correction filters from different manufacturers than the rest. In 2004, photometer 5 showed a significant reduction in its responsivity. On the filter surface of photometer 5 a cloudy deposit of unknown composition and origin was observed. After cleaning the filter surface of the photometer, the responsivity did not change.

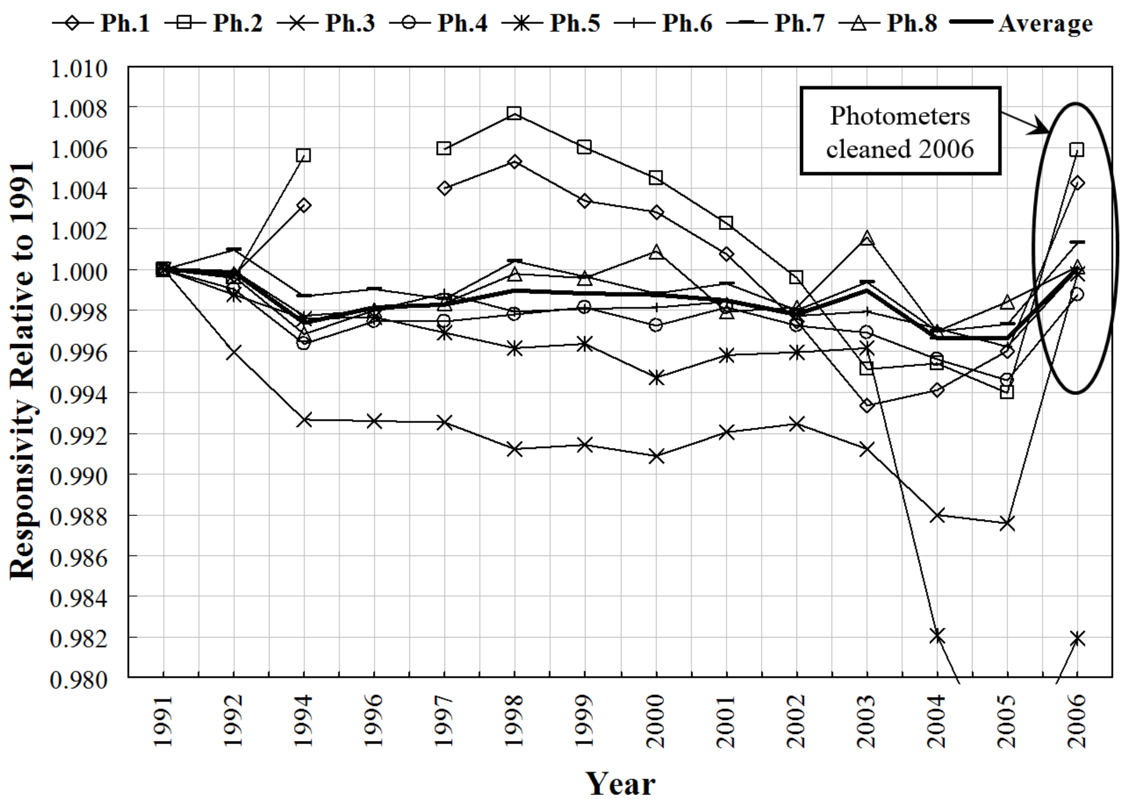

Fig. 15. Drift of illuminance responsivity of NIST standard photometers.

The filter surfaces of the photometers were not cleaned during the time period from 1991 to 2006, except for photometer 5. In 2006 the photometer filters were cleaned and the SCF had a readjustment in the spectral responsivity scale. The average drift over the 15 year period is 0.05 %. The magnitude of the long-term stability correction factor is unity. The relative standard uncertainty of the long-term correction factor is not the average drift but the maximum drift per year (0.15 %, not including the shift in 2006). As part of the NIST quality system, two working lamps are used to validate the three photometers that are chosen to perform the calibration.

3.5.3. Electrical power supply

All the standard lamps and test lamps are operated at a specified current rather than a specified voltage because lamp voltage, in general, does not reproduce well due to the variation of sockets used among customers. However, if the socket is designed well, the lamp voltage reproduces fairly well on the same socket, and the lamp voltage is useful to monitor for changes in the lamp.

The NIST photometric bench is equipped with a medium bipost-base socket which has four separate contacts, two for the current supply, and the other two for voltage measurements. For luminous intensity calibrations, the lamp voltage is reported, only for reference, without an uncertainty value. The bench is also equipped with a medium screw-base socket (E27) which has four contacts. Screw-based lamps submitted by a customer can be calibrated.

A DC constant-current power supply is used to operate standard lamps and test lamps. The lamp current is measured as the voltage across a reference current shunt (R_S = 0.1 Ω), using a calibrated 6-½ digit voltmeter. The digital voltmeter is on a one year calibration cycle. The current shunt is periodically calibrated at three different current levels with a standard uncertainty of 0.0013 %.

The lamp current is automatically controlled by a computer feedback system to keep the current drift within ± 0.002 %. The power supply is operated in an external control mode, in which the output current is regulated by an external reference voltage. The external voltage is supplied by an 18 bit D-to-A converter controlled by the computer.

An incandescent lamp operated at a fixed current, J_0, has a variation of the luminous intensity which is dependent on the following equation,

$$I_\mathrm{V} = I_0 \left(\frac{J}{J_0} \right)^{m_\mathrm{J}} , \tag{28}$$

where I_0 is the initial luminous intensity, J is the new current which is only a small deviation from the fixed current, and m_J is the current dependent coefficient equal to 7.0 with a standard uncertainty of 0.5.

Since the lamp current is controlled, the voltage of the lamp will fluctuate depending on the properties of the lamp. It is the policy of the NIST photometry calibration group to include this fluctuation in the uncertainty budget for calibrations of standard artifacts. For incandescent or halogen lamps the luminous intensity is dependent on the voltage of the lamp by the following equation

$$I_\mathrm{V} = I_0 \left(\frac{V_L}{V_0} \right)^{m_V} , \tag{29}$$

where I_0 is the initial luminous intensity, V_L is the measured voltage which is only a small deviation from the calibrated voltage, V_0, and m_V is the voltage dependent coefficient equal to 3.6 with a standard uncertainty of 0.5. To determine this correction factor the lamp is measured three times and the voltage is recorded. The measured voltage and calibrated voltage is set to the average voltage and the standard deviation of the three voltage measurements is used as the standard uncertainty of the measured voltage. The V_0 is stated not to have an uncertainty.

3.5.4. Deviation from inverse square law

Due to the lamps filament structure or properties of the lamp envelop, the lamp may not follow the inverse square law. This deviation from an ideal source is compensated for in the uncertainty budget. The correction factor has a magnitude of 1 and the standard uncertainty is determined experimentally. To determine the deviation, the lamp is turned on, allowed to warm up and then the luminous intensity is measured at several distances between 2.4 m and 3.6 m. The magnitude of the standard uncertainty for the deviation from inverse square law for a good luminous intensity standard is less than 0.03 %, but typical values may be as large as 0.10 %.

3.5.5. Uncertainty budget for luminous intensity calibrations

The analysis of the uncertainty for the luminous intensity calibration begins with a model which is an expanded Eq. (25), as given by,

$$I_{\mathrm{v}} = E_{\mathrm{v}} \cdot d^2 \cdot \left(\frac{V_J \cdot c_V}{J_0 \cdot R_{\mathrm{S}}} \right)^{m_{\mathrm{J}}} \left(\frac{V_{\mathrm{L}}}{V_0} \right)^{m_{\mathrm{V}}} \cdot c_{\mathrm{f}} \quad , \tag{30}$$

where E_{v} is measured illuminance, d is the photometric distance, V_{J} is the voltage measured across the shunt resistor for the measurement of current, c_{V} is the calibration factor of the digital voltmeter, J_0 is the calibrated current for the lamp, R_{S} is the resistance of the shunt resistor, V_{L} is the measured voltage which is only a small deviation from the calibrated voltage, V_0, and m_{V} is the voltage dependent coefficient equal to 3.6 with a standard uncertainty of 0.5. Several uncorrelated components of uncertainty have been combined in one factor, c_{f}. A list of these uncertainty components and relative standard uncertainty are summarized in Table 8.

Table 8. Uncertainty components as correction factors for luminous intensity calibration.

Symbol	Uncertainty component	Type	Relative Unc. Contribution (%)
c_{L}	Long-term stability of NIST standard photometers	B	0.15
c_{δ}	Lamp angular alignment	B	0.05
c_{I}	Deviation for the inverse square law	B	0.10
$\boldsymbol{c_{\mathrm{f}}}$	**Luminous intensity calibration correction factor**		**0.187**

Table 9 summarizes all of the data needed to analyze the uncertainty for a typical luminous intensity calibration which is modeled by Eq. (30). A correlation exists between the signal, the current measurement and the SMCF; however, the correlation coefficients for these interactions are insignificant. For this example, J_0 = 7.230 A and V_0 = 84.5 V. The sensitivity coefficient for the exponential dependent parameters would be zero because the quantity raised to the exponent is unity. However, the exponential dependent parameters have uncertainty; therefore, the sensitivity coefficient is calculated using the exponential dependent parameters plus one standard uncertainty in the numerator and minus one standard uncertainty in the denominator, as a worst case example. As an example, the sensitivity coefficient for voltage dependence in Table 9 is the luminous intensity, I_v, multiplied by the natural logarithm of 1.00014, which is the ratio of V_L plus one standard uncertainty divided by V_0.

Table 9. Uncertainty budget for typical luminous intensity calibration.

Symbol	Component	Value x_i	Standard Uncertainty $u(x_i)$	Unit	Type	Sensitivity Coefficient c_i	Unc. Contribution $u_i(y)$
E_v	Illuminance	179.828	0.363	lx	B	6.0	2.1804
d	Photometric distance	2.45000	0.00107	m	B	881.2	0.9428
V_J	Voltage across shunt	0.72130	1.0×10^{-6}	V	A	10475	0.1048
c_V	Voltmeter calibration	1.0000	0.00004		B	7555.9	0.3022
R_S	Shunt resistance	0.100006	1.3×10^{-6}	Ω	B	-75555	-0.0982
m_J	Current dependence	7.0	0.5		B	0.0074	0.0037
V_L	Lamp voltage	84.500	0.012	V	A	46.0	0.5518
m_V	Voltage dependence	3.65	0.5		B	0.15	0.0766
c_f	Correction factor	1.0000	0.00187		B	1079.4	2.0185
$\boldsymbol{I_v}$	**Luminous intensity**	**1079**		**lx**			**3.18**
Relative expanded uncertainty for typical luminous intensity calibration (*k* = 2)							**0.41 %**

The final statement of this calibration would be: The luminous intensity of the lamp standard was determined to be 1079 cd with an expanded uncertainty of 6.4 cd determined with a coverage factor k = 2. The relative expanded uncertainty for this calibration was 0.60 % with a coverage factor k = 2.

3.5.6. Calibration and quality control procedures for candela calibrations

The Photometry service group has a management system that is assessed against the ISO 17025 standard [52]. As part of that management or quality system, well defined procedures are documented for the calibration of physical standards and the validation of data taken at the time of calibration.

The step in a calibration is communication with the customer. The Photometry service personnel are available for discussion through electronic communication or telephone before the customer submits a calibration request. The NIST Photometry website provides service and contact information. The customers have reasonable access to relevant areas of the laboratory for witnessing examples of calibrations, but they are not allowed to be present during the time of actual measurements.

When a customer's lamp arrives at NIST, the test lamps are inspected to see if the bulbs or filaments are broken, or if the base is loose. Any defective lamps must be replaced or removed from calibration. The Photometry project leader will contact the customer by telephone to inform them that their lamp is defective. The test lamps are then stored in their original shipping containers.

Prior to calibration the NIST standard photometers are mounted in the photometry bench carousel and allowed to stabilize for at least 30 min. The test lamps are removed from the shipping container, and cleaned with a soft dry cloth. The bi-post base socket in the first compartment of the bench is aligned using the alignment jig and the laser.

Once the socket is aligned the check standard lamp is mounted and measured by three of the NIST standard photometers. The check standard lamp shall deviate less than 0.2 % from the running average. Figure 16 shows the result of a check standard over a four month period. After the check standard lamp is validated, the spectroradiometer used for setting the correlated color temperature of the submitted lamp is calibrated against the NIST color temperature standards. The submitted lamp is mounted in the bi-post base and the operating current is determined to set the desired correlated color temperature. The submitted lamp is operated at the determined current and measured by three of the NIST standard photometers. The submitted lamp is turned off. The determination of the luminous intensity is repeated two more times and on the last operation of the lamp the photometer carousel is moved forward to access the deviations from the inverse square law.

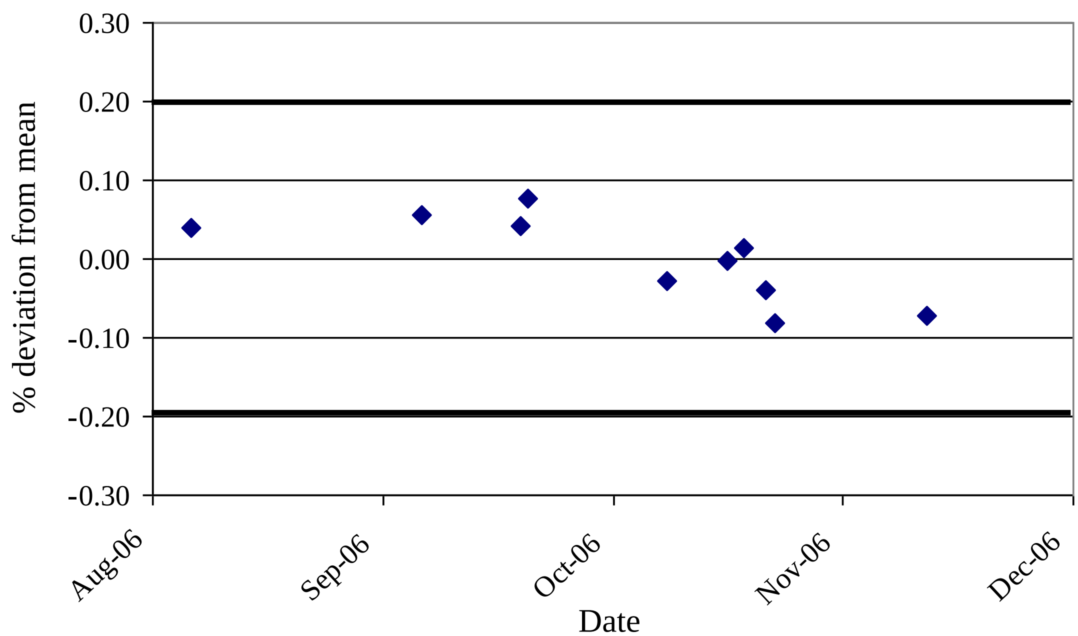

Fig. 16. Results of check standard lamp over a four month period.

After the data is analyzed the calibration report is generated. The calibration report is submitted to the alternate Photometry Service personnel for review, the Technical Manager for review, and then to the Quality Manager for the final review. When a calibration report is completed, reviewed and approved, the test lamps are packaged in the original shipping material and taken by a Photometry Staff member to the shipping facility.

After the completion of a calibration service, the customer is welcome to contact the Photometry service personnel to clarify or discuss calibration procedures and results. All communication with the customer relating to the customers' requirements or the results of the work during the period of measurement shall be documented and included in the Test Folder.

3.6. Illuminance responsivity calibrations

Significant improvement in the quality of commercial photometers and illuminance meters has been made due to availability of high quality silicon photodiodes and $V(\lambda)$ matching filters. As a result, many types of commercially available photometers can be used as photometric standards instead of traditional luminous intensity standard lamps. Standard lamps are sensitive to mechanical shocks, change with burning time, and drift during the stabilization period. Experience shows that well maintained photometers are less subject to such problems, and provide a dynamic range of several orders of magnitude. NIST experience indicates that the short-term stability of photometers is superior to lamps and although the long-term stability has not been tested for many types of photometers, a few particular types tested have shown satisfactory stability (≅0.1 % per year). It should be noted that some photometers have shown changes greater than 1 % in a year, making their use as standards difficult. In general, for luminous intensity and illuminance measurements, the use of standard photometers is recommended, but the photometers should be calibrated frequently (at least once a year) until the long-term stability data are accumulated for the particular photometers a user laboratory may employ. Photometer heads or photometers (photometer heads with a display unit) and illuminance meters are accepted for calibration by NIST. The requirements and recommendations for photometers used as transfer standards and reference standards are described below.

3.6.1. Types of photometers and illuminance meters

A standard photometer head should have either a limiting aperture (whose area is much smaller than the photodiode area) or a flat diffuser such as an opal glass in front of the V(λ)-correction filter so that the reference plane of the photometer is accurately and clearly defined. Some commercial photometer heads only have a $V(\lambda)$-correction filter attached in front of the silicon photodiode. If a photometer head does not have an aperture or a diffuser, the photodiode surface might be used as the reference plane of the photometer head. In this case, due to the refraction index of the $V(\lambda)$-correction filter which is usually several millimeters in thickness, the effective reference plane can be several millimeters from the photodiode surface. Sometimes, the front surface of the filter is simply defined as the reference plane of such photometer heads, in which case the true reference plane can be more than 1 cm from the filter surface. When the reference plane is not correctly defined, the departure from the inverse square law causes the responsivity of the photometer to vary depending on the distance to the source, and serious errors may occur when the photometer is used at close distances to the source. This is the same problem with large-size lamps, for which the inverse square law does not hold well at close distances. To avoid these difficulties, standard photometers having a limiting aperture or a flat diffuser on the front are recommended.

Some illuminance meter heads employ a dome-shaped or mesa-shaped diffuser in the front. In this case, it is usually difficult to define the correct reference plane. Such illuminance meters are not recommended to be used as standard photometers unless the meters are always used at the same distance from the source. Also, illuminance meters with poor spectral match and (or) with only a 3 digit display are not adequate for use as standard photometers.

Illuminance meters may have various structure of the light-receiving surface for cosine correction. The reference plane of the illuminance meter heads should be provided by the customer. Upon request, the reference plane of photometer heads (without an aperture or a diffuser) and illuminance meter heads can be experimentally determined.

3.6.2. Operation and handling of photometer heads and illuminance meters

Illuminance meters are generally not designed to measure illuminance at very close distances to a source. It should be noted that the measurement error may increase greatly if an illuminance meter with a reference plane incorrectly defined is placed very close to a light source (e.g., less than 0.5 m).

As previously described, the responsivity of a photometer can be a function of temperature. If the photometer is neither a temperature-controlled type nor a temperature-monitored type, the photometer must be used close to the calibration temperature to avoid errors. If not, the temperature coefficient of the photometer should be measured, and correction factors should be applied as appropriate. The photometer should be placed in the laboratory several hours in advance of use so that the photometer's temperature equilibrates to the ambient temperature.

At NIST, photometers and illuminance meters are calibrated using incandescent lamps operated at 2856 K unless otherwise requested by the customer. In this case, when the photometers are used to measure light sources other than incandescent lamps of that color temperature, spectral mismatch errors occur, and in order to quantify or correct for this error, the relative spectral responsivity of the photometers or illuminance meters must be measured.

3.6.3. Illuminance responsivity calibration and quality control procedures

Photometers and photometer heads are calibrated for illuminance responsivity in A/lx, V/lx or readings/lx. Calibration is performed on the NIST photometry bench using a 1000 W FEL type lamp operated at 2856 K (CIE Illuminant A). The calibration is performed by direct comparison with three of the NIST standard photometers. The responsivity is usually measured at two distances, 2.4 m and 3.6 m from the lamp, at typical illuminance levels of 75 lx and 180 lx. Calibrations can also be made at other illuminance levels from 0.1 lx to 3000 lx for a linearity check, if requested by customers. The procedures for initiating and completing a typical calibration are described in section 3.5.6. The specific procedures and quality control items related to illuminance responsivity calibrations follows.

Test photometers or illuminance meters are inspected to see if the head has a limiting aperture or a diffuser in front. If the head has neither, and consists of just a photodiode and a $V(\lambda)$ filter, the Photometry project leader will notify the customer by telephone that there will be additional charge for determining the reference plane of the photometer head. The front surface of photometer heads with a limiting aperture should not be cleaned or touched by anything because the edges of the aperture can be easily damaged. If dust particles are seen on the active area of the photometer head, air spray is used at distances greater than 20 cm.

Bare fingers should not touch the front surface of photometer heads with a diffuser, once cleaned. Before and during measurements, photometer heads are not touched with bare hands to avoid heating the photometer, as the responsivity of photometers is temperature dependent. A glove or dry cloth is used to hold the photometer heads. If the photometer head is supplied with a cap, it will be left on except during measurement.

Once the socket is aligned, the check standard lamp is mounted, stabilized, and measured by three of the NIST standard photometers. The check standard lamp shall deviate less than 0.2 % from the running average. Figure 16 shows the result of a check standard over a four month period. After the check standard lamp is validated, the illuminance at a reference point approximately 3.5 m from the lamp is determined by three NIST standard photometers. The photometer head under test is positioned at the same reference point and the readings are recorded. Data are usually taken within 5 min at each illuminance level. During the comparison, the luminous intensity stability of the lamp is monitored by the monitor detector installed in the photometry bench. The ambient temperature during the calibration (usually ≅25 °C) is measured and reported.

When an illuminance meter is calibrated, the errors of the reading at each illuminance level are reported. The meter reading is not adjusted. However, if the illuminance meter is so manufactured that the user can adjust the readings easily, the meter can be adjusted by NIST upon request by customers. In this case the instructions for the reading adjustment should be provided by the customer.

Illuminance meters and illuminance heads can be calibrated for specific sources other than 2856 K source upon request by customers. In this case, the calibration is first performed using the 2856 K source, and then the SMCFs for the specific sources are obtained by the following procedure. The relative spectral responsivity of the illuminance meter or illuminance head is measured by the SCF in the 350 nm to 1100 nm region at 5 nm increments. The monochromator output of the SCF is defocused on the photometer head to irradiate an area of several mm in diameter. The illuminance meter head is underfilled in this case. Measurements are made with the beam incident on several different spots of the receiving surface of the illuminance meter head, and the average is taken. This method can only be applied for illuminance meters whose relative spectral responsivity is fairly uniform over the receiving surface. From the relative spectral responsivity data and the spectral power distribution data (supplied by customer) of any particular light sources to be measured by the illuminance meter, the SMCFs for the particular sources are calculated using Eq. (22). The relative spectral responsivity data and the correction factors are reported to the customer.

3.6.4. Uncertainty of illuminance responsivity calibration

The uncertainty analysis for an illuminance responsivity calibration for an illuminance head that returns a signal that is measured with a digital voltmeter begins with a model expressed as

$$R_{\mathrm{v}} = \frac{(y - y_{\mathrm{d}})}{E_v \cdot G_{\mathrm{f}}} \cdot c_{\mathrm{f}} \quad , \tag{31}$$

where R_v is the illuminance responsivity of the photometer under test, y is the photometer signal and y_d is the dark photometer signal for the photometer under test, E_v is the illuminance, G_f is the gain factor for the photometer under test. Several uncorrelated components of uncertainty have been combined in one factor, c_f. A list of these uncertainty components and relative standard uncertainty are summarized in Table 10. The first component is the uncertainty in the distance between the NIST standard photometer reference plane and the photometer under test reference plane. The second component is the difference in the illuminance uniformity at the reference plane. If the apertures of the photometer under test and the NIST standard photometers are of similar size, the uncertainty is small. The last component is the deviation from the inverse square law of the photometer under test. The deviation from the inverse square law is usually due to an ill-defined photometer reference plane and appears as an inconsistency at two illuminance levels.

Table 10. Uncertainty components as correction factors for illuminance responsivity calibration.

Symbol	Uncertainty component	Type	Relative Unc. Contribution (%)
c_d	Reference plane determination	B	0.10
c_E	Illuminance uniformity	B	0.025
c_L	Lamp short term stability	B	0.015
c_S	Stray light detected by unit under test	B	0.05
c_δ	Detector angular alignment	B	0.02
c_I	Deviation for the inverse square law	B	0.10
$\boldsymbol{c_f}$	**Illuminance responsivity calibration correction factor**		**0.154**

Table 11 summarizes all of the data needed to analyze the uncertainty for an illuminance responsivity calibration which is modeled by Eq. (31) for a typical photometer head in the illuminance range 50 lx to 200 lx. For much lower illuminance levels, the uncertainty of calibration will increase depending on the random noise of the photometers under test.

Table 11. Uncertainty budget for a typical illuminance responsivity calibration.

Symbol	Component	Value x_i	Standard Uncertainty $u(x_i)$	Unit	Type	Sensitivity Coefficient c_i	Unc. Contribution $u_i(y)$
y	Photometer signal	2.6384	0.00035	V	A	5.56×10^{-9}	1.95×10^{-12}
y_d	Photometer dark signal	0.00011	5.20×10^{-7}	V	A	-5.56×10^{-9}	-2.89×10^{-15}
E_v	Illuminance	179.828	0.371	lx	B	-8.16×10^{-11}	-3.03×10^{-11}
G_f	Gain factor	1000010	20	V/A	B	-1.47×10^{-14}	-2.93×10^{-13}
c_f	Correction factor	1.0000	0.00154		B	1.47×10^{-8}	2.26×10^{-11}
$\boldsymbol{R_v}$	**Illuminance responsivity**	$\mathbf{1.467 \times 10^{-8}}$		**A/lx**			$\mathbf{3.78 \times 10^{-11}}$
Relative expanded uncertainty for illuminance responsivity calibration (*k* = 2)							**0.52 %**

The final statement of this calibration would be: The illuminance responsivity of the submitted detector was determined to be 1.467×10^{-8} A/lx with an expanded uncertainty of 7.6×10^{-11} A/lx determined with a coverage factor $k = 2$. The relative expanded uncertainty for this calibration was 0.52 % with a coverage factor $k = 2$.

The uncertainty analysis for an illuminance meter calibration that returns a measurement using a digital display begins with the standard uncertainty for the display illuminance and displayed dark illuminance which is the fluctuation in the reading. However, many illuminance meters will show no fluctuation in the reading. The standard uncertainty is then the precision of the display divided by the square root of three (standard uncertainty for a uniform distribution). If the display precision is 0.1 lx, the standard uncertainty is 0.0577 for the displayed signal and dark signal. The calibration factor presented in the report is the NIST scale divided by the illuminance meter under test scale; therefore, by multiplying the displayed illuminance reading by the calibration factor gives the result scaled to NIST. The illuminance meter alignment uncertainty is typically higher than an illuminance head because of mounting the device reproducibly. Inconsistency of the calibration factors is the range of the calibration factors obtained at the illuminance levels tested. For example, if the calibration factor is 0.999 at 300 lx and 1.005 at 3000 lx, the inconsistency of 0.3 % is added to the uncertainty of the IS factor. The inconsistency is most often caused by the incorrect definition of the reference plane of the illuminance meter since the calibration is conducted at different distances.

3.7. Calibration of high-illuminance photometers

Illuminance meters normally have a measurement range over several orders of magnitude, thus a large calibration range is required. A 1000 W lamp at a distance of 50 cm creates about 5000 lx at CIE Illuminant A and using mirrors behind the lamp can increase the illuminance to 10000 lx. However, calibrations at 100 klx are required for illuminance meters used in the measurement of daylight, solar simulators, lighting optics in imaging devices, and military applications.

In the detector-based method, introduced in the realization of candela and the illuminance calibration work, the illuminance scale is provided by standard photometers, not by standard lamps. Therefore, the calibration sources need not reproduce its light output, and it only needs to be stable during each burning. Thus, various types of light sources other than incandescent standard lamps can be used, if they have appropriate short-term stability, spatial uniformity, and spectral power distributions. The illuminance scale can be extended based on the wide linearity range of the standard photometers.

3.7.1. High-illuminance facility, calibration procedure and quality control

A calibration facility and procedures have been developed at NIST to establish the capability of high illuminance calibrations [53]. The calibration source is based on a modified commercial solar simulator source using a 1000 W Xenon arc lamp with optical feedback control modified to include a $V(\lambda)$-correction filter. Figure 17 shows the configuration of the high illuminance calibration facility. The illuminance level can be varied without changing the color temperature significantly and without changing the distance through the use of interchangeable apertures.

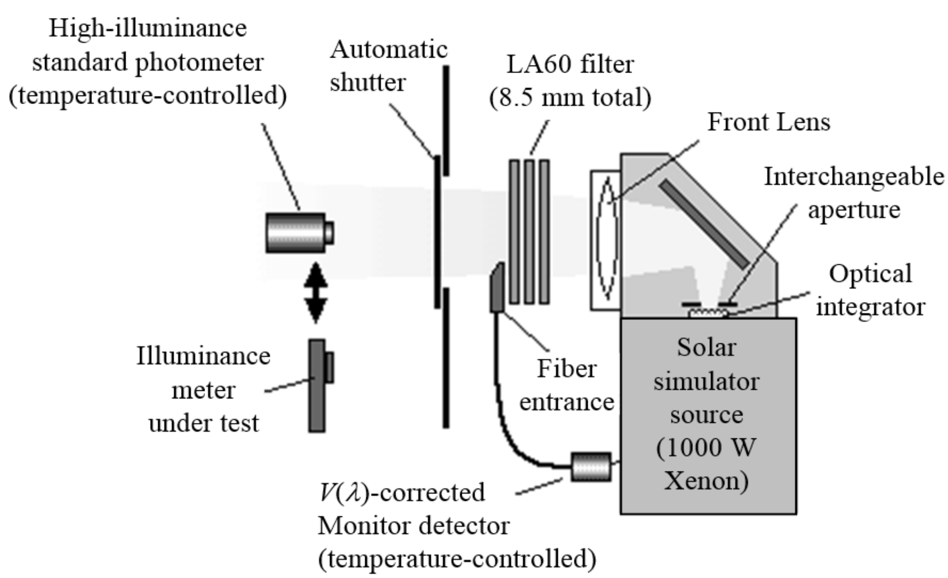

Fig. 17. Configuration of the high illuminance calibration facility.

The solar simulator source has the spectral distribution of a typical xenon lamp, having a correlated color temperature of roughly 6500 K. The source provides an illuminance field of approximately 300 klx in a 10 cm × 10 cm area at a distance of 20 cm to 40 cm from the unit. However, international recommended practice is to use a 2856 K Planckian source (CIE Illuminant A) for calibration of illuminance meters. To meet this requirement, a color correction filter was designed to match the output spectral power distribution to CIE Illuminant A. The optimum thickness of the filters was calculated using the data from the manufacturer. Among many possibilities, HOYA LA60 (16.5 cm × 16.5 cm) was chosen for the appropriate spectral matching and high transmittance. A combination with a heat absorbing filter (HA50) was also included, but without water cooling the heat absorbing filter becomes damaged over time. Figure 18 shows the calculated spectral power distribution of the source and filters. The source configuration was optimized for stability such that from a cold start to the 10 min point the illuminance drops by 0.6 % and the correlated color temperature would decrease 20 K. After 10 min of warm up the illuminance was kept stable within 0.2 % and the correlated color temperature varied by less than 8 K. The illuminance of the source can be set from 10 klx to 70 klx at a correlated color temperature of roughly 2830 K. Another set of filters was designed to produce an illuminance of 100 klx with a quasi Planckian radiation of 3400 K.

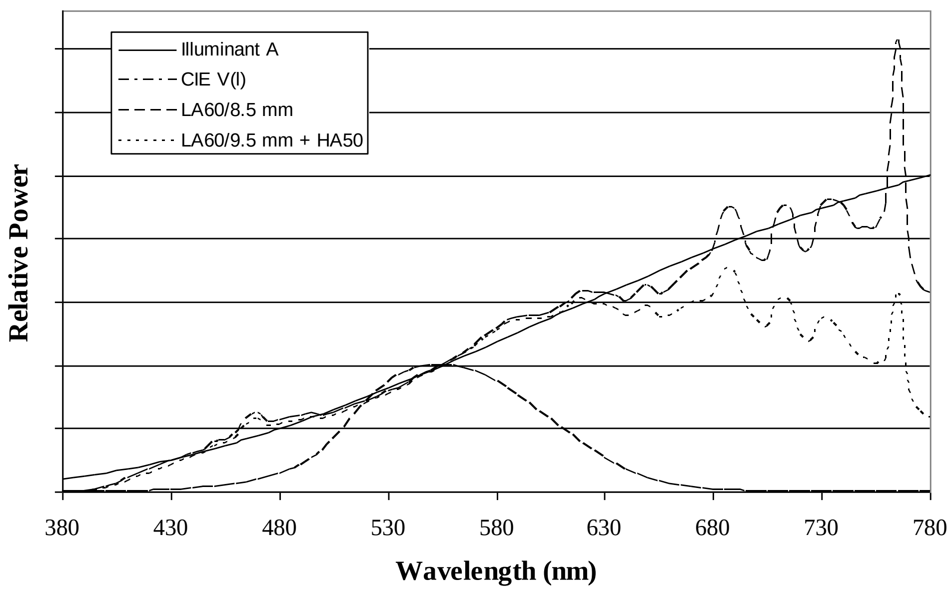

Fig. 18. Calculated spectral power distribution of the source combined with the filters.

Two high-illuminance standard photometers were developed at NIST in order to avoid possible damage to the primary NIST standard photometers. The shutter is always closed except when taking data. The high-illuminance standard photometers are calibrated against the NIST illuminance scale before calibration of the high-illuminance meter under test. The NIST standard photometers are validated against the cross check reference lamp before calibration. Procedurally the NIST high-illuminance standard photometers and the illuminance meter under test are mounted in turn, and the reading is taken with the shutter open for 10 s. This comparison is repeated three times with intervals of more than 2 min. The set of measurements can be repeated for different illuminance levels.

3.7.2. Uncertainty budget for high-illuminance calculations

The uncertainty analysis for a high-illuminance meter calibration begins with the determination of the high-illuminance at the reference plane using the NIST standard high-illuminance photometer. The model equation is the same as Eq. (24). Table 12 summarizes the uncertainty components that are included in the correction factor for the high illuminance determination. Compared to typical uncertainty components for illuminance calibrations additional factors are included for the effects of heating the photometers due to the high flux and the linearity of the detectors.

Table 12. Uncertainty components as correction factors for high-illuminance unit.

Symbol	Uncertainty component	Type	Relative Unc. Contribution (%)
c_T	Photometer temperature correction due to excessive heating	B	0.10
c_G	Photometer transimpedance gain amplifier correction	B	0.02
L_f	Long-term stability of the standard photometers	B	0.15
c_γ	Photometer alignment	B	0.002
c_y	Digital voltmeter calibration	B	0.004
F^*	SMCF	B	0.05
c_S	Spatial stray light	B	0.10
c_γ	Photometer alignment	B	0.002
$\boldsymbol{c_f}$	**NIST high-illuminance unit correction factor**		**0.213**

The uncertainty budget for the NIST high-illuminance unit is summarized in Table 13 based on the model Eq. (24). The relative standard uncertainty for the average signal voltage, y, is 0.01 %. The dark signal, y_d, which is the dark output voltage typically from unbalanced offset voltage of the transimpedance operational amplifier, is measured by closing the shutter between lamp and photometer. The relative expanded uncertainty for the NIST high-illuminance unit is 0.49 % (k = 2).

Table 13. Uncertainty budget for the NIST high-illuminance unit.

Symbol	Component	Value x_i	Standard Uncertainty $u(x_i)$	Unit	Type	Sensitivity Coefficient c_i	Unc. Contribution $u_i(y)$
y	Photometer signal	2.294×10^{-4}	1.01×10^{-8}	A	A	9.88×10^{7}	1.09
y_d	Photometer dark signal	-5.01×10^{-9}	6.11×10^{-11}	A	A	-9.88×10^{7}	-0.01
$s_{v,i}$	Illuminance responsivity	1.0118×10^{-8}	1.92×10^{-11}	A/lx	B	-2.24×10^{12}	-43.03
c_f	Correction factor	1.000	0.00213		B	26676	48.30
$\boldsymbol{E_v}$	**High-illuminance unit**	**26676**		**lx**			**64.7**
Relative expanded uncertainty for high-illuminance unit (*k* = 2)							**0.49 %**

The uncertainty analysis for a high-illuminance meter calibration that returns a measurement using a digital display begins with the standard uncertainty for the display illuminance and displayed dark illuminance which is the fluctuation in the reading. However, many high-illuminance meters will show no fluctuation in the reading. The standard uncertainty is then the precision of the display divided by the square root of three (standard uncertainty for a uniform distribution). The calibration factor presented in the report is the NIST scale divided by the high-illuminance meter under test scale; therefore, by multiplying the displayed illuminance reading by the calibration factor gives the result scaled to NIST. The high-illuminance meter alignment uncertainty is typically higher than a high-illuminance head because of mounting the device reproducibly. Inconsistency of the calibration factors is the range of the calibration factors obtained at the high-illuminance levels tested. The inconsistency is most often caused by the incorrect definition of the reference plane of the high-illuminance meter since the calibration is conducted at different distances.

The model for the high-illuminance meter calibration is expressed as

$$R_f = \frac{(Y - Y_d)}{E_v} \cdot c_f \quad , \tag{32}$$

where Y is the displayed photometer reading and Y_d is the dark photometer reading for the photometer under test, and E_v is the illuminance. Several uncorrelated components of uncertainty have been combined in one factor, c_f. A list of these uncertainty components and relative standard uncertainty are summarized in Table 14. The first component is the uncertainty in the distance between the NIST standard photometer reference plane and the photometer under test reference plane. The second component is the difference in the illuminance uniformity at the reference plane. The last component is the deviation from the inverse square law of the photometer under test.

Table 14. Uncertainty components for high-illuminance calibration factor.

Symbol	Uncertainty component	Type	Relative Unc. Contribution (%)
c_d	Reference plane determination	B	0.10
c_E	High illuminance source uniformity	B	0.15
c_L	High illuminance source short term stability	B	0.10
c_S	Stray light detected by unit under test	B	0.10
c_δ	Detector under test angular alignment	B	0.08
c_I	Deviation for the inverse square law	B	0.35
$\boldsymbol{c_f}$	**Illuminance responsivity calibration correction factor**		**0.426**

Table 15 summarizes the uncertainty budget for the determination of a high-illuminance calibration factor of an illuminance meter in a 10,000 lx to 70,000 lx range.

Table 15. Uncertainty budget for a typical high-illuminance calibration factor determination.

Symbol	Component	Value x_i	Standard Uncertainty $u(x_i)$	Unit	Type	Sensitivity Coefficient c_i	Unc. Contribution $u_i(y)$
Y	Photometer reading	26400	57.7	lx	A	3.75×10^{-5}	0.00216
Y_d	Photometer dark reading	0	57.7	lx	A	-3.75×10^{-5}	-0.00216
E_v	Illuminance	26676	64.7	lx	B	-3.71×10^{-5}	-0.00240
c_f	Correction factor	1.000	0.00426		B	0.9897	0.00420
$\boldsymbol{R_f}$	**Calibration factor**	**0.9897**					**0.0057**
Relative expanded uncertainty for high-illuminance calibration factor (*k* = 2)							**1.2 %**

The display resolution, the SMCF for the device under test, the drift due to heating of the device under test, and the nonlinearity of the response at different illuminance levels all depend on the capabilities of the high-illuminance meter that is submitted to NIST for calibration. For example, the spatial non-uniformity factor depends on the illuminance field of the source, shown in Figure 19, and the relative sizes of the apertures of the NIST high-illuminance photometers and the high-illuminance meter under test. Another important aspect is the display resolution. For example, if the precision of the display is 100 lx; the standard deviation of the photometer readings, Y and Y_d, is 57.7 lx.

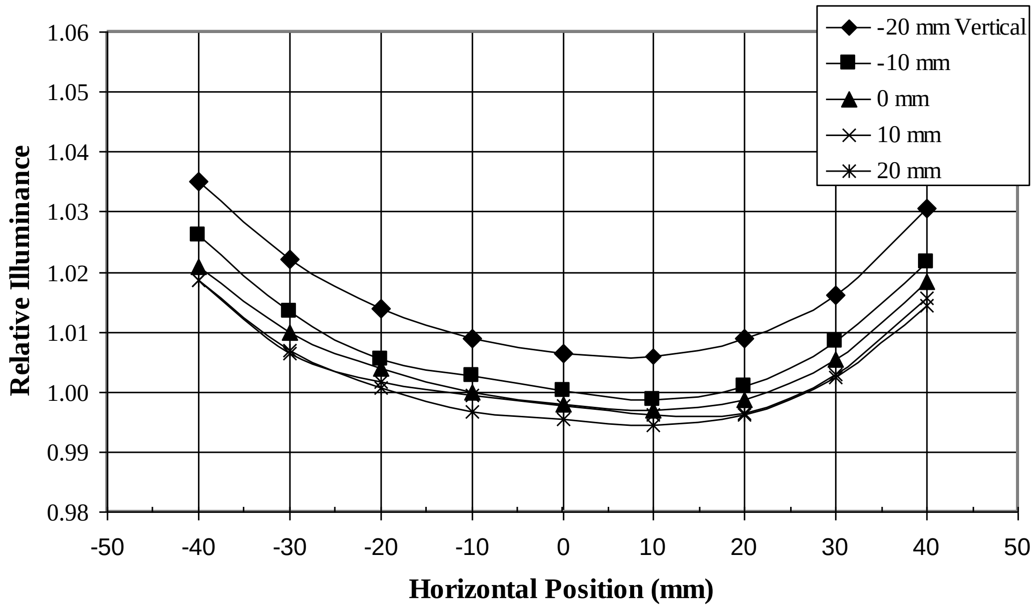

Fig. 19. Spatial non-uniformity of illuminance at 30 cm from the front lens.

From a practical point of view, the CIE Illuminant A need not be used in all calibration cases. Illuminance meters are best calibrated with the same type of source for which the meters are used. For specific purposes, such as for solar irradiance measurements, illuminance meters can be calibrated for the xenon spectrum, which is similar to the CIE D65.

4. Total luminous flux calibrations

4.1. Principles of the absolute integrating sphere method

Traditionally, the luminous flux unit is realized using goniophotometers [54]. It is often difficult, however, to build and maintain high accuracy goniophotometers which require a large dark room and costly high-precision positioning mechanisms. The measurements are also time-consuming, resulting in longer burning times for the lamps.

To alleviate these difficulties, an alternative method, the AIS (Absolute Integrating Sphere) Method has been developed at NIST using an integrating sphere with an external source [30-34]. The total flux of a lamp inside the sphere is calibrated against the known amount of flux coming into the sphere from the external source through a precision aperture. The luminous flux $\Phi_{v,e}$ (lm) from the external source introduced into the sphere is given by

$$\Phi_{v,e} = E_a A \ , \tag{33}$$

where E_a is the average illuminance (lx) over the limiting aperture of known area A. The internal source or the external source is turned on alternately. The introduced flux $\Phi_{v,e}$ is used as a reference, and the luminous flux of the internal source $\Phi_{v,i}$ is measured in comparison with the flux $\Phi_{v,e}$ as given by

$$\Phi_{v,i} = c\Phi_{v,e} y_i / y_e \ , \tag{34}$$

where y_i is the detector current for the internal source, y_e is that for the external source, and c is a correction factor containing many components described in Section 4.3. This method has the advantage that a conventional integrating sphere can be used with minor modifications. Measurements are accomplished faster, resulting in shorter burning times for the lamps. Corrections are needed for the spatial non-uniformity and the incident angle dependence of the sphere response and the spectral mismatch of the integrating sphere system. The NIST luminous flux unit has been maintained using the integrating sphere method since 1995, and is directly tied to the NIST detector-based candela established in 1992.

The AIS Method has been applied to the NIST 2.5 m integrating sphere facility. Calibrations are based on the illuminance measurement of an external source with standard photometers, thereby introducing a detector-based procedure for the total luminous flux calibration. A higher accuracy is achieved as the calibration chain is shortened with the standard lamps and the transfer process eliminated. The AIS method provides an advantage of automatically correcting for the self-absorption of the test lamps and the drift of the sphere responsivity during the measurement session. The process of the realization of the lumen and subsequent recalibration of many working standard lamps are no longer necessary. Instead, the standard photometers are to be calibrated periodically to maintain the unit.

4.2. Design of the NIST 2.5 m Integrating Sphere Facility

Figure 20 shows the geometry of the NIST 2.5 m integrating sphere. The sphere is coated with a barium-sulfate-based coating having a reflectance of approximately 98 % in the visible region. The high-reflectance coating was selected for better spatial uniformity of the sphere responsivity. The baffle surfaces are coated with the same material. The sphere basically consists of a photometer head, two baffles, an external source system, and a lamp holder. Two baffles are used to shield the detector and the opening from direct illumination by the internal source. Baffle 1 (20 cm in diameter) is normally located at 62 cm from the photometer head, but its position is moveable. Baffle 2 (15 cm in diameter) is placed as close to the opening as possible (28 cm from the opening) while not intercepting the external beam. The detector is exposed to the first reflection of the introduced flux from the external source in order to equalize the sphere responsivity for the internal source and that for the external source. The lamp holder can be mounted from the top or the bottom of the sphere to allow base-up or base-down operation of the lamp. A four-pole screw-base socket or other special socket including one for the 122 cm (4 foot) linear fluorescent lamps is attached to the lamp holder.

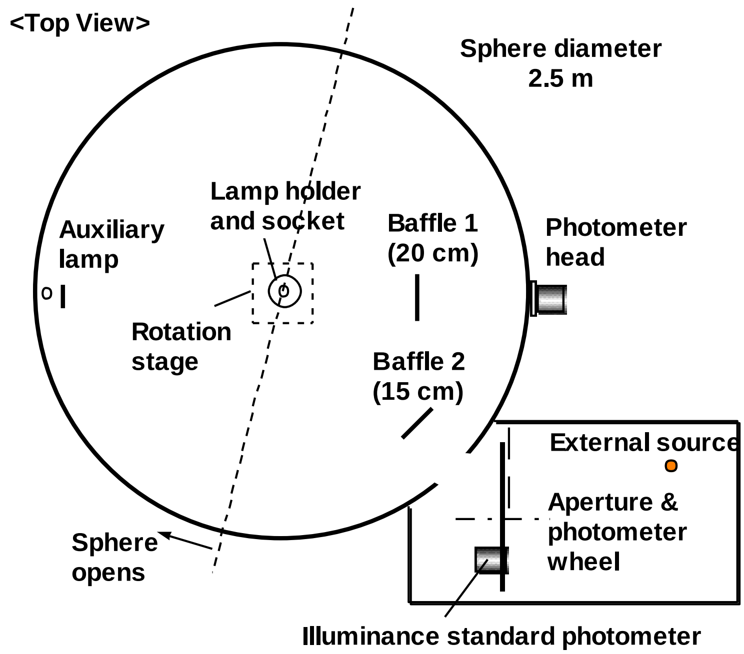

Fig. 20. Arrangement of NIST 2.5 m integrating sphere for detector-based total luminous flux calibrations.

The external source system employs an aperture/photometer wheel at the sphere opening, which is computer-controlled and has four positions. A precision aperture (40 mm or 50 mm in diameter) is mounted in one position, and a black mask in another position that works as a shutter to block the incoming beam. The wheel is placed as close to the sphere opening as possible to minimize diffraction losses. The other two positions are used to mount the standard photometers to measure the illuminance at the center of the aperture. These standard photometers are aligned so that their reference planes coincide exactly with that of the aperture (within ± 0.5 mm). The photometers are temperature-controlled, are known to have a long-term stability better than 0.1 % per year, and are annually calibrated against the NIST illuminance unit. A frosted-bulb, 1000 W FEL-type lamp, operated at 2856 K, is used as a light source, placed at 1 m from the aperture. A diode laser is used to align the orientation of the lamp to reproduce the illuminance distribution. The illuminance at the aperture is about 1100 lx, and the introduced luminous flux is approximately 2 lm. The sphere photometer signal for this external flux has a typical RMS (root mean square) noise level of 0.01 %.

The photometer for the integrating sphere is a temperature-monitored type of the same design as one used in the realization for the candela but equipped with a surface-ground opal glass for cosine response. The photometer head is mounted so that the opal surface is flush with the sphere-coating surface. The photometer response together with its built-in amplifier has been verified to be linear to within 0.03 % up to 10^{-4} A of its output current.

4.3. Uncertainty of the NIST sphere photometer system responsivity

The calibration of total luminous flux for light sources is based on determining the responsivity of the sphere system. The sphere responsivity is modeled as follows.

$$R_{\mathrm{sph}} = \frac{(y_{\mathrm{ext}} - y_d)}{E_{\mathrm{C}} \cdot A} \cdot c_{\mathrm{f}} \quad , \tag{35}$$

where y_{ext} and y_{d} is the signal and dark signal from the sphere photometer, E_{c} is the illuminance on the wheel reference plane, and A is the area of the precision aperture. Several uncorrelated components of uncertainty have been combined in one factor, c_{f}. A list of these uncertainty components and relative standard uncertainty are summarized in Table 16. The determination of these uncertainty components is described in the following sections.

Table 16. Uncertainty components for sphere photometer.

Symbol	Uncertainty component	Type	Relative Unc. Contribution (%)
c_{T}	Photometer temperature correction	B	0.05
c_{G}	Photometer transimpedance gain amplifier correction	B	0.02
c_y	Digital voltmeter calibration	B	0.008
F^*	External source SMCF	B	0.05
c_{w}	Temperature dependence of sphere wall	B	0.03
ρ	Incident angle correction	B	0.03
k_{a}	Average illuminance correction	B	0.02
c_{U}	External source spatial non-uniformity	B	0.05
c_{S}	Spatial stray light	B	0.03
$\boldsymbol{c_{\mathrm{f}}}$	**Sphere photometer responsivity correction factor**		**0.105**

4.3.1. Temperature dependence

The sphere photometer is temperature monitored but is not temperature controlled. The temperature coefficients, c_{p}, for the eight photometers range from -0.049 %/°C to -0.088 %/°C. Whenever the photometers are used, the temperature correction factor, c_{T}, is given by Eq. (12), and the output signal is multiplied by this correction factor. The following sections describe specific measurements to determine the magnitude of the other correction factors or quantities and the uncertainty of those correction factors.

The flux level of lamps under test (100 lm to 25000 lm) and that of the external beam differ by a few orders of magnitude. The measurements results are susceptible to errors due to the effect of heat by the lamp under test on the sphere system. A technique (referred to as the

AC/DC technique [55]) was used to measure the integrating sphere characteristics while the lamp under test is operated. A chopper is inserted in the beam path of the external source causing the light to be chopped at 90 Hz. When the internal lamp is turned on in the sphere, the AC signal from the chopped external beam is superimposed on the DC signal from the internal lamp. The AC signal is very small, typically 10^{-3} of the DC signal, a lock-in amplifier is used to separate and measure the AC signal with a sufficient signal-to-noise ratio. The AC signal is monitored simultaneously with the DC signal when the internal lamp is on and off. Any change of the AC signal when turning on the internal lamp indicates a change of the sphere responsivity. The cause of the change can be thermal effects by the internal lamp on the sphere coating and/or the photometer head, and/or change of the self-absorption of the internal lamp (which is not well known). Figure 21 shows the result of the AC/DC measurement of the NIST integrating sphere with a 1000 W tungsten halogen lamp (25000 lm) operated inside the sphere. Although the noise of the AC signal is high when the internal lamp is on, the average level of the signal stays near constant. No obvious sudden change of the AC signal is observed, which verifies the linearity of the photometer head. A slight gradual change (0.02 % to 0.03 %) is observed, which is negligible in most cases.

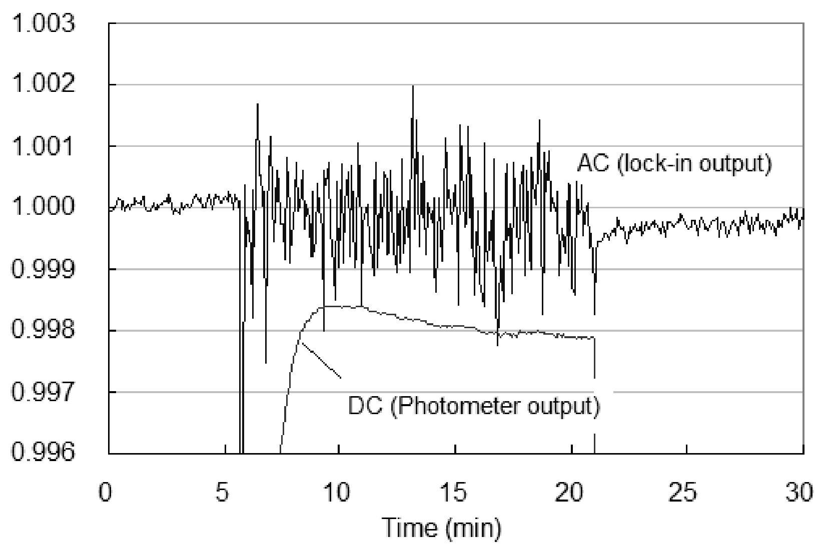

Fig. 21. Results of the AC/DC measurement of the NIST integrating sphere with a 1000-W tungsten lamp operated in the sphere.

4.3.2. Sphere photometer system SMCF

The spectral power distribution of the internal source may be different from that of the external source, and a SMCF is needed. The SMCF, F^* of the external source against the Illuminant A is given by.

$$F^*\left(s_{\mathrm{e}}(\lambda)\right)=\frac{\dfrac{\int_\lambda s_{\mathrm{A}}(\lambda)s_{\mathrm{rel,e}}(\lambda)\mathrm{d}\lambda}{\int_\lambda s_{\mathrm{A}}(\lambda)V(\lambda)\mathrm{d}\lambda}}{\dfrac{\int_\lambda s_{\mathrm{e}}(\lambda)s_{\mathrm{rel,e}}(\lambda)\mathrm{d}\lambda}{\int_\lambda s_{\mathrm{e}}(\lambda)V(\lambda)\mathrm{d}\lambda}}, \qquad (36)$$

where $s_{\mathrm{e}}(\lambda)$ is the relative spectral power distribution of the external source, $s_{\mathrm{A}}(\lambda)$ is that of the Illuminant A, $V(\lambda)$ is the spectral luminous efficiency function, and $s_{\mathrm{rel,e}}(\lambda)$ is the relative spectral responsivity of the sphere system. $s_{\mathrm{rel,e}}(\lambda)$ can be obtained by measuring the relative spectral responsivity of the detector $R_{\mathrm{d}}(\lambda)$, and the relative spectral throughput of the integrating sphere $T_{\mathrm{s}}(\lambda)$ as

$$s_{\mathrm{rel,e}}(\lambda)=R_{\mathrm{d}}(\lambda)\cdot T_{\mathrm{s}}(\lambda)\ . \qquad (37)$$

The relative spectral throughput $T_{\mathrm{s}}(\lambda)$ of the sphere was obtained using a spectroradiometer by taking the ratios of the spectral irradiance on the detector port of the sphere (in which a 500 W clear-bulb flux standard lamp was operated) and the spectral irradiance of the same lamp measured on the photometry bench. The relative spectral responsivity $R_{\mathrm{s}}(\lambda)$ of the total integrating sphere system was then obtained using Eq. (37). Since the SMCF is based on two ratio measurements, the major uncertainty components are the noise of the spectrometer and the wavelength calibration of the spectrometer.

4.3.3. Spatial non-uniformity correction factor

The spatial response distribution function (SRDF), $K(\theta, \varphi)$, is the spatial distribution of the relative sphere responsivity over the sphere wall including baffle surfaces, and is measured by scanning a narrow beam in the sphere. The integrating sphere is equipped with computer-controlled rotation stages on the top and the bottom of the sphere, which can rotate the lamp holder horizontally. At the lamp socket, another small rotation stage is mounted and rotates the beam source vertically. The beam source is scanned over the 4π solid angle. The beam source consists of a vacuum miniature lamp and a lens. A vacuum lamp is used to make the source insensitive to its burning position. The lens was used to keep the flux level as high as possible while minimizing the flux leaking outside the beam angle (approximately 5°). The total luminous flux of the beam is approximately 0.1 lm, with 97 % of the flux within the beam angle. The SRDF of the integrating sphere was measured at 5° intervals for both the azimuth angle (φ) and elevation angle (θ), and plotted as a three-dimensional chart in Figure 22. Prior to each vertical scan, the beam position was moved to a reference point so that the stability of the beam source could be monitored and corrections applied for the drift of the lamp. In Figure 22, $\theta = 0°$ at the top and $\theta = 180°$ at the bottom of the sphere, and $\varphi = 0°$ or 360° is the plane where the photometer head is located. Various structures in the sphere are seen in the data: the effect of Baffle 1 at $(\theta, \varphi) = (90°, 0°)$ and (90°, 360°), the shadow of Baffle 1 and the lamp post at $\varphi = 180°$, and the hemisphere joints (grooves at $\varphi = 70°$ and 250°). It is also observed that the responses in the upper hemisphere appear slightly lower than in the lower hemisphere. The overall uniformity of the NIST integrating sphere is considered excellent.

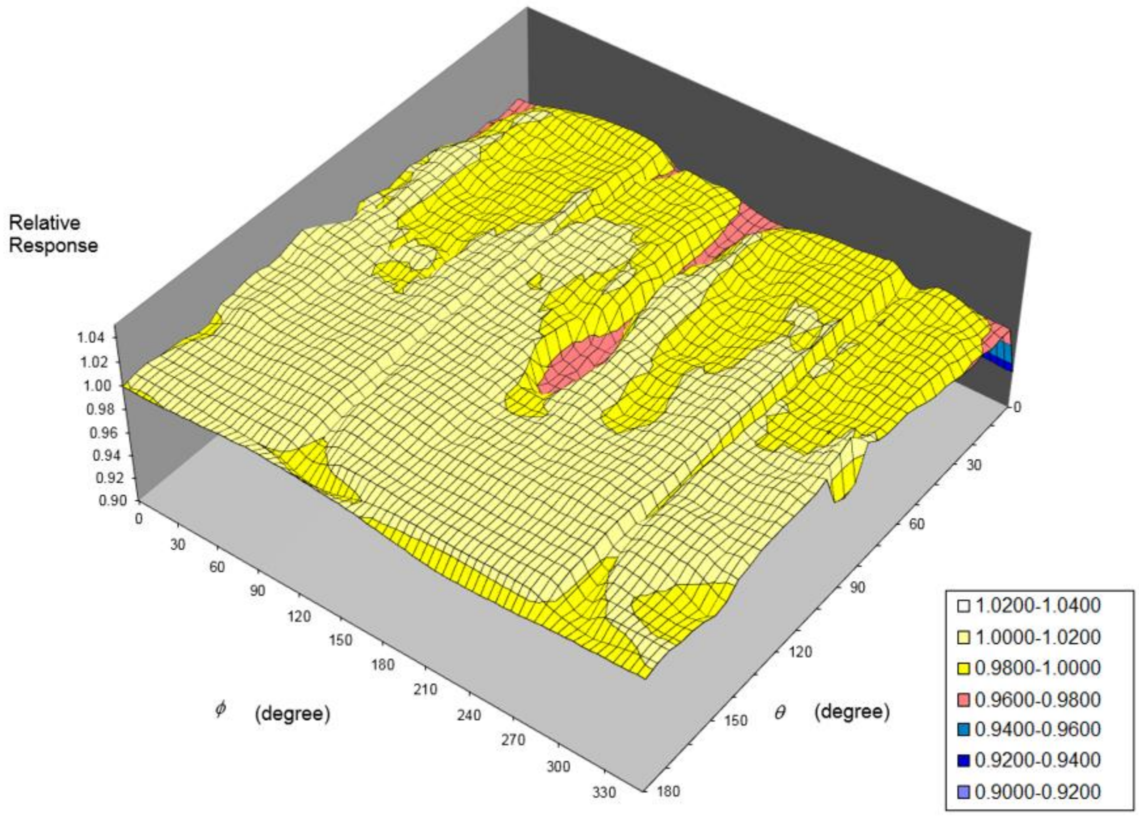

Fig. 22. Mapping of NIST 2.5 m integrating sphere responsivity (normalized SRDF).

To calculate the spatial correction factor, $K(\theta, \varphi)$ is normalized for the sphere response to an isotropic point source. The normalized SRDF, $K^*(\theta, \varphi)$, is defined as

$$K^*(\theta,\phi) = \frac{4\pi K(\theta,\phi)}{\int_{\phi=0}^{2\pi}\int_{\theta=0}^{\pi} K(\theta,\phi)\sin\theta d\theta d\phi} \,. \tag{38}$$

Using $K^*(\theta, \varphi)$, the spatial correction factor $S_{f,e}$ for the external source with respect to an isotropic point source is given by

$$S_{\mathrm{f,\,e}} = \frac{1}{K^*(\theta_e, \phi_e)}\ . \tag{39}$$

The area ± 5° around the hot spot (the area where the external beam hits the sphere wall) was further mapped at 1° intervals to determine the sphere responsivity for the hot spot. The spatial non-uniformity correction factor for the external beam was determined to be 0.9992 and is measured on an annual basis as part of the scale realization. The standard uncertainty of this measurement is 0.05 % and the annual stability of this correction factor is 0.05 %.

4.3.4. Incident angle correction factor

The light from the lamp under test is incident normal to the sphere wall, while light from the external source is incident at 45°. When the incident angle deviates from these values, the diffuse reflectance of the sphere coating changes [56], which affects the sphere response. The incident angle correction factor was measured by positioning the beam source at the center of the sphere, illuminating the hot spot, and measuring the sphere photometer response, $y_0(\theta_\mathrm{e}, \varphi_\mathrm{e})$. The beam source is moved to illuminate the hot spot along the axis of external source illumination without opening the sphere, and the sphere photometer response, $y_{45}(\theta_\mathrm{e}, \varphi_\mathrm{e})$, is measured. The ratio of the two measurements is the incident angle correction factor, 0.9993 with a standard uncertainty of 0.0003.

4.3.5. Illuminance on the reference plane of the aperture and photometer wheel

The illuminance on the aperture from the external source is determined by two photometers that are calibrated against the NIST standard photometers. The uncertainty analysis of the illuminance measurement follows the model.

$$E_\mathrm{c} = \left[\left(\frac{y_1}{R_1}\right)\left(\frac{d_0}{d_0+\Delta d_1}\right)^2\left(\frac{2856\mathrm{K}}{T_\mathrm{d}}\right)^\alpha + \left(\frac{y_2}{R_2}\right)\left(\frac{d_0}{d_0+\Delta d_2}\right)^2\left(\frac{2856\mathrm{K}}{T_\mathrm{d}}\right)^\beta\right]\frac{c_\mathrm{R}\cdot c_\mathrm{f}}{2}\ , \tag{40}$$

where y_1 and y_2 is the signal from the standard photometers, R_1 and R_2 is the illuminance responsivity of the two standard photometers, d_0 is the distance from the aperture to the external source, Δd_1 and Δd_2 is the difference between the distance from the photometer reference plane to the external source and d_0, T_d is the color temperature of the external source, and α and β are the exponential dependence of the spectral mismatch for the photometers. To remove the correlation between R_1 and R_2 the scale uncertainty has been separated into a correction factor, c_R. Several uncorrelated components of uncertainty have been combined in one factor, c_f. A list of these uncertainty components and relative standard uncertainty are summarized in Table 17. As shown in Table 18, which summarizes the uncertainty budget for the illuminance measurement on the reference plane of the aperture and photometer wheel, the distance from the external source to the aperture does not need to be determined accurately because it is a ratio in the model. The important distance aspect is setting the reference plane of the standard photometers at the same distance as the aperture. To approximate the sensitivity coefficient for d_0, the standard uncertainty for Δd_1 and Δd_2

was used instead of zero. This approximation was also used for T_d in the calculation of the sensitivity coefficients for the α and β.

Table 17. Uncertainty components for sphere external illuminance.

Symbol	Uncertainty component	Type	Relative Unc. Contribution (%)
c_T	Photometer temperature correction	B	0.005
c_G	Photometer transimpedance gain amplifier correction	B	0.02
c_y	Digital voltmeter calibration	B	0.008
c_L	Long-term stability of the photometers	B	0.05
c_γ	Angular alignment of the standard photometers	B	0.002
c_x	Stability of the external source	B	0.01
c_S	Spatial stray light	B	0.025
$\boldsymbol{c_f}$	**Sphere external illuminance correction factor**		**0.061**

The correction factor for the distribution temperature of the external source is a useful method over a small range of distribution temperatures. As shown in Table 18 the exponential dependence for the standard photometers is nearly zero. Additionally, since the standard photometers are constantly temperature controlled, the long-term stability and temperature dependence have much smaller uncertainties than the temperature monitored NIST standard photometers.

As shown in Table 18, which summarizes the uncertainty budget for the illuminance measurement on the reference plane of the aperture and photometer wheel, the distance from the external source to the aperture does not need to be determined accurately because it is a ratio in the model. The important distance aspect is setting the reference plane of the standard photometers at the same distance as the aperture. To approximate the sensitivity coefficient for d_0, the standard uncertainty for Δd_1 and Δd_2 was used instead of zero. This approximation was also used for T_d in the calculation of the sensitivity coefficients for the α and β.

Table 18. Uncertainty budget for a sphere external illuminance determination.

Symbol	Component	Value x_i	Standard Uncertainty $u(x_i)$	Unit	Type	Sensitivity Coefficient c_i	Unc. Contribution $u_i(y)$
y_1	1st photometer signal	1.8423×10^{-5}	9.0×10^{-9}	V	A	6.19×10^{6}	0.056
y_2	2nd photometer signal	1.6064×10^{-5}	3.0×10^{-9}	V	A	7.10×10^{6}	0.021
R_1	Responsivity 1st photometer	8.081×10^{-8}	4.0×10^{-11}	V/lx	B	-1.41×10^{9}	-0.056
R_2	Responsivity 2nd photometer	7.043×10^{-8}	3.5×10^{-11}	V/lx	B	-1.62×10^{9}	-0.057
d_0	Photometer-lamp distance	1.0000	0.0005	m	B	0.0912	0.000
Δd_1	Photometer 1st ref. plane	0.0000	0.0002	m	B	-227.98	-0.046
Δd_2	Photometer 2nd ref. plane	0.0000	0.0002	m	B	-228.08	-0.046
T_d	Color temperature	2856	4	K	B	1.12×10^{-3}	0.004
α	1st photometer T_d dep.	-0.014	0.050		B	-0.1595	-0.008
β	2nd photometer T_d dep.	-0.014	0.050		B	-0.1596	-0.008
c_R	Illuminance scale factor	1.000	0.0019		B	228.03	0.422
c_f	Correction factor	1.000	0.00061		B	228.03	0.139
$\boldsymbol{E_C}$	**Sphere external illum.**	**228.03**		**lx**			**0.46**
Relative expanded uncertainty for sphere external illuminance calibration factor (k = 2)							**1.2 %**

The correction factor for the distribution temperature of the external source is a useful method over a small range of distribution temperatures. As shown in Table 19 the exponential dependence for the standard photometers is nearly zero. Additionally, since the standard photometers are constantly temperature controlled, the long-term stability and temperature dependence have much smaller uncertainties than the temperature monitored NIST standard photometers.

Table 19. Uncertainty budget for a NIST sphere photometer system responsivity.

Symbol	Component	Value x_i	Standard Uncertainty $u(x_i)$	Unit	Type	Sensitivity Coefficient c_i	Unc. Contribution $u_i(y)$
y_{ext}	Sphere photometer signal	1.0274×10^{-8}	3.0×10^{-12}	A	A	2.237	6.71×10^{-12}
y_d	Sphere photometer dark	8.0×10^{-12}	8.0×10^{-14}	A	A	-2.237	-1.79×10^{-13}
E_C	External illuminance	228.03	0.453	lx	B	-1.0×10^{-10}	-4.56×10^{-11}
A	Aperture area	0.00196	3.0×10^{-8}	m^2	B	-1.2×10^{-5}	-3.52×10^{-13}
c_f	Correction factor	0.9990	0.00105		B	-2.3×10^{-8}	-2.41×10^{-11}
$\boldsymbol{R_{sph}}$	**Sphere responsivity**	$\mathbf{2.297 \times 10^{-8}}$		**A/lm**			$\mathbf{5.21 \times 10^{-11}}$
Relative expanded uncertainty for NIST sphere photometer responsivity (k = 2)							**0.45 %**

4.3.6. Average illuminance correction factor

The illuminance distribution over the aperture area is slightly non-uniform. The standard photometers in the aperture wheel have an aperture size of 10 mm. The size of the aperture is 50 mm. The illuminance distribution over the precision aperture area was measured by spatially scanning the transfer photometer to determine the average illuminance factor, k_a, which is a ratio of the average illuminance E_a to the illuminance on the aperture center, E_c. Once k_a is determined, only E_c needs to be measured to obtain E_a. For the NIST illuminance wheel the average illuminance correction factor is 0.9995 with a standard uncertainty of 0.0002.

4.3.7. Uncertainty budget for the NIST sphere photometer system responsivity

Table 19 summarizes the uncertainty analysis and budget for the NIST sphere photometer system calibration session to validate the measurements. The control limits for the validation standards are equivalent to the uncertainty of the components that are not directly related to the scale.

4.4. Total luminous flux and artifacts for calibration

For many years NIST has issued gas-filled, incandescent lamps (100 W, 200 W, 500 W, and 1000 W) with medium screw base or mogul screw base and miniature lamps ranging from 1.2 W to 30 W as luminous flux transfer standards. These lamps and other standard quality incandescent lamps, including miniature lamps, ranging from 0.1 lm to 105 lm are accepted for calibration at NIST. Linear 4-foot fluorescent lamps of any color submitted by customers are also accepted for calibration at NIST. For miniature lamps, the size of the sockets tends to be much larger relative to the size of the lamps. When a miniature lamp is mounted in a socket, the total flux may decrease significantly due to the absorption by the socket surfaces.

Sometimes miniature lamps are calibrated in combination with a particular socket, and in such cases, a combination of lamp and socket is required as a calibration artifact.

At the moment, NIST does not provide luminous flux standard lamps due to unavailability of standard quality lamps, although a search for commercially available lamps for this purpose is underway. When lamps are submitted to NIST for calibration, the lamps must be seasoned and tested for stability by the customer. Procedures for the seasoning of lamps are described in LM-54 [57]. The operating current, or operating color temperature, and burning position must be specified by the customer.

As with other standard lamps, care must be shown in the handling of luminous flux lamps. Lamps should be handled very carefully to avoid mechanical shocks to the filament, and the bulb of the lamps should not be touched with bare hands. Before calibration, the bulb of the lamps should be cleaned with a soft, lint-free cloth to remove any dust from the packing material. Lamps should be kept in a container when not used.

The model equations and operation specifics for three types of lamps NIST calibrates, approximately isotropic incandescent lamps, linear fluorescent tubes and reflector lamps are presented in the following sections.

4.4.1. Incandescent lamps – Typical budget

All incandescent lamps are operated at a specified current rather than a specified voltage because the lamp voltage, in general, does not reproduce well due to the construction of the sockets used among customers. However, lamp voltages reproduce fairly well on the same socket, and the lamp voltage is a useful indicator of changes in the lamps.

The NIST absolute integrating sphere can be equipped with a medium screw base socket, mogul screw base socket, medium bi-post base socket, or a special small socket (top surface is 3 mm in diameter) for miniature lamps with leads. These are four-pole sockets, which have four separate wires, two for the current supply and the other two for voltage measurements. For total luminous flux calibration, the lamp voltage is reported, only for reference purposes, without an uncertainty value.

A DC constant-current power supply is used to operate standard lamps and test lamps. The lamp current is measured as the voltage across a reference current shunt (0.1 Ω), using a 6-1/2 digit voltmeter with a stated uncertainty better than 0.01 %. The current shunt is periodically calibrated with an uncertainty of 0.005 %. The lamp current is automatically controlled by a computer feedback system to keep the current drift within ± 0.002 %. The power supply is operated in an external control mode, in which the output current is regulated by an external reference voltage. The external voltage is supplied by two 12 bit D-to-A converters (giving 23 bits of resolution), which is controlled by the computer.

Incandescent lamps are operated in the sphere center with the base up position unless otherwise stated. The lamps are operated at the lamp current or at the color temperature specified by the customer. When the color temperature is specified, the lamp current is first determined by color temperature measurements as described in Section 6. When the lamp current is specified, the color temperature of the lamp is measured and reported together with the luminous flux value. The lamps are allowed to stabilize, usually for 10 min. The color temperature values are used for the SMCFs. The lamp current is ramped up and down slowly (approximately 30 s). Photometric measurements are made after the lamp has stabilized.

The model for the total luminous flux calibration of incandescent lamps is expressed as

$$\Phi_{\text{test}} = \frac{(y - y_{\text{d}})}{R_{\text{sph}}} \cdot \left(\frac{U \cdot c_U}{J_0 \cdot R} \right)^{m_{\text{J}}} c_{\text{f}} , \tag{41}$$

where y is the sphere photometer signal [A], y_{d} is the dark sphere photometer signal [A], R_{sph} is the photometric responsivity of the sphere photometer system [A/lm], U is the voltage measured across the shunt resistor for the measurement of current, J_0 is the calibrated current for the lamp, R is the resistance of the shunt resistor, and m_{J} is the exponential dependence of the lamp luminous flux with respect to the operating current. Several uncorrelated components of uncertainty have been combined in one factor, c_{f}. A list of these uncertainty components and relative standard uncertainty are summarized in Table 20.

Table 20. Uncertainty components for total flux calibration.

Symbol	Uncertainty component	Type	Relative Unc. Contribution (%)
c_{N}	Near-field absorption losses	B	0.01
c_{T}	Sphere photometer temperature correction	B	0.05
c_{G}	Photometer transimpedance gain amplifier correction	B	0.02
c_y	Digital voltmeter calibration	B	0.008
c_{W}	Sphere wall temperature dependence	B	0.03
F^*	Source SMCF	B	0.05
S_{f}	Source spatial non-uniformity correction	B	0.02
c_{S}	Spatial stray light	B	0.05
$\boldsymbol{c_{\text{f}}}$	**Incandescent lamp total flux correction factor**		**0.097**

The spatial non-uniformity correction factor for the internal source with respect to an isotropic point source is given by,

$$S_{\text{f}} = 1 \Big/ \int_{\phi=0}^{2\pi} \int_{\theta=0}^{\pi} I^*(\theta,\phi) K^*(\theta,\phi) \sin\theta d\theta d\phi , \tag{42}$$

where $K^*(\theta, \varphi)$ is defined by Eq. (38) and $I^*(\theta, \varphi)$ is the normalized luminous intensity distribution of the internal source as given by

$$I^*(\theta,\phi) = I_{rel}(\theta,\phi) \Big/ \int_{\phi=0}^{2\pi} \int_{\theta=0}^{\pi} I_{rel}(\theta,\phi) \sin\theta d\theta d\phi \, , \qquad (43)$$

where $I_{\mathrm{rel}}(\theta, \varphi)$ is the relative luminous intensity distribution of the internal source under test. The correction factor for several types of flux standard lamps were determined to be 0.9995 to 1.0002. The variation of the spatial correction factor due to horizontal rotation of these lamps was calculated to be ± 0.0002.

The uncertainty budget for the total luminous flux calibration of incandescent lamps is shown in Table 21 where the set operating current, J_0, is 5.097 A.

Table 21. Uncertainty budget for total luminous flux calibration of a typical incandescent lamp.

Symbol	Component	Value x_i	Standard Uncertainty $u(x_i)$	Unit	Type	Sensitivity Coefficient c_i	Unc. Contribution $u_i(y)$
y	Sphere photometer signal	4.85×10^{-5}	9.00×10^{-9}	A	A	4.35×10^{7}	0.39
y_{d}	Sphere photometer dark	7.00×10^{-9}	3.00×10^{-10}	A	A	-4.35×10^{7}	-0.01
R_{sph}	Sphere responsivity	2.297×10^{-8}	5.21×10^{-11}	A/lm	B	-9.19×10^{10}	-4.79
U	Shunt voltage drop	0.50970	2.00×10^{-5}	V	A	28580	0.57
c_{U}	Voltmeter calibration	1.0000	2.74×10^{-5}		B	14567	0.40
R	Shunt resistance	0.100001	2.00×10^{-6}	Ω	B	-1.5×10^{5}	-0.29
m_{J}	Current dependence	6.900	0.500		B	0.0654	0.03
c_{f}	Correction factor	0.9995	0.00096		B	2112	2.03
Φ_{test}	**Total luminous flux**	**2111**		**lm**			**5.3**
Relative expanded uncertainty for total luminous flux incandescent lamp calibration (*k* = 2)							**0.45 %**

4.4.2. Fluorescent lamps – Typical budget

Linear fluorescent lamps are always operated in the horizontal position. The test lamp axis was aligned to be in line with the photometer and the 10 cm sphere baffle. Linear fluorescent lamps should be operated on AC power at a specified current, using a reference ballast. All fluorescent lamps are operated at a specified current rather than a specified voltage because the lamp voltage, in general, does not reproduce well from facility to facility due to the construction of the sockets used among customers. However, lamp voltages reproduce fairly well on the same socket, and the lamp voltage is a useful indicator of changes in the lamps. Calibration can be performed with the cathode power either on or off by request from the customer. The luminous flux of fluorescent lamps changes significantly with ambient temperature. The ambient temperature (usually measured at the back side of the baffle) must be controlled within 25 °C ± 1 °C. The details for the electrical and photometric measurements of fluorescent lamps are described in the reference [58].

The operating circuit diagram for fluorescent tube calibrations is shown in Figure 23, which is in accordance with the ANSI standard [see section 6.1 of reference [59] for various fluorescent lamps. The circuit consists of a regulated variable AC power supply (set to 60 Hz), a step-up transformer, a reference ballast composed of an adjustable linear reactor and an adjustable resistor, a cathode heating transformer, a 2-channel AC power meter, and the test fluorescent lamp. The 2-channel AC power meter has an RMS measurement capability within a 10 kHz bandwidth. It has been confirmed that the input impedance of this instrument does not affect the circuit conditions. Both the step-up transformer and cathode heating transformer were connected to the variable AC power supply to synchronize the frequency and the phase.

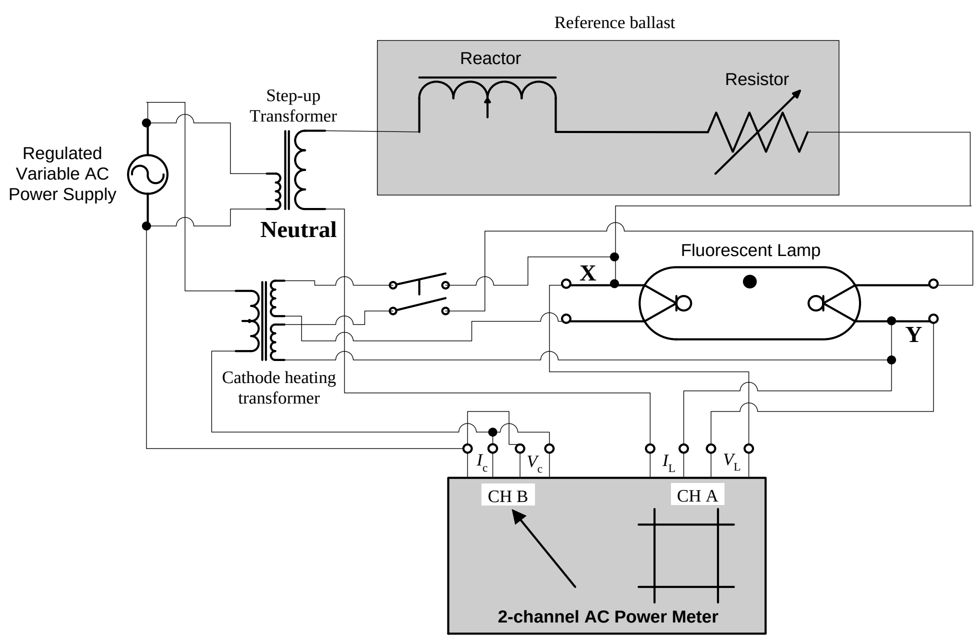

Fig. 23. Circuit diagram for the calibration of test fluorescent lamps.

The hot pin X is marked on one of the two bases of the test lamp. The test lamp is connected to the lamp-holder in such a way that the hot pin X was connected to the hot terminal X at the lamp-holder. The lamp current IL, the arc voltage VL, and the arc power were measured at CH A of the 2 channel AC power meter. The lamp operating current is set manually adjusting the output voltage of the AC power supply.

Prior to calibration, the reference ballast is adjusted (and fixed for all test lamps) with the test lamp shortened in the circuit to meet the required reference ballast's specifications. The required reference ballast specifications are found in references [60] and [51]. All AC values given in this report are in RMS values. The cathode transformer is calibrated, in advance, in terms of the primary voltage needed to provide the desired secondary voltage under normal load conditions, and the power loss in the transformer under this normal load condition. The lamp is mounted on the socket, and turned on, and the supply voltage is adjusted so that the lamp current equals the specified value. When the lamp current is adjusted, the cathode power is usually kept on. Measurements can be made with the cathode power off if requested by customer. During photometric measurements, the supply voltage, the lamp current, the lamp voltage, and the lamp power, and the cathode power are measured and recorded. If the cathode power is kept on during the measurements, the sum of lamp power and cathode power (corrected by the power loss of the cathode transformer) is reported as the total lamp power.

The model for the total luminous flux calibration of fluorescent lamps is expressed as

$$\Phi_{\mathrm{test}} = \frac{(y - y_{\mathrm{d}})}{R_{\mathrm{sph}}} \cdot \left(\frac{J_L}{J_0}\right)^{m_\mathrm{J}} B_R \cdot c_{\mathrm{f}} , \qquad (44)$$

with

$$B_{\mathrm{R}} = \left(\frac{V}{V_{\mathrm{B}}}\right)^{m_{\mathrm{V}}} \left(\frac{J}{J_{\mathrm{B}}}\right)^{m_{\mathrm{J}}} \left(\frac{P}{P_{\mathrm{B}}}\right)^{m_{\mathrm{P}}} , \qquad (45)$$

where y is the sphere photometer signal [A], y_0 is the dark sphere photometer signal [A], R_{sph} is the photometric responsivity of the sphere photometer system [A/lm], J_{L} is the measurement of lamp current, J_0 is the calibrated current for the lamp, and m_{J} is the exponential dependence of the lamp luminous flux with respect to the operating current. B_{R} is the correction factor based on the reference ballast settings where V is the input voltage when setting the reference ballast, V_{B} is the calibrated input voltage, m_{V} is the exponential dependence of the input voltage on the final lumen output, J is the short circuit current when setting the reference ballast, J_{B} is the calibrated short circuit current, m_{J} is the exponential dependence of the short circuit current on the final lumen output, P is the ballast watt loss when setting the reference ballast, P_{B} is the calibrated ballast watt loss, and m_{P} is the exponential dependence of the ballast watt loss on the final lumen output. Several uncorrelated components of uncertainty have been combined in one factor, c_f. A list of these uncertainty components and relative standard uncertainty are summarized in Table 22.

Table 22. Uncertainty components for total flux calibration.

Symbol	Uncertainty component	Type	Relative Unc. Contribution (%)
c_L	Lamp ambient temperature correction	B	0.40
c_N	Near-field absorption losses	B	0.10
c_T	Sphere photometer temperature correction	B	0.05
c_G	Photometer transimpedance gain amplifier correction	B	0.02
c_y	Digital voltmeter calibration	B	0.008
c_W	Sphere wall temperature dependence	B	0.03
F^*	Source SMCF	B	0.15
S_f	Source spatial non-uniformity correction	B	0.12
c_S	Spatial stray light	B	0.05
$\boldsymbol{c_f}$	**Fluorescent lamp total flux correction factor**		**0.462**

The performance characteristics of a fluorescent lamp including light output are strongly influenced by the mercury vapor pressure inside the lamp. The mercury vapor pressure is determined by the coolest part of the fluorescent lamp glass [62]. The ambient temperature determines the temperature of the fluorescent lamp glass. Generally all fluorescent lamps follow the same temperature curve, because the output is based on mercury vapor pressure which is dependent on temperature. Lamps with mercury amalgams follow a different curve. An amalgam is a mercury alloy that determines the mercury pressure by absorbing or releasing mercury as a function of temperature. The amalgam reduces the dependence of the ambient temperature over a wide range. Figure 24 shows a typical normalized linear fluorescent tube light output with respect to the ambient temperature for lamps without amalgam. The equation in Figure 24 is the light output dependence on ambient temperature. The standard uncertainty of the sphere ambient temperature, T_A, which is measured on the photometer side of the baffle, is 1.0 °C. Since there are thermal gradients in the sphere, the measured ambient temperature only correlates to the ambient temperature directly in contact with the lamp glass. To account for this uncertainty in the correlation, the standard uncertainty for the correction factor T_L is the determined by multiplying the uncertainty in T_A by 3 and then multiply by the derivative of the equation evaluated at T_A.

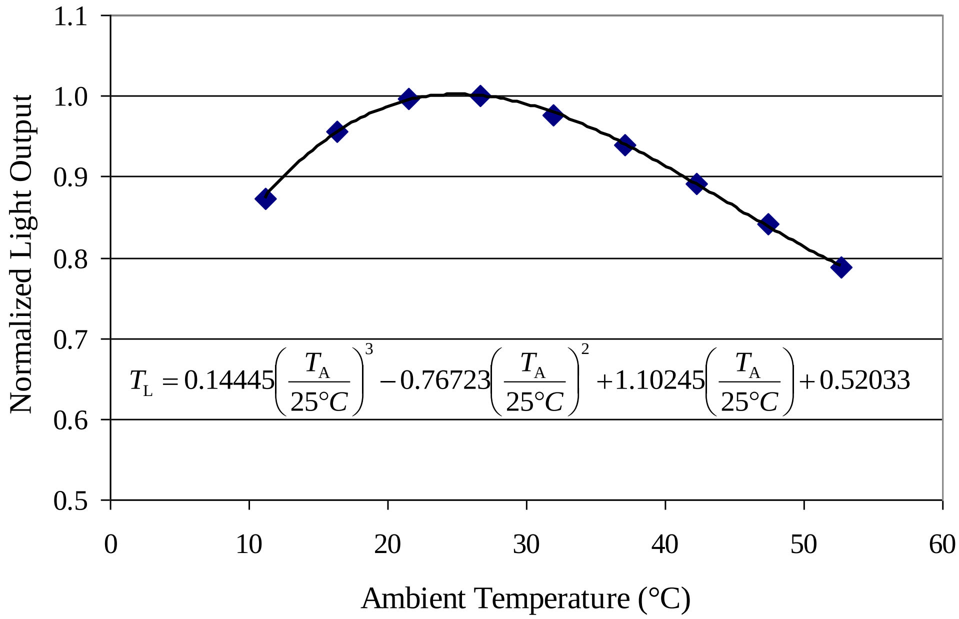

Fig. 24. Typical normalized linear fluorescent tube light output as a function of ambient temperature.

Near-field absorption losses occur when the lamp is close to a surface were multiple reflections are possible causing a significant increase in absorption. If the length of the 4 foot linear fluorescent tube is parallel to the holder, the light from the lamp is reflected and absorbed by the holder. The closer the holder is to the lamp, the more opportunities for the light to be absorbed by the holder and not detected by the sphere photometer. These near-field interactions cannot be corrected. The holder must be made such that the lamp is as far away from the holder as possible.

The reference ballast dependencies on voltage, current and power loss settings were determined by altering each parameter independently by ± 5 %. Due to the fluctuations in the linear fluorescent tube an exponential fit to the individual parameters could not statistically be achieved. The fluctuations for the repeatability of the linear fluorescent tube were on the order of 0.17 %. The reference ballast parameters are set better than 0.25 % therefore the standard deviation in the flux measurement was assumed to be 0.02 %.

The uncertainty budget for the total luminous flux calibration of fluorescent lamps is shown in Table 23 where the operating conditions are for a 32 W, 48 inch, T8, rapid-start type fluorescent lamp (J_0 = 0.265 A, V_B = 241.2 V, J_B = 0.265 A, P_B = 4.8 W).

Table 23. Uncertainty budget for total luminous flux calibration of a typical fluorescent lamp.

Symbol	Component	Value x_i	Standard Uncertainty $u(x_i)$	Unit	Type	Sensitivity Coefficient c_i	Unc. Contribution $u_i(y)$
y	Sphere photometer signal	6.34×10^{-5}	2.50×10^{-8}	A	A	4.35×10^{7}	1.09
y_d	Sphere photometer dark	9.00×10^{-5}	3.00×10^{-10}	A	A	-4.35×10^{7}	-0.01
R_sph	Sphere responsivity	2.297×10^{-8}	5.21×10^{-11}	A/lm	B	-1.20×10^{11}	-6.26
J_L	Lamp current	0.2650	7.00×10^{-4}	A	B	10413	7.29
m_J	Current dependence	1.000	0.200		B	7.28	1.46
B_R	Ballast dependence	1.000	0.0002		A	2760	0.55
c_f	Correction factor	0.9995	0.00462		B	2761	12.76
Φ_test	**Total luminous flux**	**2760**		**lm**			**20.5**
Rel. expanded uncertainty for total luminous flux fluorescent lamp cal. (k = 2)							**1.5 %**

4.4.3. Reflector lamps – Typical budget

Reflector lamps and typical incandescent lamps are operated similarly. The reflector lamps are operated in the sphere center with the base up position unless otherwise stated. If supplied by the customer, a light trapping can is mounted above the reflector lamp to capture light backward leaking light in accordance with LM-41. The lamps are operated at the lamp current or at the color temperature specified by the customer. When the color temperature is specified, the lamp current is first determined by color temperature measurements as described in Section 6. When the lamp current is specified, the color temperature of the lamp is measured and reported together with the luminous flux value. The lamps are allowed to stabilize, usually for 10 min. The color temperature values are used for the SMCFs. The lamp current is ramped up and down slowly (approximately 30 s). Photometric measurements are made after the lamp has stabilized (approximately 10 min after turning on or a time specified by the customer).

The model for the total luminous flux calibration of reflector lamps is expressed in Eq. (41). The uncertainty budget for the total luminous flux calibration of reflector lamps is shown in Table 24 where the set operating current, J_0, is 0.7600 A and the operating voltage is 119.4 V. Reflector lamps have three uncertainty components which are significantly larger than typical incandescent lamps. One uncertainty component is the near-field correction factor. Since the light trapping can is close to the lamp, the uncertainty of the near-field correction factor is large, typically 0.15 %. Additionally, the space between the can and the lamp cause a loss in the light that should be measured causing a larger uncertainty in the near-field correction factor. The second uncertainty component is the spatial non-uniformity correction factor. A simple model for the intensity distribution of the reflector lamp whether it is a flood or spot lamp is applied to the spatial sphere responsivity. Since the lamp shines directly on seam of the sphere, a disc covered with the sphere wall reflecting coating is positioned at the bottom of the sphere. The spatial sphere responsivity is measured with the disc in position. A typical spatial non-uniformity correction factors for a flood lamp is 1.007 and for a spot lamp 1.009 with a standard uncertainty of 0.44 %. A third uncertainty component that is typically larger for reflector lamps than typical incandescent lamps is the operating voltage correction factor.

Table 24. Uncertainty budget for total luminous flux calibration of a typical reflector lamp.

Symbol	Component	Value x_i	Standard Uncertainty $u(x_i)$	Unit	Type	Sensitivity Coefficient c_i	Unc. Contribution $u_i(y)$
y	Sphere photometer signal	3.15×10^{-5}	9.00×10^{-9}	A	A	4.39×10^{7}	0.40
y_d	Sphere photometer dark	7.00×10^{-9}	3.00×10^{-10}	A	A	-4.39×10^{7}	-0.01
R_{sph}	Sphere responsivity	2.297×10^{-8}	5.21×10^{-11}	A/lm	B	-6.02×10^{10}	-3.14
U	Shunt voltage drop	0.07600	8.00×10^{-6}	V	A	125586	1.00
c_U	Voltmeter calibration	1.0000	5.27×10^{-5}		B	9545	0.50
R	Shunt resistance	0.100001	2.00×10^{-6}	Ω	B	-9.5×10^{4}	-0.19
m_J	Current dependence	6.900	0.500		B	0.0429	0.02
c_f	Correction factor	1.0088	0.00478		B	1371	6.56
Φ_{test}	**Total luminous flux**	**1383**		**lm**			**10.6**
Rel. expanded uncertainty for total luminous flux reflector lamp cal. (k = 2)							**1.5 %**

5. Luminance calibrations

5.1. NIST luminance unit and uncertainty budget

Luminance units are commonly established using a white reflectance standard or a transmitting diffuser illuminated by a luminous intensity standard lamp [48]. The determination of the luminance factor of the material includes comparison of the incident and outgoing illuminances, which differ by three to four orders of magnitude, and which makes precise calibration difficult. The uncertainty is also limited by that of the standard lamp used.

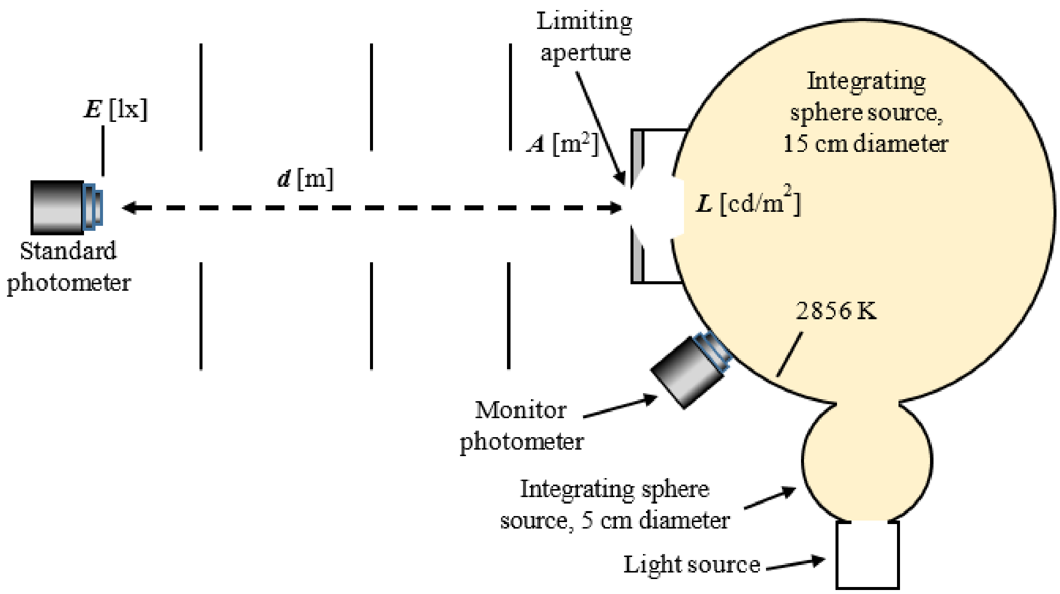

Fig. 25. Arrangement for NIST luminance unit realization.

Using the NIST standard photometers, a detector-based luminance unit is realized on a reference integrating-sphere source operated at 2856 K. Figure 25 shows the arrangement. The 15 cm diameter sphere has a double sphere structure with a $V(\lambda)$-corrected monitor detector on the sphere wall. The large sphere is irradiated by an intermediate 5 cm sphere which is irradiated by a quartz halogen lamp. The sphere source is operated by a constant-current power supply. A precision aperture 6 mm in diameter is attached to the exit port (50 mm diameter) of the sphere source. The sphere source and the photometers are placed on the NIST photometry bench in a light tight box to reduce stray light. The sphere is aligned using the alignment laser and the side telescope. The side telescope sets the distance by aligning the aperture front surface with the origin of the bench. The sphere source is adjusted to produce a correlated color temperature of 2856 K and allowed to stabilize for 30 min before calibration since the responsivity of the monitor detector drifts as the sphere warms up. The illuminance 2.45 m from the sphere source is measured by the NIST standard photometers that hold the illuminance unit. The average luminance L (cd/m^2) over the aperture plane is determined from the illuminance E (lx), the distance, d (m), and the aperture area, A (m^2), as given by

$$L = k \cdot E \frac{d^2}{A}, \tag{46}$$

where k is a geometrical correction factor determined by the radius, r_a, of the aperture, the radius, r_d, of the detector sensitive area, and the distance, d, as given by

$$k \approx 1 + \left(\frac{r_a}{d}\right)^2 + \left(\frac{r_d}{d}\right)^2 ; r_a, r_d < \frac{d}{10}. \tag{47}$$

The error, 1- k, is negligible with distance d = 2.45 m. The diffraction loss with the 6 mm aperture [63] is calculated to be negligible (< 0.01 %) in the geometry used in this measurement. When the luminance, L, is determined, the monitor detector signal, y, is recorded, and the monitor detector responsivity, R_{lum} [V/(cd/m^2)], is determined. This procedure is completed each time a luminance or luminance responsivity calibration is to be performed.

For routine calibrations of luminance when a luminance surface with larger area is needed, the precision aperture is removed from the sphere source, and the sphere port can be full open (50 mm diameter) or equipped with another aperture (25 mm diameter). In these cases, the luminance changes due to the interreflections between the aperture surface, and the sphere wall. This change of luminance is determined by the signal from the monitor detector installed on the sphere wall. The model for the NIST luminance unit realization is expressed as

$$L = \frac{(y - y_{\mathrm{d}}) \cdot d^2}{R_{\mathrm{v,i}} \cdot A} \cdot c_{\mathrm{f}} , \tag{48}$$

where y is the NIST standard photometer signal, y_d is the dark signal, d is the photometric distance, $R_{v,i}$ is the NIST standard photometer responsivity, A is the area of the sphere aperture. Several uncorrelated components of uncertainty have been combined in one factor, c_f. A list of these uncertainty components and relative standard uncertainty are summarized in Table 25. The uncertainty budget for the NIST luminance unit realization in Table 26 shows that the relative expanded uncertainty of the monitor responsivity is 0.5 % (k = 2).

Table 25. Uncertainty components for NIST luminance unit.

Symbol	Uncertainty component	Type	Relative Unc. Contribution (%)
c_L	Stability of the light source	B	0.05
c_T	Photometer temperature correction	B	0.05
L_f	Long-term stability of the NIST standard photometers	B	0.15
F^*	SMCF for NIST standard photometers	B	0.02
c_G	Photometer transimpedance gain amplifier correction	B	0.02
c_y	Digital voltmeter calibration	B	0.008
c_γ	Angular alignment of the NIST standard photometers	B	0.002
c_α	Angular alignment of the sphere source	B	0.002
k	Geometric correction factor	B	0.005
c_S	Spatial stray light	B	0.02
$\boldsymbol{c_f}$	**Luminance unit correction factor**		**0.170**

Table 26. Uncertainty budget for NIST luminance unit.

Symbol	Component	Value x_i	Standard Uncertainty $u(x_i)$	Unit	Type	Sensitivity Coefficient c_i	Unc. Contribution $u_i(y)$
y	NIST photometer signal	1.268×10^{-10}	2.00×10^{-14}	A	A	2.10×10^{13}	0.42
y_d	NIST photometer dark	1.10×10^{-13}	5.20×10^{-15}	A	A	-2.10×10^{13}	-0.11
$R_{v,i}$	NIST std responsivity	1.012×10^{-8}	1.88×10^{-11}	A/lx	B	-2.63×10^{11}	-4.94
d	Photometric distance	2.45000	0.00062	m	B	2170	1.35
A	Source aperture	2.827×10^{-5}	2.80×10^{-8}	m^2	B	-9.40×10^7	-2.63
c_f	Correction factor	1.000	0.00170		B	2658	4.52
L	**NIST Luminance unit**	**2658**		**cd/m^2**			**7.3**
Rel. expanded uncertainty for NIST luminance unit (*k* = 2)							**0.55 %**

To transfer the scale the sphere monitor photometer needs to be calibrated. Simultaneously as the luminance is realized on the sphere, the monitor photometer is measured and the monitor responsivity is determined as shown in the following equation

$$R_{\mathrm{Lum}} = \frac{(y - y_{\mathrm{d}}) \cdot c_y}{L} , \tag{49}$$

The uncertainty for the monitor responsivity is the square root of the sum of the squares since all the components are uncorrelated. The additional uncertainty components for y, y_{d}, and c_{y} are small compared $u(L)$, so the relative expanded uncertainty of the monitor responsivity is also 0.55 % (k = 2).

5.2. Calibration of luminance meters

A luminance meter under test is calibrated against the reference luminance source (described in Section 5.1) operated at 2856 K using the following procedures. Prior to calibration, the reference sphere source is turned on and allowed to stabilize for 30 min in the photometry bench to minimize sensitivity to ambient temperature. The reference sphere source is aligned so that the center of the exit port of the source is on the optical axis of the NIST photometry bench, and that the front surface around the exit port is normal to the optical axis. The monitor detector is calibrated against the NIST illuminance scale.

The luminance meter under test is placed and aligned on the optical axis at 1 m to 3 m from the source depending on the measurement angle or field of view of the luminance meter. The luminance meter is focused on the plane of the exit port, aiming at the center of the exit port of the reference sphere source. The luminance values indicated by the luminance meter under test are compared with the luminance values determined from the monitor detector signal of the reference sphere source. The room temperature at calibration is usually 24 °C. The uncertainty for a typical luminance meter calibration follows the expression,

$$R_{\mathrm{f}} = \frac{(Y - Y_{\mathrm{d}}) \cdot R_{\mathrm{lum}}}{y} \cdot c_{\mathrm{f}} , \tag{50}$$

where R_{f} is a calibration factor, Y is the displayed luminance and Y_{d} is the displayed dark luminance for the luminance meter under test, y is the sphere monitor signal [V], R_{lum} is the responsivity of the sphere monitor detector. Several uncorrelated components of uncertainty have been combined in one factor, c_{f}. A list of these uncertainty components and relative standard uncertainty are summarized in Table 27.

Table 27. Uncertainty components for luminance meter calibration.

Symbol	Uncertainty component	Type	Relative Unc. Contribution (%)
c_L	Stability of the sphere source	B	0.015
c_T	Sphere monitor temperature dependence	B	0.05
c_U	Luminance uniformity of the sphere source	B	0.05
c_y	Digital voltmeter calibration	B	0.008
c_S	Spatial stray light	B	0.05
$\boldsymbol{c_f}$	**Luminance meter calibration correction factor**		**0.088**

For many luminance meters the uncertainty in the displayed luminance is the display resolution. The uncertainty budget for the calibration of a typical luminance meter is shown in Table 28. This budget does not include the uncertainty factor for the out-of-field sensitivity of the test instrument. If the luminance meter's out-of-field blocking is poor, the responsivity of the instrument is affected by the illuminance of the area outside the measurement angle. Therefore, the calibration value is reported with the measurement geometry used at the calibration, and may not be valid with other geometries

Table 28. Uncertainty budget for a typical luminance meter calibration.

Symbol	Component	Value x_i	Standard Uncertainty $u(x_i)$	Unit	Type	Sensitivity Coefficient c_i	Unc. Contribution $u_i(y)$
Y	Luminance meter reading	2335	0.5774	cd/m^2	B	0.00043	0.00025
Y_d	Luminance meter dark	0	0.5774	cd/m^2	B	-0.00043	-0.00025
R_{lum}	Monitor responsivity	2.035×10^{-4}	5.61×10^{-7}	V/[cd/m^2]	B	4902	0.00275
y	Monitor signal	0.4763	0.00011	V	A	-2.095	-0.00023
c_f	Correction factor	1.000	0.00088		B	0.9976	0.00088
R_f	**Calibration factor**	**0.9976**					**0.59 %**
Rel. expanded uncertainty for luminance meter calibration (k = 2)							**0.59 %**

Luminance meters used for particular sources other than incandescent sources can be calibrated for those specific sources (e.g., color displays) upon request by customers. In this case, the calibration is first performed using the 2856 K source as described above. Then, the SMCFs for the sources are obtained using the following procedures.

The relative spectral responsivity of the NIST luminance meter is measured by the SCF [25] in the 350 nm to 1100 nm region. The monochromator output of the SCF is defocused on a PTFE (polytetrafluoroethylene) plaque to irradiate an area of several mm in diameter. The luminance meter under test is placed so that it will measure the luminance of the spot on the PTFE plaque at 0/45 geometry, and that the irradiated spot underfills the measurement area of the luminance meter. This method can only be applied for luminance meters whose relative spectral responsivity is fairly spatially uniform within the measurement angle. From the relative spectral responsivity data and the spectral power distribution data (supplied by customer) of the light sources to be measured by the luminance meter, the SMCFs are calculated. The relative spectral responsivity data and the correction factors are reported to the customer.

5.3. Calibration of high-luminance meters

Based on the high-illuminance source described in section 3.6, a high-luminance surface can be created by combining it with a reflecting or transmitting diffuser of a known luminance coefficient to allow calibration of luminance meters. The calibration of reflecting and transmitting diffusers for luminance coefficient is described in section 5.6. Two transmitting diffusers, an acrylic diffuser and an opal glass, were tested along with one reflecting diffuser constructed from pressed PTFE powder. The transmitting diffusers were arranged with 0° incidence and 0° viewing geometry. The pressed PTFE plaque was arranged at a 45° incidence and 45° viewing angle instead of the normal 0/45 due to space limitations. The high-luminance surfaces where measured with the NIST high-illuminance photometers equipped with luminance optics with a 1° measurement angle. The acrylic diffuser had a maximum luminance of 55 kcd/m^2, the opal diffuser had a maximum luminance of 45 kcd/m^2, and the PTFE diffuser had maximum luminance of 70 kcd/m^2 for a Xenon spectral distribution. For CIE Illuminant A the range is 5000 cd/m^2 to 30,000 cd/m^2.

The uncertainty analysis for a high-luminance meter calibration follows the model.

$$R_{\mathrm{f}} = \frac{(Y - Y_{\mathrm{d}}) \cdot R_{\mathrm{v,L}}}{(y - y_{\mathrm{d}})} \cdot c_{\mathrm{f}} , \qquad (51)$$

where $R_{\mathrm{v,L}}$ is the responsivity of the NIST high-luminance standard photometer which includes the uncertainty of the transfer of the scale, Y is the displayed luminance and Y_{d} is the displayed dark luminance for the luminance meter under test, y is the NIST high-luminance photometer reading and y_{d} is the dark reading. Several uncorrelated components of uncertainty have been combined in one factor, c_{f}. A list of these uncertainty components and relative standard uncertainty are summarized in Table 29. Table 30 shows a typical uncertainty budget for the calibration of a high-luminance meter.

Table 29. Uncertainty components for high luminance meter calibration.

Symbol	Uncertainty component	Type	Relative Unc. Contribution (%)
c_L	Stability of the luminance source	B	0.10
c_U	Luminance uniformity of the source	B	0.15
L_f	Long-term stability of the high-luminance std. photometer	B	0.15
c_T	Temperature dependence of the high-luminance std. photometer	B	0.10
F^*	SMCF for NIST standard photometers	B	0.05
c_G	Photometer transimpedance gain amplifier correction	B	0.15
c_y	Digital voltmeter calibration	B	0.008
c_H	Temperature dependence of the luminance meter under test	B	0.15
c_S	Spatial stray light	B	0.10
$\boldsymbol{c_f}$	**High-luminance meter calibration correction factor**		**0.350**

Table 30. Uncertainty budget for a typical high-luminance meter calibration.

Symbol	Component	Value x_i	Standard Uncertainty $u(x_i)$	Unit	Type	Sensitivity Coefficient c_i	Unc. Contribution $u_i(y)$
Y	Luminance meter display	15560	5.77	cd/m^2	B	6.538×10^{-5}	3.77×10^{-4}
Y_d	Luminance meter dark	0	5.77	cd/m^2	B	-6.538×10^{-5}	-3.77×10^{-4}
$R_{v,L}$	Std. Photometer resp.	1.497×10^{-4}	4.4×10^{-7}	V/[cd/m^2]	B	6796	2.99×10^{-3}
y	Std. Photometer signal	2.2897	0.00011	V	A	-0.4443	-4.89×10^{-5}
y_d	Std. Photometer dark	0.00003	4.1×10^{-7}	V	A	0.4443	1.82×10^{-7}
c_f	Correction factor	1.0000	0.00350		B	1.0173	3.56×10^{-3}
R_f	**Cal. factor**	**1.0173**					**0.0047**
Rel. expanded uncertainty for high-luminance meter calibration (k = 2)							**0.92 %**

5.4. Calibration of luminance sources

Luminance sources under test are calibrated against the reference sphere source described in 5.1 using the following procedures. The reference sphere source is turned on and stabilized for 30 min before the scale is realized. A reference luminance meter is calibrated against the reference sphere source. The reference luminance meter has measurement angles of 6’, 20’, 1°, and 3°. The luminance meter is equipped with a 3 1/2 digit display and an analog output, the voltage of which is measured with a digital voltmeter. The stray light error (due to the surrounding field outside the measured area) of this luminance meter was checked according to the CIE Pub. 69 [48] and found to be less than 0.1 %.

The sphere source under test is aligned so that the center of the exit port of the source is on the optical axis and so that the front surface around the exit port is normal to the optical axis. The reference luminance meter is placed on the optical axis at approximately 1.5 m from the source for a measurement area of 9 mm in diameter, with the measurement angle of the reference luminance meter to be 0.33 °. The luminance meter is focused on the plane of the exit port. The test source is turned on and allowed to stabilize for the time period specified by the customer. The room temperature during the calibration is usually 24 °C. The color temperature of the source is also measured using the facilities and procedures described in Section 6.

The uncertainty analysis for a luminance source calibration follows the model,

$$R_{\mathrm{f}} = \frac{(L - L_{\mathrm{d}}) \cdot R_{\mathrm{v,L}}}{(y - y_{\mathrm{d}})} \cdot c_{\mathrm{f}} , \tag{52}$$

where $R_{\mathrm{v,L}}$ is the responsivity of the reference luminance photometer which includes the uncertainty of the transfer of the scale, L is the displayed luminance and L_{d} is the displayed dark luminance for the luminance source under test, y is the reference luminance photometer reading and y_{d} is the dark reading. Several uncorrelated components of uncertainty have been combined in one factor, c_{f}. A list of these uncertainty components and relative standard uncertainty are summarized in Table 31. Table 32 shows a typical uncertainty budget for the calibration of a luminance source.

Table 31. Uncertainty components for luminance source calibration.

Symbol	Uncertainty component	Type	Relative Unc. Contribution (%)
c_L	Stability of the luminance source	B	0.10
L_f	Long-term stability of the reference luminance meter	B	0.15
c_O	Out-of-field sensitivity of the reference luminance meter	B	0.05
F^*	SMCF for the reference luminance meter	B	0.05
c_G	Ref. luminance meter gain amplifier correction	B	0.15
c_y	Digital voltmeter calibration	B	0.008
c_S	Spatial stray light	B	0.05
$\boldsymbol{c_f}$	**Luminance source calibration correction factor**		**0.250**

Table 32. Uncertainty budget for a typical luminance source calibration.

Symbol	Component	Value x_i	Standard Uncertainty $u(x_i)$	Unit	Type	Sensitivity Coefficient c_i	Unc. Contribution $u_i(y)$
L	Source luminance display	2450	0.577	cd/m^2	B	4.09×10^{-4}	2.36×10^{-4}
L_d	Source luminance dark	0	0.577	cd/m^2	B	-4.09×10^{-4}	-2.36×10^{-4}
$R_{v,L}$	Std. Luminance resp.	1.497×10^{-3}	4.4×10^{-6}	V/[cd/m^2]	B	669	2.94×10^{-3}
y	Std. Luminance signal	3.6637	0.00011	V	A	-0.2732	-3.01×10^{-5}
y_d	Std. Luminance dark	0.00003	4.1×10^{-7}	V	A	0.2732	1.12×10^{-7}
c_f	Correction factor	1.0000	0.00250		B	1.0011	2.50×10^{-3}
R_f	**Calibration factor**	**1.0011**					**0.0039**
Rel. expanded uncertainty for luminance source calibration (k = 2)							**0.77 %**

5.5. Artifacts for calibration

Commercially available luminance sources and luminance meters of various types, submitted by the customers, are accepted for calibration at NIST. For sphere sources, operating current or voltage, or a set point for the monitor detector, and the stabilization time must be specified by customer. The customers are responsible for ensuring stability of the sources. For luminance meters, luminance levels and measurement angles must be specified for calibration. The luminance range for calibration is 1 cd/m^2 to 3000 cd/m^2.

NIST issues opal glasses calibrated for luminance coefficient (ratio of luminance to illuminance), and recalibrates submitted opal glasses. The opal glass issued by NIST is 50 mm x 50 mm in size and 3 mm in thickness. It has a diaphragm of 25 mm diameter attached on the flashed side of the opal glass.

In general, use of opal glass requires a luminous intensity standard lamp and a photometric bench (distance measurement capability) in a dark room. Sphere sources usually do not need such facilities (of course, ambient light must be reduced) and are more convenient in terms of instrumentation. Use of sphere sources with a monitor detector is highly recommended because the monitor detector can maintain the scale more reliably than the lamp of the source (almost regardless of the operating time of the source). If there is no monitor detector, it is recommended that the source be recalibrated after every 50 h of use. The luminance of typical commercial sphere sources can change (decrease) by 1 % to 2 % and color temperature by 10 K to 20 K per 100 h of operation at 2856 K. It should be noted, however, that a sphere monitor detector, without temperature control, can drift by ≅0.5 % during the first hour while the sphere warms up. It should also be noted that the sphere coating or the monitor detector will be contaminated or degraded after use or storage of a long period of time. Even when the scale is maintained by the monitor detector or when the source is not used, it is recommended that the sphere source be calibrated yearly. The exit port of the sphere source should always be capped when not used.

5.6. Calibration of diffusers for luminance coefficient

5.6.1. Calibration procedure for opal glass luminance coefficient

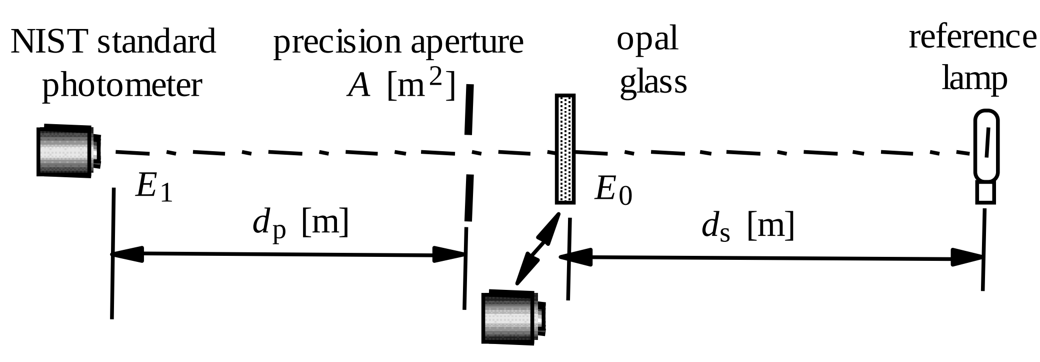

Fig. 26. Configuration for the realization of opal glass luminance coefficient.

An opal glass under test is calibrated for luminance coefficient (ratio of luminance to illuminance, unit [sr^{-1}]) of diffuse transmission, by comparison with three reference opal glass standards. The reference opal glasses are calibrated by directly measuring the incident illuminance by using the NIST standard photometers and the transmitted luminance on the opal glass surface by using the same NIST standard photometers and a calibrated precision aperture as shown in Figure 26. When the illuminance, E_0 [lx], and the luminance, L [cd/m^2], which is determined from the second illuminance measurement, E_1, the distance, and the precision aperture area, A, are measured, the luminance coefficient, q [sr^{-1}], of the opal glass is given by

$$q = \frac{E_1 \cdot d^2}{E_0 \cdot A \cdot \Omega_0} \quad . \tag{53}$$

The uncertainty analysis for luminance coefficient of the NIST reference opal glass calibration follows the model,

$$q_0 = \frac{\left(y_1 - y_{\mathrm{d},1}\right) \cdot d^2}{\left(y_0 - y_{\mathrm{d},0}\right) \cdot A \cdot \Omega_0} \cdot c_{\mathrm{f}} \quad , \tag{54}$$

where y_0 and $y_{\mathrm{d},0}$ are the photometer signal and dark signal measuring the lamp, y_1 and $y_{\mathrm{d},1}$ are the photometer signal and dark signal measuring the light from the opal glass, d is the distance from the photometer to the opal glass reference plane, A is the area of the precision aperture, and Ω_0 is the unit solid angle. Several uncorrelated components of uncertainty have been combined in one factor, c_{f}. A list of these uncertainty components and relative standard uncertainty are summarized in Table 33. Table 34 shows a typical uncertainty budget for the calibration of a luminance source.

Table 33. Uncertainty components for NIST reference opal glasses.

Symbol	Uncertainty component	Type	Relative Unc. Contribution (%)
c_L	Stability of the lamp during calibration	B	0.05
c_U	Illuminance nonuniformity at the opal glass reference plane	B	0.08
c_T	Temperature correction of the photometer	B	0.05
c_O	Temperature correction of the opal glass	B	0.02
$F^*(s_{ml})$	SMCF for measuring lamp	B	0.03
$F^*(s_{og})$	SMCF for measuring opal glass	B	0.05
c_γ	Angular alignment of the photometer measuring the lamp	B	0.005
c_γ	Angular alignment of the photometer measuring the opal glass	B	0.005
c_γ	Angular alignment of the opal glass	B	0.02
c_I	Deviation from the inverse square law of light from opal glass	B	0.002
c_G	Ref. luminance meter gain amplifier correction	B	0.02
c_y	Digital voltmeter calibration	B	0.008
c_S	Spatial stray light	B	0.05
$\boldsymbol{c_f}$	**Luminance source calibration correction factor**		**0.250**

Table 34. Uncertainty budget for a NIST reference opal glass calibration.

Symbol	Component	Value x_i	Standard Uncertainty $u(x_i)$	Unit	Type	Sensitivity Coefficient c_i	Unc. Contribution $u_i(y)$
y_1	Opal glass signal	8.2819×10^{-5}	1.1×10^{-8}	V	A	-0.0640	-1.92×10^{-6}
$y_{d,1}$	Opal glass dark signal	-5.0×10^{-9}	6.1×10^{-11}	V	A	0.0640	3.33×10^{-8}
d	Photometric distance	1.5000	0.0008	m	B	0.2045	1.64×10^{-4}
y_0	Lamp signal	2.3976	0.00003	V	A	-302.7	-1.51×10^{-4}
$y_{d,0}$	Lamp dark signal	0.00011	5.2×10^{-7}	V	A	1852.1	2.04×10^{-5}
A	Precision aperture area	5.067×10^{-4}	5.0×10^{-7}	m^2	B	-1852.1	-1.13×10^{-7}
c_f	Correction factor	1.0000	0.00136		B	0.1534	2.09×10^{-4}
q_0	**Luminance coefficient**	**0.1534**					**0.00031**
Rel. expanded uncertainty for NIST reference opal glass calibration (*k* = 2)							**0.40 %**

For calibration of customers' opal glasses, the instruments are placed on the NIST photometry bench in a light tight box. The reference opal glasses and the opal glass under test are placed alternately and irradiated by a 1000 W frosted quartz halogen lamp operated at a color temperature of 2856 K (unless otherwise stated in the report) at a distance of approximately 2 m from the opal glass. A reference luminance meter is placed 1.5 m from the opal glass. The centers of the lamp filament, the opal glass, and the luminance meter lens are aligned on the optical axis. The opal glasses are placed with the aperture side facing the luminance meter. The glass surface is aligned to be perpendicular to the optical axis. The luminance meter is aimed at the center of the circular aperture area and set to a measurement angle of 20'. With these dimensions, the luminance of the center area of 9 mm in diameter is measured. The luminance coefficient of the opal glass under test is calculated by comparison to the reference opal glasses.

The color temperature of the transmitted light is shifted due to the spectral transmittance of the opal glass and decreases typically by 100 K to 200 K. As an option, if a set of a luminous intensity standard lamp and an opal glass are submitted for calibration, the operating current of the lamp can be set so that the transmitted light from the opal glass produces color temperature of 2856 K (See Section 6 for color temperature calibration), and the luminance coefficient of the opal glass can be calibrated under that condition.

NIST issues opal glasses of 50 mm square, 3 mm thick, having an aperture of 25 mm in diameter, as calibrated standards for luminance coefficient. A luminance standard can be obtained by combining these standards and an incandescent lamp operated at approximately 2856 K. The opal glass should be placed so that the transparent glass side (with no aperture) faces the lamp. The luminance standard will be on the opal side with the aperture. The luminance, L [cd/m^2], of the illuminated opal glass is

$$L = q \cdot E \ , \tag{55}$$

where q is the luminance coefficient [sr^{-1}] and E is the illuminance [lx] on the reference plane of the opal glass. The reference plane is 2 mm inside from the surface of the transparent glass side. Illuminance can be measured by placing a standard photometer at the reference plane of the opal glass after the opal glass is removed. Illuminance can also be determined by using a luminous intensity standard lamp applying the inverse square law. In this case the distance should be measured from the reference plane of the opal glass.

It is recommended that the distance, d, be greater than 1 m because a small distance error creates a large luminance error at shorter distances. It should be noted that the luminance coefficient, q, is calibrated for the central 9 mm diameter area of the opal glass (unless otherwise stated in the calibration report) and in the direction normal to the opal surface. Luminance may vary up to ± 1 % typically, outside that central area. Luminance may also vary if viewed at different angles.

An opal glass is sensitive to stray light on both sides of the glass. Extreme care should be taken to minimize ambient reflection from both the front side and the back side. It is important that an opal glass is illuminated uniformly over its entire surface area, since light incident on one part of the glass affects to luminance on other parts by volume diffusion. For example, a holder for the glass should not block the light falling on the edges of the glass. No labels should be affixed on the glass surface after calibration. The calibration will not be valid if the aperture is removed from the opal glass or if the black coating around the edges of the glass is removed.

The uncertainty analysis for luminance coefficient of an opal glass calibration follows the model,

$$L = q \cdot E \ , \tag{56}$$

where L_0 and $L_{d,0}$ are the reference luminance meter signal and dark signal for the reference opal glass, L_1 and $L_{d,1}$ are the reference luminance meter signal and dark signal for the opal glass under test, q_0 is the reference opal glass luminance coefficient. The correction factors c_f include the gain differences between the signals, the position alignment correction of the opal glass under test with respect to the reference opal glass, stability of the lamp during calibration, temperature correction of the opal glass, SMCF for measuring the opal glasses, angular alignment of the reference opal glass, angular alignment of the opal glass under test, and combined stray light in the measurements. The relative expanded uncertainty (k = 2) for calibration of NIST-issued opal glasses is 0.46 %. For calibration of customer-submitted opal glasses of sizes different from the reference opal glasses, additional uncertainty factors such as the difference in stray light around the opal glass, the calibration to a different measuring angle (3° or 0.1°) of the reference luminance meter, and the non-uniformity of illuminance field, are taken into account.

5.6.2. Calibration procedure for reflectance plaque luminance coefficient

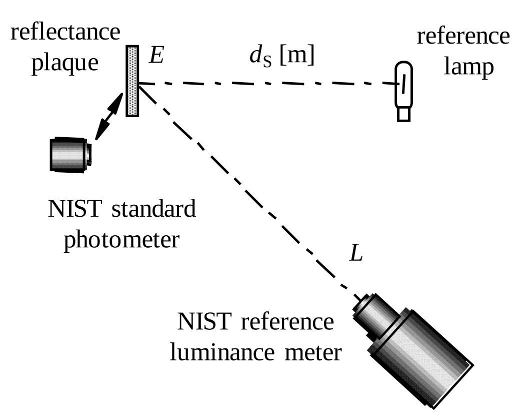

Fig. 27. Configuration for the realization of reflectance plaque luminance coefficient.

A reflectance plaque under test is calibrated for luminance coefficient (ratio of luminance to illuminance, unit [sr^{-1}]) of diffuse reflectance, by directly measuring the incident illuminance normal to the plaque by using the NIST standard photometers and the reflected luminance from the plaque surface 45° to the normal by using the NIST reference luminance meter as shown in Figure 27. The uncertainty analysis for the luminance coefficient of a reflectance plaque uses the following model,

$$q = \frac{(L - L_{\mathrm{d}})}{(E - E_{\mathrm{d}})} \cdot c_{\mathrm{f}} \quad , \tag{57}$$

where E is the illuminance on the reflectance plaque, E_{d} is the dark signal of the NIST standard photometer, L is the luminance from the reflectance plaque, and L_{d} is the dark signal of the NIST reference luminance meter. Since the calibration of the NIST reference luminance meter is correlated to the scale transferred from the NIST standard photometers, the uncertainty due to the photometric scale is pulled out. The photometric scale does not need to be counted twice. Several uncorrelated components of uncertainty have been combined in one factor, c_{f}. A list of these uncertainty components and relative standard uncertainty are summarized in Table 35. Compared to the opal glasses, the color temperature of the reflected light is typically shifted very little due to the spectral reflectance of the plaque and decreases typically by 1 K. Table 36 shows a typical uncertainty budget for the calibration of a luminance source.

Table 35. Uncertainty components for reflectance plaque.

Symbol	Uncertainty component	Type	Relative Unc. Contribution (%)	
			Plaque	opal
c_{L}	Stability of the lamp during calibration	B	0.05	0.05
c_{U}	Illuminance nonuniformity at reflectance plaque ref. plane	B	0.10	0.03
c_{T}	Temperature correction of the photometer	B	0.03	0.03
$F^*(s_{\mathrm{ml}})$	SMCF for measuring lamp	B	0.03	0.03
$F^*(s_{\mathrm{mp}})$	SMCF for measuring plaque	B	0.03	0.03
c_{γ}	Angular alignment of the photometer measuring the lamp	B	0.005	0.005
c_{γ}	Angular alignment of the opal glass	B	0.005	0.005
c_{G}	Ref. luminance meter gain amplifier correction	B	0.02	0.02
c_{y}	Digital voltmeter calibration	B	0.008	0.008
c_{S}	Spatial stray light	B	0.05	0.02
$\boldsymbol{c_{\mathrm{f}}}$	**Reflectance plaque calibration correction factor**		0.135	0.084

Table 36. Uncertainty budget for a typical reference plaque luminance coefficient calibration.

Symbol	Component	Value x_i	Standard Uncertainty $u(x_i)$	Unit	Type	Sensitivity Coefficient c_i	Unc. Contribution $u_i(y)$
E	Illuminance	257.340	0.10265	lx	B	-0.0012	-1.27×10^{-4}
E_d	Illuminance dark	0.002	8.0×10^{-7}	lx	B	0.0012	9.87×10^{-10}
L	Luminance	81.945	0.174	cd/m^2	B	0.0039	6.75×10^{-4}
L_d	Luminance dark	0.004	8.5×10^{-7}	cd/m^2	B	-0.0039	-3.30×10^{-8}
c_f	Correction factor	1.00000	0.00141		B	0.3184	4.49×10^{-4}
q	**Luminance coefficient**	**0.3184**					**0.0010**
Rel. expanded uncertainty for reflectance plaque luminance coefficient cal. (k = 2)							**0.65 %**

6. Color temperature calibrations

6.1. General Description

Color temperature is a concept used to express the color of a light source in a simple manner using just one number. According to the CIE [18], color temperature is defined as "the temperature of a Planckian radiator whose radiation has the same chromaticity as that of a given stimulus." The spectral power distribution of the test source is not necessarily identical or even similar to that of a blackbody. Strictly speaking, however, the chromaticity coordinate of most of the light sources including incandescent lamps do not fall on the Planckian locus. The CIE definition does not say how close the chromaticity should be to be considered as "the same." Therefore, the definition of color temperature is somewhat vague, and this term is considered to be a general term to introduce the concept.

For practical calibration of sources used in photometry, either "distribution temperature" or "correlated color temperature" is used. Another similar concept is a radiance temperature, which is defined as "Temperature of the Planckian radiator for which the radiance at the specified wavelength has the same spectral concentration as for the thermal radiator considered" [18]. Radiance temperature is used only for blackbodies and transfer lamps to blackbodies.

Distribution temperature is defined as the "temperature of the Planckian radiator whose relative spectral distribution $S_t(\lambda)$ is the same or nearly the same as that of the radiation considered in the spectral range of interest" by CIE [18]. Practically speaking, distribution temperature is a concept to represent the relative spectral power distribution of a near Planckian source, such as an incandescent lamp, by one number. CIE [64] gives more precise definition of distribution temperature (T_d) given by the equation.

$$\min \int_{\lambda_1}^{\lambda_2} \left[1 - \frac{S_t(\lambda)}{a S_b(\lambda, T_d)} \right]^2 \mathrm{d}\lambda \text{ where } S_b(\lambda, T_d) = \frac{1}{\lambda^5 \left[\exp\left(\frac{c_2}{\lambda T_d} \right) - 1 \right]} . \quad (58)$$

The distribution temperature of the source with relative spectral distribution $S_t(\lambda)$ is the temperature T_d of the Planckian radiation $S_b(\lambda)$ when the value of Eq. (58) is minimized by varying T_d and normalization factor *a*. CIE also specifies that the wavelength region shall be 380 nm to 780 nm, and the wavelength interval for calculation shall be less than 10 nm. It is also specified that the difference of the relative spectral power distribution of the radiation considered and that of a Planckian radiation should be less than 10 % in order to use distribution temperature.

Correlated color temperature (T_c) is used for sources, such as discharge lamps, whose spectral power distribution is significantly different from that of Planckian radiation and is defined as the "temperature of the Planckian radiator whose perceived color most closely resembles that of a given stimulus at the same brightness and under specified viewing conditions" [18] Practically, T_c is obtained from the chromaticity coordinate (on the CIE 1960 u,v diagram) of the point on the Planckian locus which is at the closest distance from that of the light source in question [65].

If the relative spectral power distribution of the given radiation is identical to that of the Planckian radiator, the values of color temperature, T_d, and T_c are the same. The differences between distribution temperature and correlated color temperature for typical incandescent lamps are only 2 K or 3 K, but can be much larger depending on lamp type.

6.2. NIST color temperature scale

NIST has traditionally used the term "color temperature" for incandescent lamps even though their chromaticity coordinates are not exactly the same as the Planckian radiator. The NIST color temperature scale is based on the computation of T_c from the relative spectral power distributions of sources.

The NIST color temperature scale is derived from the NIST spectral irradiance scale [23, 24]. Spectral responsivity measurements are used to calibrate the response of a filter radiometer, which in turn is used to estimate the temperature of a blackbody radiator and hence provide the reference standard for spectral irradiance measurements. These reference standards, both for detectors and sources, are transferred to working standards for external calibrations, and used internally in deriving reference standards for colorimetric measurements. Three 1000 W FEL type quartz halogen lamps are maintained as the NIST color temperature primary standard lamps in the range of 2000 K to 3200 K. These lamps have demonstrated good stability of operation in this color temperature range [66]. The spectral irradiance of these lamps is calibrated periodically against the NIST spectral irradiance scale at 2000 K, 2300 K, 2600 K, 2856 K, and 3200 K. The correlated color temperatures of these lamps are computed from the spectral irradiance values according to the procedures recommended by reference [65].

The standard uncertainty of the correlated color temperature of these lamps has been evaluated using the methods described in references [67-69]. The standard uncertainty determined for the five correlated color temperature points is 1.0 K at 2000 K, 1.2 K at 2300 K,1.6 K at 2600 K,1.8 K at 2856 K, and 2.3 K at 3200 K.

6.3. Artifacts for calibration

For many years in the past, NIST issued 500 W Airway Beacon lamps as color temperature standards. These lamps are still accepted for recalibration at NIST. These lamps have medium bi-post bases, clear bulbs, and C-13B filaments. The lamp designation number is etched on the bulb. The appearance and the electrical polarity of this type of lamp are shown in Figure 11.

NIST now issues FEL type 1000 W quartz halogen lamps calibrated for color temperature. This is the same type of lamp used for luminous intensity standards. The lamps are potted on a medium bi-post base, and seasoned on DC power for at least 48 h at 8.4 A. The lamps are then tested for stability 3 times for 24 h at 7.2 A. Lamps are usually calibrated at a color temperature of 2856 K, but can be used for color temperature standards in the range of 2000 K to 3200 K. The operating current and voltage of the lamp are approximately 7.2 A and 85 V at 2856 K. The lamp designation numbers and the electrical polarity are engraved on an identification plate affixed on the lamp base as shown in Figure 11.

The burning position of the lamp with respect to the optical axis is critical to the transfer of correlated color temperature. Due to shadowing of the coiled-coiled filament, the angular distribution of the correlated color temperature fluctuates on the order of 8 K. The angular alignment of the reference lamp contributes a standard uncertainty of 1.5 K. Additionally the angular alignment of the lamp under test contributes a standard uncertainty of 1.5 K.

The reference lamps cannot be calibrated frequently enough to reduce the uncertainty of lamp aging to negligible. The reference lamps are calibrated after every 24 h of operation. The standard uncertainty due to lamp aging ranges from 0.7 K at 2000 K up to 1.8 K at 3200 K.

The uncertainty in the correlated color temperature due to the setting of the current has the following dependence,

$$T_c = T_0 \left(\frac{U \cdot c_U}{J_0 \cdot R} \right)^{m_\mathrm{T}} \quad . \tag{59}$$

where T_0 is the calibrated correlated color temperature, U is the measured voltage, c_U is the calibration factor for the digital voltmeter, J_0 is the calibrated current, R is the calibrated resistance of the shunt resistor, and m_T is the exponential dependence which has a value of 0.7 and a standard uncertainty of 0.05. The uncertainty in the correlated color temperature due to the fluctuation in the lamp is characterized by the fluctuation in the voltage over several operations of the lamp. The model for the fluctuation in the lamp is

$$T_c = T_0 \left(\frac{V}{V_0} \right)^{m_V} \quad . \tag{60}$$

where T_0 is the calibrated correlated color temperature, V is the measured voltage, V_0 is the average voltage, and m_V is the exponential dependence which has a value of 0.37 and a standard uncertainty of 0.05.

6.4. Equipment and instruments for calibration

Figure 28 shows the arrangement used for color temperature calibration. A PTFE plaque is placed in the photometry bench. The plaque is placed approximately 1 m from the lamp, and irradiated at normal incidence. The diffuse reflection at 45° is directed to a spectroradiometer. The plaque is mounted on a kinematic base, and can be removed when the luminous intensity is measured.

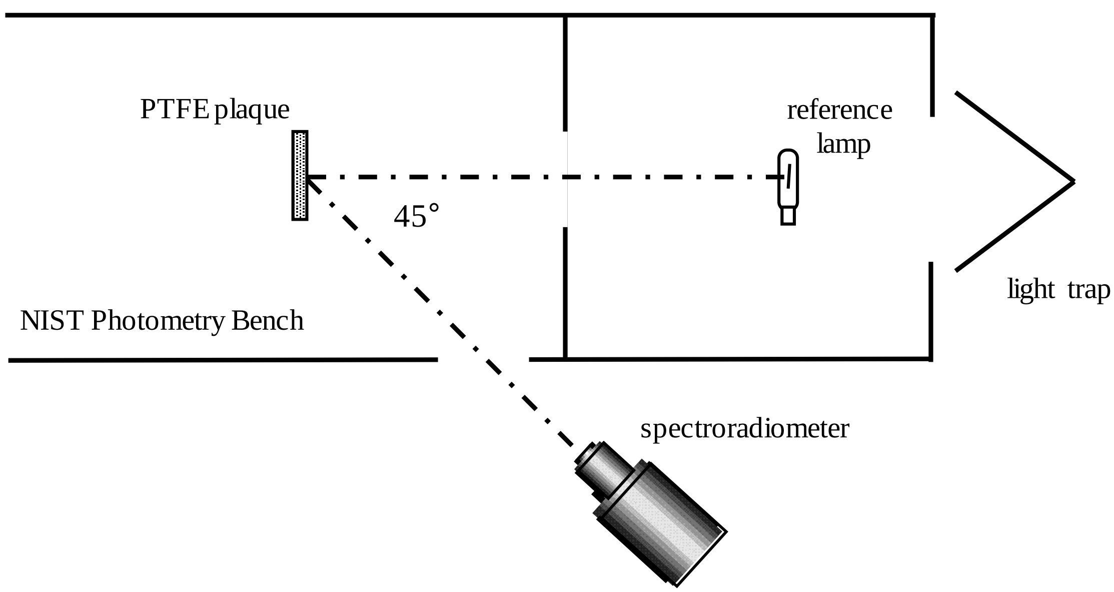

Fig. 28. Configuration for color temperature calibration.

The spectroradiometer is a diode-array system, consisting of imaging optics in front, a single diffraction grating, and a cooled photodiode array, and is calibrated against the NIST spectral irradiance standards. This spectroradiometer has measurement angles of 0.125° circular and 0.5°×1.5° rectangular. The rectangular aperture is used for color temperature calibrations. The short measurement time (normally less than 10 s) of the spectroradiometer allows for the determination of the operating current of a lamp for a specified color temperature precisely within a few min, minimizing the labor time and the lamp burning time. The spectroradiometer calculates chromaticity coordinates and the correlated color temperature of the source.

This type of spectroradiometer, however, is subject to fairly large stray light errors due to a single diffraction grating installed in a compact unit. When the radiometer is calibrated using a 2856 K Planckian source, there will be errors when sources of different color temperatures are measured. For calibrations at NIST, therefore, this spectroradiometer is used basically to transfer the same color temperature from the standard lamp to the test lamp. For this reason, the color temperature standards for several different color temperatures are maintained.

Since the procedures for the spectral calibration of the instrument are not simple and the responsivity of the spectroradiometer is fairly stable over a long period of time, prior to each calibration of test lamps, the spectroradiometer's color temperature reading is calibrated by measuring two color temperature working standard lamps, and correction values as shown in Figure 29 is determined and applied to the measured values. If the measurement point lies between the calibration points of the standard lamps, the correction value is determined by interpolation based on the second order polynomial function. The uncertainty for correlated color temperature calibrations other than the set points of 2000 K, 2300 K, 2600 K, 2856 K, and 3200 K has the additional uncertainty component due to the prediction band analysis.

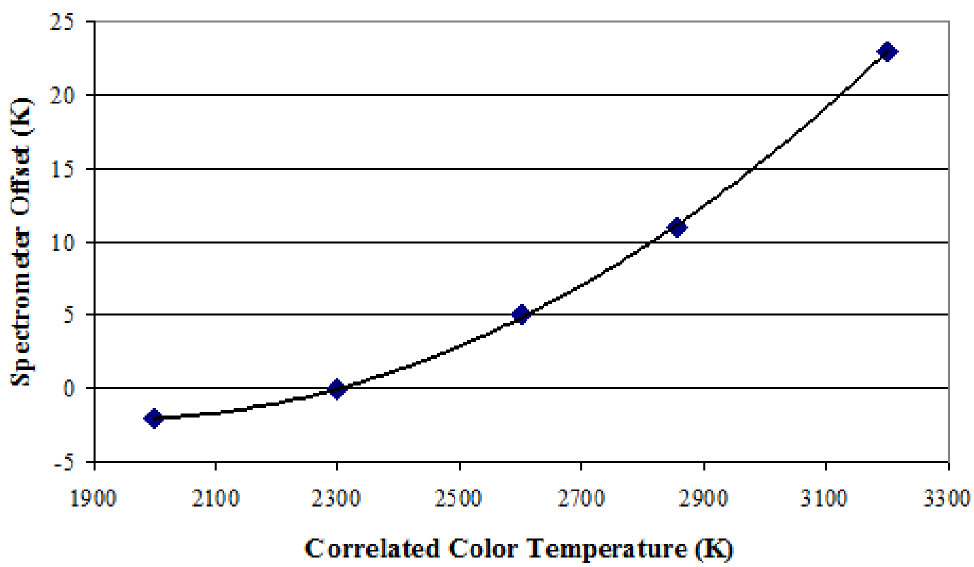

Fig. 29. Color temperature correction values for the NIST diode-array spectroradiometer.

The equipment and arrangement for the calibration has two significant components of uncertainty. The first component due to the arrangement is the 1 m distance between the lamp and the plaque, which is different from the distance of 50 cm specified for the calibrated reference lamp. The uncertainty was analyzed by scanning the area at 50 cm and the area at 1 m using a fiber optic spectrometer with an opal glass input optic. The correction factor for this difference in distance is zero and the standard uncertainty ranges from 1.1 K for 2000 K to 2.3 K for 3200 K. The second component due to equipment is the spectral stray-light errors that occur within the spectroradiometer. Reference [70] describes the spectral stray-light errors and method for correcting. The correction factor for stray light is zero with the standard uncertainty of 1.0 K.

6.5. Calibration procedures

Prior to the measurement of test lamps, the spectroradiometer's color temperature reading is calibrated against two color temperature working standard lamps at the color temperature points required for the calibration. The test lamp is mounted on the photometry bench and aligned with the same procedure as the luminous intensity measurements. The lamp is operated in the base-down position, with the identifying number on the opposite side from the spectroradiometer. Lamp orientation is accomplished by aligning the lamp socket so that the lamp posts are held vertically, and the plane formed by the axes of the posts is perpendicular to the optical axis of the spectroradiometer. An alignment jig (a mirror mounted on a bi-post base to be parallel to the plane formed by the axes of the posts) is used in combination with a laser and an end-viewing telescope. The distance from the lamp to the input optics (a PTFE plaque) of the spectroradiometer is approximately 1 m.

The lamp is operated on DC power. The electrical polarity is marked on the identification plate of the lamp. The test lamp is slowly (≅30 s) ramped up to the specified current, and allowed to stabilize for at least ten minutes before calibration. When a lamp current is to be determined for a specified color temperature, the lamp current is adjusted repeatedly until the spectroradiometer indicates the specified color temperature. The lamp current and voltage are recorded when the lamp reaches that color temperature. When the same lamp is calibrated for different color temperatures, at least 3 min are allowed before any measurements after the lamp current is changed from one color temperature to another.

Color temperature calibrations at NIST are most often done at 2856 K. Requests for calibration at any other color temperatures from 2000 K to 3200 K are accepted.

6.6. Uncertainty of correlated color temperature calibration

The offset calibration for the transfer spectroradiometer is done at five specific correlated color temperatures. The uncertainty analysis of the offset calibration uses the model.

$$O_{\mathrm{T}} = (T_0 - T_c)\left(\frac{U \cdot c_{\mathrm{U}}}{J_0 \cdot R}\right)^{m_{\mathrm{T}}}\left(\frac{V}{V_0}\right)^{m_{\mathrm{V}}} + L_{\mathrm{f}} + D + \phi_{\mathrm{L}} \quad . \tag{61}$$

where L_{f} is uncertainty due to the aging stability of the lamps, D is the uncertainty due to distance correction factor, and φ_L is the uncertainty due to angular alignment of the lamp. Table 37 summarizes uncertainty budget for calibration of the spectrometer at 2856 K where J_0 is 7.230 A.

Table 37. Uncertainty budget for the offset calibration of the transfer spectroradiometer at 2856 K.

Symbol	Component	Value x_i	Standard Uncertainty $u(x_i)$	Unit	Type	Sensitivity Coefficient c_i	Unc. Contribution $u_i(y)$
T_0	Calibrated color temp.	2856	1.8	K	B	1.00	1.8
T_c	Measured color temp.	2845	0.6	K	A	-1.00	-0.6
U	Shunt voltage	0.72300	2.1×10^{-6}	V	A	10.7	2.2×10^{-5}
c_U	Voltmeter calibration	1.0	0.00004		B	0.06	2.3×10^{-6}
R	Shunt resistance	0.10001	1.3×10^{-6}	Ω	B	-0.006	-8.3×10^{-9}
m_T	Current dependence	0.70	0.05		B	0.0005	2.4×10^{-5}
V	Lamp voltage	84.356	0.00041	V	A	0.05	2.0×10^{-5}
m_V	Voltage dependence	0.37	0.05		B	5.5×10^{-5}	2.7×10^{-6}
L_f	Aging of the lamps	0	1.5	K	B	1.00	1.5
D	Distance correction	0	2.0	K	B	1.00	2.0
ϕ_L	Lamp angular alignment	0	1.5	K	B	1.00	1.5
O_T	**Temperature offset**	**11**					**3.48**
Expanded uncertainty for spectroradiometer temperature offset cal. at 2856 K (*k* = 2)							**7.0 K**

Typical offsets and the standard uncertainty of the offset calibration are shown in Table 38. To set the current of a submitted lamp at an arbitrary correlated color temperature, the offset is determined from a second order polynomial that is fit to the offsets of the five correlated color temperatures from the reference lamps. The uncertainty of the offset for the arbitrary correlated color temperature is determined from a prediction band analysis. The uncertainty analysis of the correlated color temperature calibration for a lamp under test uses the model,

$$T_c = (T_m - O_T)\left(\frac{U \cdot c_U}{J_0 \cdot R}\right)^{m_T}\left(\frac{V}{V_0}\right)^{m_V} + S_L + \phi_L \ . \qquad (62)$$

where T_m is the measured correlated color temperature, O_T is the offset calibration of the spectrometer determined from the polynomial fit, and S_L is the stray light correction factor. Table 39 summarizes uncertainty budget for calibration of the spectrometer at 2856 K where J_0 is 7.230 A.

Table 38. Typical offsets and standard uncertainties of the offsets.

T_{cp}	Offset	Standard uncertainty
2000 K	-2 K	2.3 K
2300 K	0 K	2.7 K
2600 K	5 K	3.1 K
2856 K	11 K	3.5 K
3200 K	23 K	4.0 K

Table 39. Uncertainty budget for the correlated color temperature calibration at 2856 K.

Symbol	Component	Value x_i	Standard Uncertainty $u(x_i)$	Unit	Type	Sensitivity Coefficient c_i	Unc. Contribution $u_i(y)$
T_m	Measured color temp.	2845	0.6	K	A	1.00	0.6
O_T	Temperature offset	11	3.5	K	B	-1.00	-3.5
U	Shunt voltage	0.72300	2.1×10^{-6}	V	A	10.7	2.2×10^{-5}
c_U	Voltmeter calibration	1.0	0.00004		B	0.06	2.3×10^{-6}
R	Shunt resistance	0.10001	1.3×10^{-6}	Ω	B	-0.006	-8.3×10^{-9}
m_T	Current dependence	0.70	0.05		B	0.0005	2.4×10^{-5}
V	Lamp voltage	84.356	0.00041	V	A	0.05	2.0×10^{-5}
m_V	Voltage dependence	0.37	0.05		B	5.5×10^{-5}	2.7×10^{-6}
S_L	Stray light	0	1.0	K	B	1.00	1.0
γ_L	Lamp angular alignment	0	1.5	K	B	1.00	1.5
T_c	**Color temperature**	**2856**					**3.96**
Expanded uncertainty for correlated color temperature calibration at 2856 K (*k* = 2)							**7.9 K**

7. Flash photometer calibrations

7.1. General description

To achieve accurate flashing-light measurements, a luminous exposure unit has been realized at NIST for calibration of flash photometers. Four flash standard photometers equipped with current integrators were built and calibrated against the NIST illuminance standard photometers. Two different approaches have been taken to calibrate these standard photometers; one based on electrical calibration of the current integrator, and the other based on electronic pulsing of a steady-state photometric standard. The units realized using the two independent methods were intercompared, and the uncertainty of the luminous exposure unit realization was evaluated. A procedure for calibration of flashing-light photometers for anticollision flashing lights has also been established and is described below.

7.2. Methods for realization of the luminous exposure unit

Two independent methods were employed to derive the luminous exposure unit [lx·s] to allow verification of the uncertainty of the realized unit. With either method, the unit [lx·s] has been derived from the NIST illuminance unit [lx] based on the following analyses.

7.2.1. Electrical method

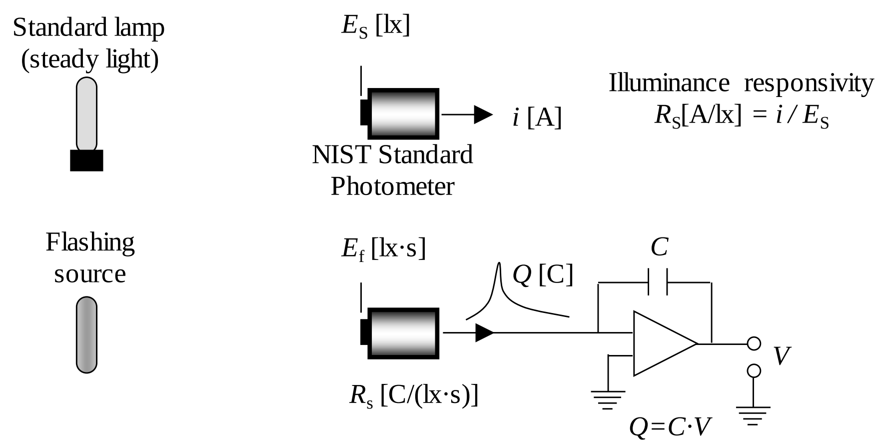

Fig. 30. Derivation of the luminous exposure unit using the electrical method.

Figure 30 shows the principle of this method. A standard photometer consisting of a photodiode and a $V(\lambda)$ filter is first calibrated for illuminance responsivity using an illuminance standard (steady light). The responsivity of this photometer for luminous exposure is equal in magnitude to the illuminance responsivity and has the units C/(lx·s) since the ampere is coulomb per second. To measure a flashing light, the standard photometer is connected to a current integrator. The photometer output current is integrated using a capacitor with capacitance C. The output voltage V is related to the electric charge Q in the capacitor and the capacitance C by the formula,

$$V = Q/C \ . \tag{63}$$

The luminous exposure E_f is given by

$$E_f = Q/R_S \ . \tag{64}$$

From Eqs. (63) and (64), the responsivity R_f [V/(lx·s)] of the photometer including the current integrator is given by

$$R_f = R_S / C \ . \tag{65}$$

From the output voltage of the current integrator, the luminous exposure E_f is obtained by

$$E_f = V / R_f \ . \tag{66}$$

The subscripts s and f in the variables represent steady light and flashing light, respectively. As shown in Eq. (65), the derivation of the luminous exposure unit from the steady-state photometric unit in this method depends on the calibration of the feedback capacitor for the capacitance C.

7.2.2. Pulsed photometry method

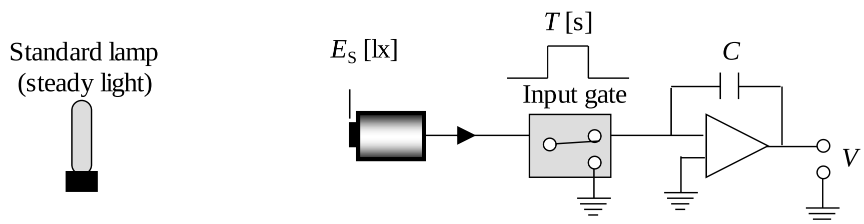

Fig. 31. Derivation of the luminous exposure unit using the pulsed photometry method.

This method is an improvement over the well-known chopper method. Instead of using a light chopper, an electronic gate is used for much higher accuracy in the calibration. Figure 31 shows the principle of this method. The standard photometer is connected to a current integrator which has an input gate controlled by an accurate time base. The photometer head is placed at a point of known illuminance E_s [lx] under steady light illumination, and the input gate opens for T [s], and the output voltage V [V] is measured. The capacitor in the integrator is completely discharged before opening the gate. The responsivity R_f [V/(lx·s)] of the photometer including the current integrator is given by

$$R_f = V / (E_S \cdot T). \tag{67}$$

In this method, the capacitance of the feedback capacitor of the integrator needs not be known. Instead, the calibration accuracy depends on the accuracy of the time base. It should be noted that the photometer output should never be left open (no-load condition) before an integration starts. The no-load condition would yield an open voltage from the photodiode, which would then create an additional charge in the photodiode junction capacitor and in the stray capacitors of the wires. These electric charges would flow into the integrator when the photodiode is connected and cause a serious error.

7.3. Flash standard photometers

Four flash photometers have been built for use as the primary standards for luminous exposure measurements at NIST. Each flash standard photometer head consists of a precision aperture, $V(\lambda)$ filter, a silicon photodiode, and is equipped with a thermoelectric device which maintains the photodiode/filter temperature at 25 °C ± 0.1 °C and a current-integrator unit. For calibration with steady light, the photometers are also equipped with detachable current-to-voltage converters, which have gain settings from 10^4 [V/A] to 10^{10} [V/A] and are calibrated with an uncertainty of 0.02 %. This integrator operates in two modes: calibration mode (for the pulsed photometry method) and measurement mode (for flashing light). The main integrator has three ranges (1000 lx·s, 100 lx·s, and 10 lx·s) and are capable of measuring over two orders of magnitude at each range with sufficient signal-to-noise ratios, thus covering a measurement range over four orders of magnitude. The flash of an anticollision flashing light repeats at a rate of approximately 1 s^{-1}. Therefore, the photometer operation must synchronize with the timing of the flashes. An additional photometer head is used to detect the starting of the flashes and to feed the signals (FLASH) to the integrator for synchronized operation. The current integrator is interfaced to a computer so that the data acquisition is also synchronized.

The circuit operates as follows. The START signal initiates discharge of the capacitors for 50 ms. In calibration mode, integration starts and continues for exactly 1 s. In the measurement mode, integration starts before the start of a flash and continues until a certain time (50 ms to 200 ms) after the start of the flash. In this way, the circuit will not miss the rising edge of the pulse. The measurement of the output voltages by the digital voltmeter starts immediately after integration has ended. Thus, each flash is measured and data is stored in the computer while measuring as many flashes as necessary. There are small dark readings due to the input bias current and the offset voltage of the operational amplifier. The dark readings of the integrators are almost negligible (less than 0.1 %) at illuminance levels higher than 100 lx·s, but need to be corrected at lower illuminance levels, especially with integration for 1 s. The dark readings are taken in the DARK mode, in which the circuit is operated with the input gate switch kept open. At illuminance levels lower than 1 lx·s, the dark readings need to be corrected by light-dark measurement because the readings by the DARK mode are not exactly the same as the light-dark readings due to the shunt resistance of the photodiode. The 1 s time base is a quartz-based timer, and its pulse width was calibrated using a calibrated frequency counter to be 1.0000 s ± 0.0001 s. The operate/release time of the reed relays including bouncing is included in the uncertainty budget. It is important that the photodiode output be grounded before integration starts, particularly in calibration mode. To achieve this, the gate switch and the discharge switch are both closed before starting the integration. The integration is started by opening the discharge switch, and integration is ended by opening the gate switch.

The responsivities of the four NIST flash standard photometers were calibrated using the two methods described. For the electrical method, under illumination by a 1000 W quartz halogen lamp operated at 2856 K, the photometer heads were first calibrated against the NIST illuminance standard photometers to determine the illuminance responsivities of the photometer heads. The capacitances of the feedback capacitors of all of the current integrators were calibrated using a calibrated current source having an uncertainty of 0.065 %. The current offset of the source was corrected by zero readings. A current y [A] is fed to the detector input, and the current integrator was operated in the calibration mode (1 s integration). With the duration of the time base T [s] and the output voltage V [V], the capacitance C [F] of the feedback capacitor is given by

$$C = yT/V \ . \tag{68}$$

During repeated measurements of the same capacitors, noticeable changes (less than a few tenths of a percent) of the measured capacitance values were observed, the reason for which was determined to be temperature dependence of the capacitors. To assure the capacitances of the feedback capacitors to be stable, all of the current integrator units were warmed up for more than two hours before use. To verify the accuracy of the capacitance calibration mentioned above, the capacitors of one of the units were also officially calibrated by the NIST Quantum Measurement Division. The calibration was performed using a capacitor bridge at 1 kHz with an uncertainty of 0.05 %, with the capacitors under test installed on the circuit board so that all the stray capacitances of wires are included. The differences between the two methods may arise from the reed relay operating time and the difference in the measurement frequency. The uncertainty of the capacitance measurement using the current source is assessed to be 0.15 % from this comparison of results. The responsivities R_f [V/(lx·s)] of the flash standard photometers at each range were determined using Eq. (65).

For the pulsed photometry method, the flash standard photometers were calibrated under illumination by a 1000 W quartz halogen lamp operated at 2856 K, with the current integrator operated in the calibration mode using the 1 s time base. The illuminance was determined with the NIST illuminance standard photometers, and the responsivities R_f of the flash standard photometers were determined using Eq. (65). Table 40 shows the results of the calibration of the flash standard photometers using the two methods. The flashing-light responsivities R_f of the four photometers in the three ranges, determined with the two independent methods, agreed to within 0.2 %, well within the uncertainty of calibration. Both methods proved to be appropriate for this purpose

Table 40. Results of the flash standard photometers calibration using the two methods.

Range	Method	Luminous exposure responsivity [V/(lx·s)]			
		#1	#2	#3	#4
1000	Electrical method	0.010489	0.010546	0.010670	0.010688
	Pulsed photometry	0.010478	0.010538	0.010672	0.010689
Ratio		**1.0011**	**1.0008**	**0.9998**	**0.9999**
100	Electrical method	0.10777	0.10438	0.10726	0.10449
	Pulsed photometry	0.10767	0.10431	0.10727	0.10447
Ratio		**1.0010**	**1.0007**	**1.0000**	**1.0003**
10	Electrical method	1.0309	1.0362	1.0531	1.0556
	Pulsed photometry	1.0299	1.0341	1.0534	1.0540
Ratio		**1.0009**	**1.0021**	**0.9997**	**1.0015**

One component of uncertainty analyzed over the last nine years is the long-term stability of the NIST flash standard photometers including the current-integration circuit units. The unit realization is performed every year on three of the NIST flash standard photometers as shown in Figure 32 and the average luminous exposure responsivity changed < 0.5 % over a nine year period.

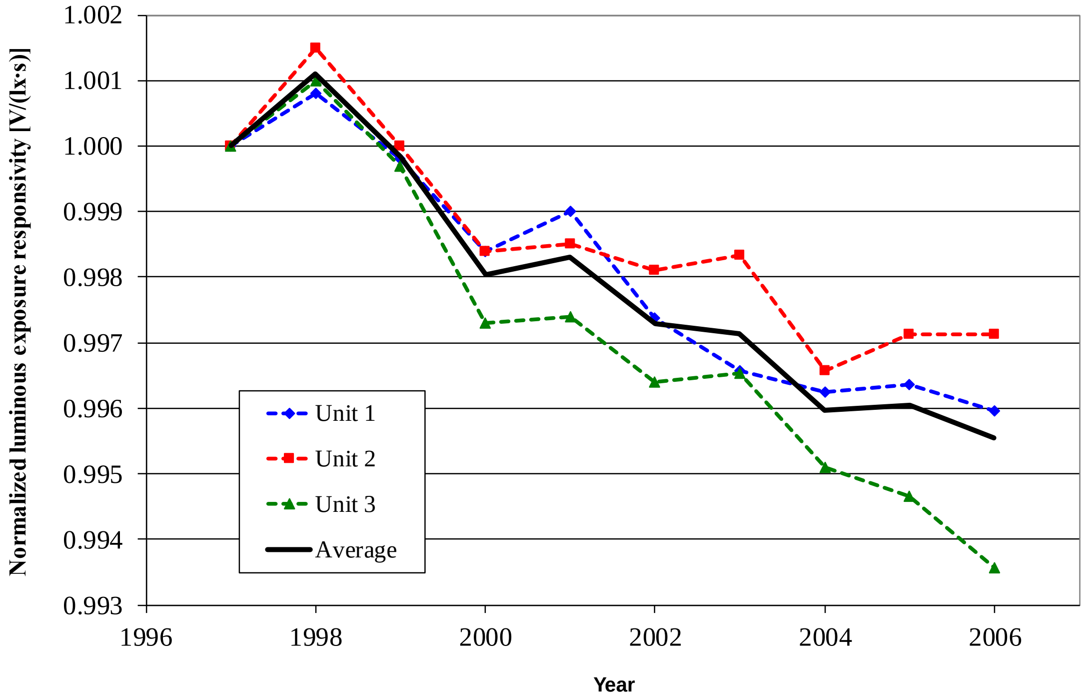

Fig. 32. The normalized luminous exposure responsivity [V/(lx·s)] of the three NIST flash photometers that maintain the unit.

7.4. Calibration scheme for flash photometers

Since xenon flashing-light sources do not reproduce their photometric values well enough as calibration sources, typically photometers are submitted to be calibrated against NIST standard flash photometers. An arrangement as shown in Figure 33 is used to perform the calibration of flash photometers submitted by customers. The measurements are made on the NIST photometry bench. A xenon anticollision flashing light is used as a source to provide luminous exposure, and photometers are calibrated for both white (Xenon) and red (Aviation Red) flashing lights. Figure 34 shows the spectral power distributions of the xenon flashing-light source and filtered red flashing-light source used in this calibration. Calibration in two colors also provides some information on the $V(\lambda)$ matching of the photometer under test. Calibrations are normally performed at two luminous exposure levels (100 lx·s and 10 lx·s) for white anticollision flashing light so that the linearity of the test photometer can be checked. These luminous exposure levels correspond to effective intensities of 5000 cd and 500 cd at a photometric distance of 3.3 m, respectively. (The required minimum level from the FAA, or Federal Aviation Administration, for white anticollision flashing lights is 400 cd.) A neutral density filter along with a larger aperture is inserted in the optical path to adjust the luminous exposure level, and an Aviation Red filter is inserted to conduct the calibration for the red anticollision flashing light. The photometer under test is calibrated by substitution with the NIST flash standard photometers. A monitor photometer is used to monitor the variations of individual flashes while substituting the standard photometer and a test photometer to allow corrections. The uncertainty of the calibration depends largely on the repeatability and the linearity of the photometer under test, and therefore, is reported individually.

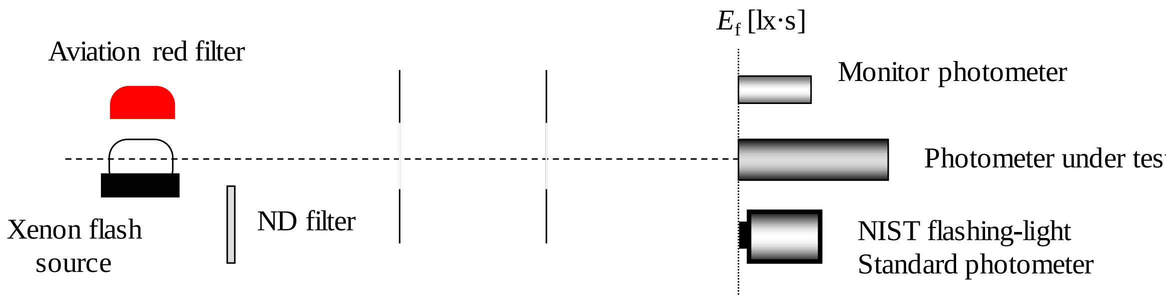

Fig. 33. Arrangement for the calibration of flash photometers.

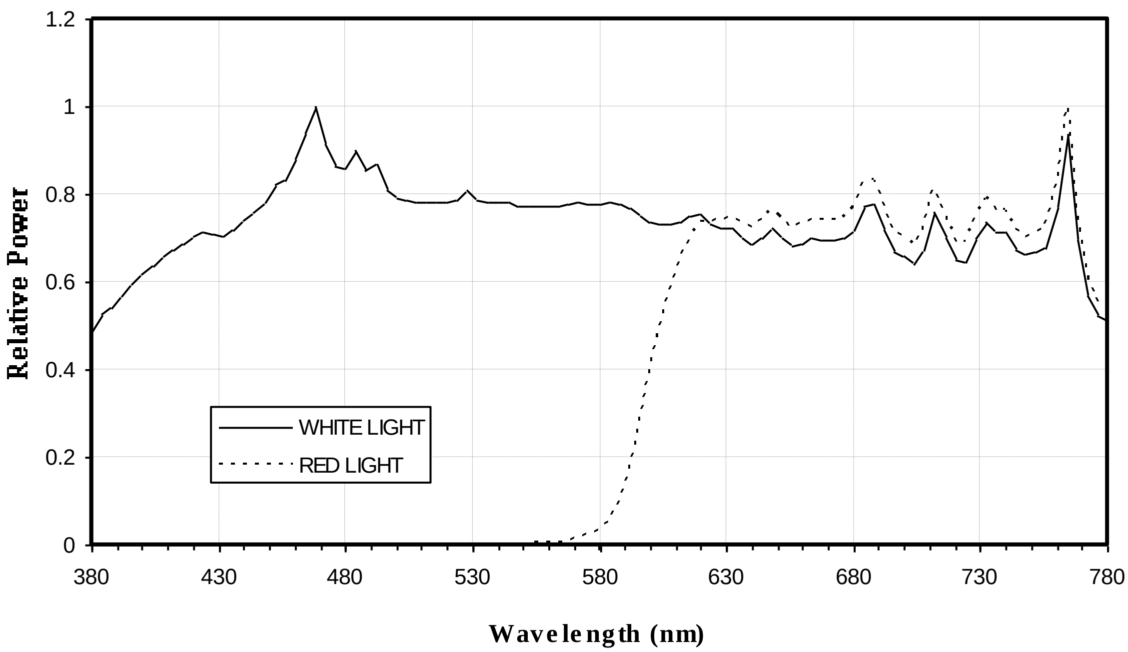

Fig. 34. The spectral power distributions of the xenon flashing-light source and filtered red flashing-light source used in this calibration.

Photometers under test are calibrated for their luminous exposure responsivities. However, many of the anticollision flashing light photometers only indicate effective intensity. The calibration of such instruments is handled as follows. The effective intensity is five times the time-integrated luminous intensity for all four methods for a very narrow, single pulse, as one emitted by a xenon flash tube. For calibrations at NIST, the effective intensity is defined by the Blondel-Rey equation:

$$I_{\mathrm{e}} = \frac{\int_{t_0}^{t_1} I(t)\mathrm{d}t}{(0.2 + t_1 - t_0)} \, , \tag{69}$$

where t_0 is the start time and t_1 is the end time of the flash. The term 0.2 s is the Blondel-Rey constant. The effective intensity is defined as the luminous intensity of a steady-state light source which gives equivalent detectability to that of a given pulse of light. If a flash photometer indicates effective intensity, the photometric distance (the distance between the photometer and the source) should be specified for the instrument. With the specified photometric distance d, the luminous exposure E_{f} is calculated from the reading of the effective intensity I_{e} by

$$E_{\mathrm{f}} = (0.2 + t_1 - t_0) I_e \big/ d^2 \; . \tag{70}$$

The duration (t_1 - t_0) can be neglected in the practical measurements of xenon anticollision lights because the durations of most xenon anticollision lights are normally 1 ms or less and because there is no clear definition of the duration of a flash. Also, many types of commercial flash photometers are not equipped with a means to measure the duration of flashes. Thus, photometers that only indicate effective intensity can be calibrated against standard flash photometers for luminous exposure responsivities rather than against standard sources of effective intensity. There is no need for measuring the real distance between the calibration source and the photometer in the calibration setup, and the calibration source needs not to have an excellent reproducibility since the calibration is performed using the detector-based procedure. The reference plane of the test photometer head should be clearly defined by the user so that it can be aligned precisely to the same position as that of the standard flash photometer.

7.5. Uncertainty analysis of luminous exposure and flash photometer calibrations

The uncertainty analysis for the luminous exposure responsivity, R_{f}, of the NIST standard flash photometer including the current integrator using the electrical method follows the model.

$$R_{\mathrm{f}} = \frac{R_{\mathrm{s}}}{C} \cdot D_{\mathrm{L}} \; . \tag{71}$$

where R_{s} is the illuminance responsivity of the NIST standard flash photometer calibrated using a steady lamp, C is the capacitance of the feedback capacitor of the current integrator, and D_{L} is a correction factor for the linearity of the detector. The uncertainty budget for luminous exposure responsivity using the electrical method is shown in Table 41.

Table 41. Uncertainty budget for luminous exposure responsivity using the electrical method.

Symbol	Uncertainty component	Type	Relative Unc. Contribution (%)
R_S	Illuminance responsivity of NIST standard flash photometer	B	0.22
C	Capacitance of the current integrator	B	0.15
D_L	Factor for the linearity of the detector	B	0.10
R_f	Rel. combined std. uncertainty for luminous exposure resp.		**0.280**

The uncertainty analysis for the luminous exposure, E_f, determined using the NIST standard flash photometer including the current integrator using the electrical method follows the model

$$E_f = \frac{V \cdot c_v}{R_f} \cdot c_D \cdot F^* \cdot c_T \cdot c_S \cdot c_\gamma \ , \tag{72}$$

where V is the current integrator signal, c_v is the voltmeter correction factor, R_f is the illuminance responsivity of the NIST standard flash photometer calibrated using a steady lamp, c_D is the short-term stability of the capacitors which includes the signal decay over 1 s, F^* is the SMCF, c_T is the temperature sensitivity of the photometer, c_S is the stray light correction factor, and c_γ is the angular alignment of the detector. The uncertainty budget for luminous exposure responsivity using the electrical method is shown in Table 42.

Table 42. Uncertainty budget for the luminous exposure unit using the electrical method.

Symbol	Uncertainty component	Type	Relative Unc. Contribution (%)
V	Current integrator signal	A	0.050
c_{v}	Voltmeter correction factor	B	0.008
R_{f}	Illuminance responsivity of the standard flash photometer	B	0.284
c_{D}	Short term stability of the capacitors	B	0.100
F^*	SMCF	B	0.010
c_{T}	Temperature sensitivity of the photometer	B	0.100
c_{S}	Stray light correction factor	B	0.011
c_{γ}	Angular alignment of the detector	B	0.002
E_{f}	Rel. combined std. uncertainty for time-integrated illuminance		**0.32**
Relative expanded uncertainty for luminous exposure (*k* = 2)			**0.64 %**

The uncertainty analysis for the luminous exposure responsivity, R_{f}, of the NIST standard flash photometer including the current integrator using the pulsed photometric method follows the model

$$R_{\mathrm{f}} = \frac{V \cdot c_v}{E_S \cdot T} \cdot c_D \cdot D_{\mathrm{L}} \quad , \tag{73}$$

where V is the current integrator signal, c_{v} is the voltmeter correction factor, E_{S} is the illuminance on the reference plane of the NIST standard flash photometer using a steady lamp, T is the time period when the input gate is open, c_{D} is the short-term stability of the capacitors which includes the signal decay over 1 s, and D_{L} is a correction factor for the linearity of the detector. The uncertainty budget for luminous exposure responsivity using the pulsed photometric method is shown in Table 43.

Table 43. Uncertainty budget for luminous exposure responsivity using the pulsed photometric method.

Symbol	Uncertainty component	Type	Relative Unc. Contribution (%)
V	Current integrator signal	A	0.01
c_v	Voltmeter correction factor	B	0.00
E_S	Illuminance on the NIST standard flash photometer	B	0.22
T	Time input gate is open	B	0.01
c_D	Short term stability of the capacitors	B	0.10
D_L	Factor for the linearity of the detector	B	0.10
R_f	Rel. combined std. uncertainty for luminous exposure resp.		**0.28**

The uncertainty analysis for the luminous exposure, E_f, determined using the NIST standard flash photometer including the current integrator using the pulsed photometric method follows the model presented in Eq. (72). The relative expanded uncertainty for luminous exposure using the pulsed photometric method is 0.64 % (k = 2).

The uncertainty analysis for the calibration for a flash photometer follows the model,

$$R = \frac{E_T \cdot R_M \cdot R_f}{V_M \cdot c_V} \cdot c_L \cdot F^* \cdot c_U \cdot c_d \cdot c_T \cdot c_S \cdot c_\gamma, \tag{74}$$

where R is the luminous exposure responsivity of the test flash photometer, E_T is the luminous exposure measured by the flash photometer under test, R_f is the luminous exposure responsivity of the NIST standard flash photometers using the pulsed photometric method, V_M is the current integrator signal for the monitor photometer, R_M is the ratio of the monitor photometer to the NIST standard flash photometer, c_L is the long-term stability of the NIST standard flash photometer, F^* is the SMCF for xenon or Aviation red light, c_U is the correction factor for the luminous exposure non-uniformity, c_d is the correction factor for the distance difference between the reference planes of the NIST standard flash photometer and the flash photometer under test, c_T is the temperature stability of the monitor photometer, c_S is the stray light correction factor, and c_γ is the angular alignment correction factor for the flash photometer under test. The uncertainty budget for calibration of luminous exposure responsivity using the pulsed photometric method is shown in Table 44.

Table 44. Uncertainty budget for calibration of luminous exposure responsivity using the pulsed photometric method.

Symbol	Uncertainty component	Type	Relative Unc. Contribution (%)
E_{T}	Luminous exposure	B	0.05
R_{f}	Luminous exposure resp. of NIST standard flash photometer	B	0.27
V_{M}	Current integrator signal for monitor photometer	A	0.04
c_V	Voltmeter correction factor	B	0.00
R_{M}	Ratio of the monitor photometer to the standard photometer	B	0.11
c_{L}	Long-term stability of the NIST standard flash photometer	B	0.25
F^*	SMCF	B	0.20
c_{U}	Time-integrated illuminance non-uniformity	B	0.10
c_d	Distance difference between reference planes	B	0.03
c_T	Temperature stability of the monitor photometer	B	0.01
c_S	Stray light correction factor	B	0.05
c_γ	Angular alignment for the flash photometer under test	B	0.01
R	Relative combined standard uncertainty for luminous exposure responsivity		**0.45**
Relative expanded uncertainty for luminous exposure responsivity (*k* = 2)			**0.89 %**

References

[1] Booker, R.L. and McSparron, D.A., "Photometric Calibrations," *NBS Special Publication* **250**-15 (1987).

[2] Cromer, C.L., Eppeldauer, G., Hardis, J.E., Larason, T.C. and Parr, A.C., "National Institute of Standards and Technology detector-based photometric scale," *Applied Optics*, **32**-16, 2936-2948 (1993).

[3] Ohno, Y., Cromer, C.L., Hardis, J.E., and Eppeldauer, G., "The Detector-based Candela Scale and Related Photometric Calibration Procedures at NIST," *The Journal of the Illuminating Engineering Society of North America*, **23**-1, 88-98 (1994).

[4] Ohno, Y., "Detector-Based Luminous Flux Calibration using the Absolute Integrating-Sphere Method," *Metrologia*, **35**-4, 473-478 (1998).

[5] Taylor, B.N. and Kuyatt, C.E., "Guidelines for Evaluating and Expressing the Uncertainty of NIST Measurement Results," *NIST Technical Note* **1297** (1994).

[6] NIST, "Calibration Services Users Guide SP 250 Appendix Fee Schedule," *Special Publication* **250**, https://www.nist.gov/sites/default/files/documents/2017/01/13/feeschedule2017.pdf.

[7] CIE Compte Rendu, p. 67 (1924).

[8] CIE Compte Rendu, Table II, pp. 25-26 (1931).

[9] CIE, "Colorimetry – Part 1:CIE Standard Colorimetric Observers," *CIE Standard S014-1/E:2006* (2006).

[10] CIE, "The Basis of Physical Photometry," *CIE Publication No.18.2* (1983).

[11] CIPM, Comité Consultatif de Photométrie et Radiométrie 10e Session–1982, Bureau International Des Poids et Mesures, Pavillon de Breteuil, F-92310, Sèvres, France (1982). The same content is published in BIPM Monographie - Principles Governing Photometry (1983), Bureau International Des Poids et Mesures, Pavillon de Breteuil, F-92310, Sèvres, France.

[12] CIE Disk D001 Photometric and Colorimetric Tables (1988).

[13] CGPM, "Comptes Rendus des Séances de la 16e Conférence Générale des Poids et Mesures," Paris, Bureau International des Poids et Mesures, F-92310 Sèvres, France, p. 10 (1979).

[14] CIE Compte Rendu, Vol. **3**, Table II, pp. 37-39 (1951).

[15] CIPM Procés-Verbaux **44**, 4 (1976).

[16] CIE, "Mesopic photometry: History, special problems and practical solutions," *CIE Publication No. 81* (1989).

[17] CIE, "Vision and Lighting in Mesopic Conditions," *Proceedings of the CIE Symposium*, CIE x028:2005, León, Spain (2005).

[18] CIE, "CIE International Lighting Vocabulary," *CIE Publication No. 17.4* (1987).

[19] ISO, "Quantities and units: ISO Standards Handbook," Third edition (1993).

[20] Taylor, B.N., Editor, "Interpretation of the SI for the United States and Metric Conversion Policy for Federal Agencies," *NIST Special Publication* **814**, (1991).

[21] Taylor, B.N., "Guide for the use of the International System of Units (SI)," *NIST Special Publication* **811**, (1995).

[22] Illuminating Engineering Society of North America, "The IESNA Lighting Handbook 9th Edition: Appendix," pp. 5-7 (2000).

[23] Walker, J.H., Saunders, R.D., Jackson, J.K., and McSparron, D.A., "Spectral Irradiance Calibrations," *NBS Special Publication* **250**-20 (1987).

[24] Yoon, H.W., Gibson, C.E., and Barnes, P.Y., "The realization of the NIST Detector-based Spectral Irradiance Scale," *Metrologia*, **40**, S172-S176 (2003).
[25] Mielenz, K.D., Saunders, R. D., Parr, A. C., and Hsia, J. J., "The new international temperature scale of 1990 and its effect on radiometric, photometric, and colorimetric measurements and standards," *CIE Proceedings 22nd Session 1-1*, Melbourne 1991, Div.2, 65-68 (1991).
[26] Houston, J.M., Rice, J.P., "NIST reference cryogenic radiometer designed for versatile performance," *Metrologia*, **43**, S31-S35 (2006).
[27] Gentile, T.R., Houston, J.M., Hardis, J.E., Cromer, C.L., and Parr, A.C., "The NIST High-Accuracy Cryogenic Radiometer," *Applied Optics* **35**-7, 1056-1068 (1996).
[28] Larason, T.C., Bruce, S.S., and Parr, A.C., "Spectroradiometric Detector Measurements: Part I - Ultraviolet Detectors and Part II: Visible to Near-Infrared Detectors," *NIST Special Publications* **250**-41, U.S. Government Printing Office, Washington, D.C. (1998).
[29] Physikalisch-Technische Bundesanstalt (PTB), *PTB Report*, PTB-Opt-62 (1999).
[30] Ohno, Y., "Integrating Sphere Simulation - Application to Total Flux Scale Realization," *Applied Optics*, **33**-13, 2637-2647 (1994).
[31] Ohno, Y., "New Method for Realizing a Total Luminous Flux Scale using an Integrating Sphere with an External Source," *The Journal of the Illuminating Engineering Society of North America*, **24**-1, 106-115 (1995).
[32] Ohno, Y., "Realization of NIST Luminous Flux Scale Using an Integrating Sphere with an External Source," *CIE Proceedings, 23rd Session, New Delhi* (1995).
[33] Ohno, Y., "Realization of NIST 1995 Luminous Flux Scale using Integrating Sphere Method," *The Journal of the Illuminating Engineering Society of North America*, **25**-1, 13-22 (1996).
[34] Ohno, Y. and Zong, Y., "Detector-Based Integrating Sphere Photometry," *Proceedings, CIE 24th Session – Warsaw'99*, 155 – 160 (1999).
[35] White House Commission on Aviation Safety and Security, "Final Report to President Clinton," (February 1997).
[36] SAE, "Minimum Performance Standard for Anticollision Light Systems," *AS 8017A* (1986).
[37] CIE, "International Lighting Vocabulary," *CIE Publication No.17.4* (1987).
[38] Allard, M.E. "Mémoire sur l'Intensité et la Portée des Phares," Imprimerie Nationale, Paris 62-73 (1876).
[39] A. Blondel and J. Rey, "Sur la perception des lumiéres bréves à la limite de leur portée." *Journal de Physique,* juillet et aout, 643 (1911).
[40] H.J. Schmidt-Clausen, "The influence of the angular size, adaptation luminance, pulse shape and light colur on the Blondel-Rey constant a." *The perception and application of flashing lights*, **95**-111, Adam Hilger, London (1971).
[41] Ohno, Y. and Couzin, D. "Modified Allard Method for Effective Intensity of Flashing Lights," *Proceedings of the CIE Expert Symposium 2002*, Veszprém, Hungary (2002).
[42] Y. Ohno and Y. Zong, "Establishment of the NIST Flashing Light Photometric Unit," *Proceedings of the SPIE: Photometric Engineering of Sources and Systems*, **3140**, 2-11 1997.
[43] CIE, "Colorimetry – Part 2:CIE Standard Illuminants," *CIE Standard S014-2/E:2006* (2006).

[44] Fowler, J.B., and Litorja, M., "Geometric Area Measurements of Circular Apertures for Radiometry at NIST," *Metrologia*, **40**, no. 1, S9-S12 (2003).
[45] Eppeldauer, G. and Hardis, J.E., "Fourteen-decade photocurrent measurements with large-area silicon photodiodes at room temperature," *Applied Optics*, **30**-22, 3091-3099 (1991).
[46] Eppeldauer, G., "Temperature Monitored/Controlled Silicon Photodiodes for Standardization," *Surveillance Technologies, SPIE Proceedings 1479*, 71-77 (1991).
[47] Stearns, E.I and Stearns, R.E, "An example of a method for correcting radiance data for bandpass error," *Color Research and Application*, **13**, 257-259 (1988).
[48] CIE, "Methods of characterizing illuminance meters and luminance meters," CIE Publication No. 69 (1987).
[49] Thompson, A. and Chen, H., "Beamcon III, a Linearity Measurement Instrument for Optical Detectors," *Journal of Research of the National Institute of Standards and Technology*, **99**-6: 751-755 (1994).
[50] Eppeldauer, G. and Hardis, J.E., "Fourteen-decade photocurrent measurements with large-area silicon photodiodes at room temperature," *Applied Optics*, **30**-22, 3091-3099 (1991).
[51] ISO, "Guide to the Expression of Uncertainty in Measurement" (1995).
[52] ISO, "General requirements for the competence of testing and calibration laboratories," ISO/IEC 17025, Geneva, Switzerland (2005).
[53] Ohno, Y., "High Illuminance Calibration Facility and Procedures," *The Journal of the Illuminating Engineering Society of North America*, **27**(2) (1998).
[54] CIE, "Measurements of Luminous Flux," *CIE Publication* No.84 (1987).
[55] Ohno, Y., Köhler, R., and Stock, M., "AC/DC Technique for the Absolute Integrating Sphere Method," *Metrologia*, **37**, 583-586 (2000).
[56] Venable, W.H., Hsia, J.J., and Weidner, V.R., "Establishing a Scale of Directional-Hemispherical Reflectance Factor I: The Van den Akker Method," *Journal of Research of the National Bureau of Standards*, **82**-1:29-55 (1977).
[57] IES, "IES Guide to Lamp Seasoning," IES LM-54-12, New York, New York (2012).
[58] IES, "IES Approved Method for the Electrical and Photometric Measurements of Fluorescent Lamps," *LM-9-1999* (1999).
[59] ANSI, "Fluorescent Lamps – Guide for Electrical Measurements," *C78.375-2004* (2004).
[60] ANSI, "Double-Capped Fluorescent Lamps - Dimensional and Electrical Characteristics," *ANSI_IEC C78.81-2005* (2005).
[61] ANSI, "Reference Ballasts for Fluorescent Lamps," *C82.3-2002* (2002).
[62] IES, Understanding and Controlling the Effects of Temperature on Fluorescent Lamp Systems," *TM-6-1996* (1996).
[63] Blevin, W.R., "Diffraction Losses in Radiometry and Photometry," *Metrologia*, **7**, 39-44 (1970).
[64] CIE, "CIE Collection in Photometry and Radiometry," *CIE Publication No.114* (1994).
[65] CIE, "Colorimetry," CIE Publication No. 15, 3rd edition, Vienna, Austria (2004).
[66] Ohno, Y. and Jackson, J. K., "Characterization of modified FEL quartz-halogen lamps for photometric standards," *Metrologia*, **32**-6, 693-696 (1996).
[67] J.L. Gardner, "Uncertainty Propagation for NIST Visible Spectral Standards," *Journal of Research of the National Institute of Standards and Technology*, **109**, 305-318 (2004).

[68] J. L. Gardner, Correlated colour temperature—uncertainty and estimation, *Metrologia* **37**, 381-384 (2000).
[69] J. Fontecha, J. Campos, A. Corrons, and A. Pons, "An analytical method for estimating correlated colour temperature uncertainty," *Metrologia* **39**, 53-536 (2002).
[70] Zong, Y., Brown, S.W., Johnson, B.C., Lykke, K.R., and Ohno, Y., "Simple spectral stray light correction method for array spectroradiometers," *Applied Optics*, **45**, Issue 6, pp. 1111-1119 (2006). https://doi.org/10.1364/AO.45.001111

Appendix A: List of symbols used in document

Φ_V luminous flux
γ_P angular alignment of the photometer
γ_L angular alignment of the lamp
Ω solid angle

A area
C_d correction factor for distance difference between photometer reference planes
c_p temperature coefficient for photometers
C_S spectral responsivity scale for SCF
c_r calibration factor for the digital voltmeter for a voltage ratio measurement
c_U calibration factor for the digital voltmeter for a voltage determination
c_y calibration factor for the digital voltmeter for a signal measurement
d distance
d_B distance measured by the electronic linear encoder
d_L distance from the photometry bench origin to the lamp reference plane
d_P distance from the carriage reference plane to the standard photometer reference plane
E_U correction factor for illuminance uniformity at photometer reference plane
E_V illuminance
F^* SMCF
G_f gain factor
G_S geometrical correction factor for SCF calibration
H_f correction factor due to the heating of a photometer
H_V luminous exposure
$I^*(\theta,\phi)$ the normalized luminous intensity distribution of the internal source
I_S correction factor for the deviation versus inverse square law
I_V luminous intensity
J_0 set calibration current
$K(\theta,\phi)$ the spatial response distribution function (SRDF)
$K^*(\theta,\phi)$ the normalized spatial response to an isotropic point source
k_a illuminance non-uniformity correction factor for sphere wheel reference plane
K_m maximum spectral luminous efficacy (of radiation) for photopic vision
L_f long term stability of a photometer
L_V luminance
m_J exponential dependence of the voltage measurement across the shunt resistor
m_L exponential dependence of the voltage measurement across the lamp
M_V luminous exitance
N_S numerical aperture of the SCF
Q_V luminous energy

$R_d(\lambda)$	relative spectral responsivity of the sphere detector
R	shunt resistor resistance
R_S	integrating sphere photometric responsivity
$R_S(\lambda)$	relative spectral responsivity of the integrating sphere
$R_{v,f}$	photometric responsivity (A/lm)
$R_{v,i}$	illuminance responsivity (A/lx)
$s(\lambda)$	spectral responsivity
$S_A(\lambda)$	spectral power distribution of CIE illuminant A
S_{fe}	external source spatial non-uniformity correction factor
S_L	correction factor for short term stability of a light source
s_{rel}	relative spectral responsivity of the detector
S_{SL}	stray light correction factor
S_t	spectral power distribution of the test lamp
T_c	color temperature
T_{cp}	correlated color temperature
T_d	distribution temperature
T_P	photometer temperature
T_S	temperature correction factor during calibration
$T_S(\lambda)$	relative spectral throughput of the integrating sphere
T_w	temperature correction factor for sphere wall
U_0	calibrated voltage of the lamp
U_J	voltage measurement across the shunt resistor
U_L	voltage measurement across the lamp
$V(\lambda)$	spectral luminous efficiency function for photopic vision
W_S	wavelength scale of spectral responsivity
y	signal (A or V)
y_d	dark signal

Appendix B: Sensitivity coefficients

Sensitivity coefficients for Table 10

$$I_{\mathrm{v}} = E_v \cdot d^2 \cdot \left(\frac{U_J \cdot c_U}{J_0 \cdot R_{\mathrm{S}}}\right)^{m_{\mathrm{J}}} \left(\frac{U_{\mathrm{L}}}{U_0}\right)^{m_{\mathrm{U}}} \cdot c_{\mathrm{f}}$$

1) $\frac{\partial I_{\mathrm{v}}}{\partial E_{\mathrm{v}}} = \frac{I_{\mathrm{v}}}{E_{\mathrm{v}}}$

2) $\frac{\partial I_{\mathrm{v}}}{\partial d} = \frac{2 I_{\mathrm{v}}}{d}$

3) $\frac{\partial I_{\mathrm{v}}}{\partial U_{\mathrm{J}}} = m_{\mathrm{J}} \frac{I_{\mathrm{v}}}{U_{\mathrm{J}}}$

4) $\frac{\partial I_{\mathrm{v}}}{\partial c_{\mathrm{U}}} = m_{\mathrm{J}} \frac{I_{\mathrm{v}}}{c_{\mathrm{U}}}$

5) $\frac{\partial I_{\mathrm{v}}}{\partial R_{\mathrm{S}}} = m_{\mathrm{J}} \frac{-I_{\mathrm{v}}}{R_{\mathrm{S}}}$

6) $\frac{\partial I_{\mathrm{v}}}{\partial m_{\mathrm{J}}} = I_{\mathrm{v}} \cdot \ln\left(\frac{U_{\mathrm{J}} \cdot c_{\mathrm{U}}}{J_0 \cdot R_{\mathrm{S}}}\right)$

7) $\frac{\partial I_{\mathrm{v}}}{\partial U_{\mathrm{L}}} = m_{\mathrm{U}} \frac{I_{\mathrm{v}}}{U_{\mathrm{L}}}$

8) $\frac{\partial I_{\mathrm{v}}}{\partial m_{\mathrm{U}}} = I_{\mathrm{v}} \cdot \ln\left(\frac{U_{\mathrm{L}}}{U_0}\right)$

9) $\frac{\partial I_{\mathrm{v}}}{\partial c_{\mathrm{f}}} = \frac{I_{\mathrm{v}}}{c_{\mathrm{f}}}$

Sensitivity coefficients for Table 8

$$R_{\mathrm{v}} = \frac{(y - y_{\mathrm{d}}) \cdot G_{\mathrm{f,\,r}} \cdot c_{\mathrm{r}} \cdot R_{\mathrm{v,i}}}{(y_{\mathrm{r}} - y_{\mathrm{d,r}}) \cdot G_{\mathrm{f}}} \cdot C_{\mathrm{d}} \cdot E_{\mathrm{U}} \cdot S_{\mathrm{L}} \cdot T_{\mathrm{S}} \cdot L_{\mathrm{f}} \cdot M_{\mathrm{f}} \cdot S_{\mathrm{SL}} \cdot \gamma_{\mathrm{P}} \cdot \gamma_{\mathrm{P,r}} \cdot I_{\mathrm{S}}$$

1) $\frac{\partial R_{\mathrm{v}}}{\partial y} = \frac{R_{\mathrm{v}}}{(y - y_{\mathrm{d}})}$

2) $\frac{\partial R_{\mathrm{v}}}{\partial y_{\mathrm{d}}} = \frac{-R_{\mathrm{v}}}{(y - y_{\mathrm{d}})}$

3) $\frac{\partial R_{\mathrm{v}}}{\partial c_{\mathrm{r}}} = \frac{R_{\mathrm{v}}}{c_{\mathrm{r}}}$

4) $\frac{\partial R_{\mathrm{v}}}{\partial G_{\mathrm{f,\,r}}} = \frac{R_{\mathrm{v}}}{G_{\mathrm{f,\,r}}}$

5) $\frac{\partial R_{\mathrm{v}}}{\partial R_{\mathrm{v,i}}} = \frac{R_{\mathrm{v}}}{R_{\mathrm{v,i}}}$

6) $\frac{\partial R_{\mathrm{v}}}{\partial y_r} = \frac{-R_{\mathrm{v}}}{(y_r - y_{\mathrm{d,r}})}$

7) $\frac{\partial R_{\mathrm{v}}}{\partial y_{\mathrm{d,r}}} = \frac{R_{\mathrm{v}}}{(y_{\mathrm{r}} - y_{\mathrm{d,r}})}$

8) $\frac{\partial R_{\mathrm{v}}}{\partial G_{\mathrm{f}}} = \frac{-R_{\mathrm{v}}}{G_{\mathrm{f}}}$

9) $\frac{\partial R_{\mathrm{v}}}{\partial C_{\mathrm{d}}} = \frac{R_{\mathrm{v}}}{C_{\mathrm{d}}}$

10) $\frac{\partial R_{\mathrm{v}}}{\partial E_{\mathrm{U}}} = \frac{R_{\mathrm{v}}}{E_{\mathrm{U}}}$

11) $\frac{\partial R_{\mathrm{v}}}{\partial S_{\mathrm{L}}} = \frac{R_{\mathrm{v}}}{S_{\mathrm{L}}}$

12) $\frac{\partial R_{\mathrm{v}}}{\partial T_{\mathrm{S}}} = \frac{R_{\mathrm{v}}}{T_{\mathrm{S}}}$

13) $\frac{\partial R_{\mathrm{v}}}{\partial L_{\mathrm{f}}} = \frac{R_{\mathrm{v}}}{L_{\mathrm{f}}}$

14) $\frac{\partial R_{\mathrm{v}}}{\partial M_{\mathrm{f}}} = \frac{R_{\mathrm{v}}}{M_{\mathrm{f}}}$

15) $\frac{\partial R_{\mathrm{v}}}{\partial S_{\mathrm{SL}}} = \frac{R_{\mathrm{v}}}{S_{\mathrm{SL}}}$

16) $\frac{\partial R_{\mathrm{v}}}{\partial \gamma_{\mathrm{P}}} = \frac{R_{\mathrm{v}}}{\gamma_{\mathrm{P}}}$

17) $\frac{\partial R_{\mathrm{v}}}{\partial \gamma_{\mathrm{P,r}}} = \frac{R_{\mathrm{v}}}{\gamma_{\mathrm{P,r}}}$

18) $\frac{\partial R_{\mathrm{v}}}{\partial I_{\mathrm{S}}} = \frac{R_{\mathrm{v}}}{I_{\mathrm{S}}}$

Sensitivity coefficients for Table 9

$$R_{\mathrm{f}} = \frac{(Y - Y_{\mathrm{d}}) \cdot G_{\mathrm{r}} \cdot R_{\mathrm{v,i}}}{(y_{\mathrm{r}} - y_{\mathrm{d,r}}) \cdot c_{\mathrm{y}}} \cdot C_{\mathrm{d}} \cdot E_{\mathrm{U}} \cdot S_{\mathrm{L}} \cdot T_{\mathrm{S}} \cdot L_{\mathrm{f}} \cdot M_{\mathrm{f}} \cdot S_{\mathrm{SL}} \cdot \gamma_{\mathrm{P}} \cdot \gamma_{\mathrm{P,r}} \cdot I_{\mathrm{S}}$$

1) $\dfrac{\partial R_{\mathrm{f}}}{\partial Y} = \dfrac{R_{\mathrm{f}}}{(Y - Y_{\mathrm{d}})}$ 2) $\dfrac{\partial R_{\mathrm{f}}}{\partial Y_{\mathrm{d}}} = \dfrac{-R_{\mathrm{f}}}{(Y - Y_{\mathrm{d}})}$ 3) $\dfrac{\partial R_{\mathrm{f}}}{\partial c_y} = \dfrac{R_{\mathrm{f}}}{c_y}$

4) $\dfrac{\partial R_{\mathrm{f}}}{\partial G_{\mathrm{r}}} = \dfrac{R_{\mathrm{f}}}{G_{\mathrm{r}}}$ 5) $\dfrac{\partial R_{\mathrm{f}}}{\partial R_{\mathrm{v,i}}} = \dfrac{R_{\mathrm{f}}}{R_{\mathrm{v,i}}}$ 6) $\dfrac{\partial R_{\mathrm{f}}}{\partial y_r} = \dfrac{-R_{\mathrm{f}}}{(y_r - y_{\mathrm{d,r}})}$

7) $\dfrac{\partial R_{\mathrm{f}}}{\partial y_{\mathrm{d,r}}} = \dfrac{R_{\mathrm{f}}}{(y_{\mathrm{r}} - y_{\mathrm{d,r}})}$ 8) $\dfrac{\partial R_{\mathrm{f}}}{\partial C_{\mathrm{d}}} = \dfrac{R_{\mathrm{f}}}{C_{\mathrm{d}}}$ 9) $\dfrac{\partial R_{\mathrm{f}}}{\partial E_{\mathrm{U}}} = \dfrac{R_{\mathrm{f}}}{E_{\mathrm{U}}}$

10) $\dfrac{\partial R_{\mathrm{f}}}{\partial S_{\mathrm{L}}} = \dfrac{R_{\mathrm{f}}}{S_{\mathrm{L}}}$ 11) $\dfrac{\partial R_{\mathrm{f}}}{\partial T_{\mathrm{S}}} = \dfrac{R_{\mathrm{f}}}{T_{\mathrm{S}}}$ 12) $\dfrac{\partial R_{\mathrm{f}}}{\partial L_{\mathrm{f}}} = \dfrac{R_{\mathrm{f}}}{L_{\mathrm{f}}}$

13) $\dfrac{\partial R_{\mathrm{f}}}{\partial M_{\mathrm{f}}} = \dfrac{R_{\mathrm{f}}}{M_{\mathrm{f}}}$ 14) $\dfrac{\partial R_{\mathrm{f}}}{\partial S_{\mathrm{SL}}} = \dfrac{R_{\mathrm{f}}}{S_{\mathrm{SL}}}$ 15) $\dfrac{\partial R_{\mathrm{f}}}{\partial \gamma_{\mathrm{P}}} = \dfrac{R_{\mathrm{f}}}{\gamma_{\mathrm{P}}}$

16) $\dfrac{\partial R_{\mathrm{f}}}{\partial \gamma_{\mathrm{P,r}}} = \dfrac{R_{\mathrm{f}}}{\gamma_{\mathrm{P,r}}}$ 17) $\dfrac{\partial R_{\mathrm{f}}}{\partial I_{\mathrm{S}}} = \dfrac{R_{\mathrm{f}}}{I_{\mathrm{S}}}$

Sensitivity coefficients for Table 10

$$R_{\mathrm{f}} = \frac{(Y - Y_{\mathrm{d}}) \cdot G_{\mathrm{r}} \cdot R_{\mathrm{v,i}}}{(y_{\mathrm{r}} - y_{\mathrm{d,r}}) \cdot c_{\mathrm{y}}} \cdot C_{\mathrm{d}} \cdot E_{\mathrm{U}} \cdot S_{\mathrm{L}} \cdot H_{\mathrm{f}} \cdot H_{\mathrm{r}} \cdot L_{\mathrm{f}} \cdot M_{\mathrm{f}} \cdot M_{\mathrm{f,r}} \cdot S_{\mathrm{SL}} \cdot \gamma_{\mathrm{P}} \cdot \gamma_{\mathrm{P,r}} \cdot I_{\mathrm{S}}$$

1) $\dfrac{\partial R_{\mathrm{f}}}{\partial Y} = \dfrac{R_{\mathrm{f}}}{(Y - Y_{\mathrm{d}})}$ 2) $\dfrac{\partial R_{\mathrm{f}}}{\partial Y_{\mathrm{d}}} = \dfrac{-R_{\mathrm{f}}}{(Y - Y_{\mathrm{d}})}$ 3) $\dfrac{\partial R_{\mathrm{f}}}{\partial c_y} = \dfrac{R_{\mathrm{f}}}{c_y}$

4) $\dfrac{\partial R_{\mathrm{f}}}{\partial G_{\mathrm{r}}} = \dfrac{R_{\mathrm{f}}}{G_{\mathrm{r}}}$ 5) $\dfrac{\partial R_{\mathrm{f}}}{\partial R_{\mathrm{v,i}}} = \dfrac{R_{\mathrm{f}}}{R_{\mathrm{v,i}}}$ 6) $\dfrac{\partial R_{\mathrm{f}}}{\partial y_r} = \dfrac{-R_{\mathrm{f}}}{(y_r - y_{\mathrm{d,r}})}$

7) $\dfrac{\partial R_{\mathrm{f}}}{\partial y_{\mathrm{d,r}}} = \dfrac{R_{\mathrm{f}}}{(y_{\mathrm{r}} - y_{\mathrm{d,r}})}$ 8) $\dfrac{\partial R_{\mathrm{f}}}{\partial C_{\mathrm{d}}} = \dfrac{R_{\mathrm{f}}}{C_{\mathrm{d}}}$ 9) $\dfrac{\partial R_{\mathrm{f}}}{\partial E_{\mathrm{U}}} = \dfrac{R_{\mathrm{f}}}{E_{\mathrm{U}}}$

10) $\dfrac{\partial R_{\mathrm{f}}}{\partial S_{\mathrm{L}}} = \dfrac{R_{\mathrm{f}}}{S_{\mathrm{L}}}$ 11) $\dfrac{\partial R_{\mathrm{f}}}{\partial H_{\mathrm{f}}} = \dfrac{R_{\mathrm{f}}}{H_{\mathrm{f}}}$ 12) $\dfrac{\partial R_{\mathrm{f}}}{\partial H_{\mathrm{r}}} = \dfrac{R_{\mathrm{f}}}{H_{\mathrm{r}}}$

13) $\dfrac{\partial R_{\mathrm{f}}}{\partial L_{\mathrm{f}}} = \dfrac{R_{\mathrm{f}}}{L_{\mathrm{f}}}$ 14) $\dfrac{\partial R_{\mathrm{f}}}{\partial M_{\mathrm{f}}} = \dfrac{R_{\mathrm{f}}}{M_{\mathrm{f}}}$ 15) $\dfrac{\partial R_{\mathrm{f}}}{\partial M_{\mathrm{f,\,r}}} = \dfrac{R_{\mathrm{f}}}{M_{\mathrm{f,\,r}}}$

16) $\dfrac{\partial R_{\mathrm{f}}}{\partial S_{\mathrm{SL}}} = \dfrac{R_{\mathrm{f}}}{S_{\mathrm{SL}}}$ 17) $\dfrac{\partial R_{\mathrm{f}}}{\partial \gamma_{\mathrm{P}}} = \dfrac{R_{\mathrm{f}}}{\gamma_{\mathrm{P}}}$ 18) $\dfrac{\partial R_{\mathrm{f}}}{\partial \gamma_{\mathrm{P,r}}} = \dfrac{R_{\mathrm{f}}}{\gamma_{\mathrm{P,r}}}$

19) $\dfrac{\partial R_{\mathrm{f}}}{\partial I_{\mathrm{S}}} = \dfrac{R_{\mathrm{f}}}{I_{\mathrm{S}}}$

Sensitivity coefficients for Table 11

$$E_{\mathrm{c}} = \left[P_1 + P_2\right]\frac{c_y \cdot c_{\mathrm{R}}}{2G_{\mathrm{r}}} \cdot L_{\mathrm{f}} \cdot S_{\mathrm{L}} \cdot T_{\mathrm{S}} \cdot S_{\mathrm{SL}} \cdot \gamma_{\mathrm{P}}$$

$$P_1 = \left(\frac{y_1}{R_1}\right)\left(\frac{d_0}{d_0 + \Delta d_1}\right)^2\left(\frac{2856\mathrm{K}}{T_{\mathrm{d}}}\right)^{\alpha} \text{ and } P_2 = \left(\frac{y_2}{R_2}\right)\left(\frac{d_0}{d_0 + \Delta d_2}\right)^2\left(\frac{2856\mathrm{K}}{T_{\mathrm{d}}}\right)^{\beta}$$

1) $\dfrac{\partial E_{\mathrm{c}}}{\partial y_1} = \dfrac{P_1}{y_1}\dfrac{c_y \cdot c_{\mathrm{R}}}{2G_{\mathrm{r}}} \cdot L_{\mathrm{f}} \cdot S_{\mathrm{L}} \cdot T_{\mathrm{S}} \cdot S_{\mathrm{SL}} \cdot \gamma_{\mathrm{P}}$

2) $\dfrac{\partial E_{\mathrm{c}}}{\partial y_2} = \dfrac{P_2}{y_2}\dfrac{c_y \cdot c_{\mathrm{R}}}{2G_{\mathrm{r}}} \cdot L_{\mathrm{f}} \cdot S_{\mathrm{L}} \cdot T_{\mathrm{S}} \cdot S_{\mathrm{SL}} \cdot \gamma_{\mathrm{P}}$

3) $\dfrac{\partial E_{\mathrm{c}}}{\partial R_1} = \dfrac{-P_1}{R_1}\dfrac{c_y \cdot c_{\mathrm{R}}}{2G_{\mathrm{r}}} \cdot L_{\mathrm{f}} \cdot S_{\mathrm{L}} \cdot T_{\mathrm{S}} \cdot S_{\mathrm{SL}} \cdot \gamma_{\mathrm{P}}$

4) $\dfrac{\partial E_{\mathrm{c}}}{\partial R_2} = \dfrac{-P_2}{R_2}\dfrac{c_y \cdot c_{\mathrm{R}}}{2G_{\mathrm{r}}} \cdot L_{\mathrm{f}} \cdot S_{\mathrm{L}} \cdot T_{\mathrm{S}} \cdot S_{\mathrm{SL}} \cdot \gamma_{\mathrm{P}}$

5) $\dfrac{\partial E_{\mathrm{c}}}{\partial d_0} = \left[\dfrac{P_1 \cdot \Delta d_1}{d_0\left(d_0 + \Delta d_1\right)} + \dfrac{P_2 \cdot \Delta d_2}{d_0\left(d_0 + \Delta d_2\right)}\right]\dfrac{c_y \cdot c_{\mathrm{R}}}{G_{\mathrm{r}}} \cdot L_{\mathrm{f}} \cdot S_{\mathrm{L}} \cdot T_{\mathrm{S}} \cdot S_{\mathrm{SL}} \cdot \gamma_{\mathrm{P}}$

6) $\dfrac{\partial E_{\mathrm{c}}}{\partial \Delta d_1} = \dfrac{-P_1}{\left(d_0 + \Delta d_1\right)}\dfrac{c_y \cdot c_{\mathrm{R}}}{G_{\mathrm{r}}} \cdot L_{\mathrm{f}} \cdot S_{\mathrm{L}} \cdot T_{\mathrm{S}} \cdot S_{\mathrm{SL}} \cdot \gamma_{\mathrm{P}}$

7) $\dfrac{\partial E_{\mathrm{c}}}{\partial \Delta d_2} = \dfrac{-P_2}{\left(d_0 + \Delta d_2\right)}\dfrac{c_y \cdot c_{\mathrm{R}}}{G_{\mathrm{r}}} \cdot L_{\mathrm{f}} \cdot S_{\mathrm{L}} \cdot T_{\mathrm{S}} \cdot S_{\mathrm{SL}} \cdot \gamma_{\mathrm{P}}$

8) $\dfrac{\partial E_\mathrm{c}}{\partial T_\mathrm{d}} = \left[-\alpha P_1 - \beta P_2\right] \dfrac{c_y \cdot c_\mathrm{R}}{T_\mathrm{d} \cdot 2G_\mathrm{r}} \cdot L_\mathrm{f} \cdot S_\mathrm{L} \cdot T_\mathrm{S} \cdot S_\mathrm{SL} \cdot \gamma_\mathrm{P}$

9) $\dfrac{\partial E_\mathrm{c}}{\partial \alpha} = P_1 \ln\left(\dfrac{2856\mathrm{K}}{T_\mathrm{d}}\right) \dfrac{c_y \cdot c_\mathrm{R}}{2G_\mathrm{r}} \cdot L_\mathrm{f} \cdot S_\mathrm{L} \cdot T_\mathrm{S} \cdot S_\mathrm{SL} \cdot \gamma_\mathrm{P}$

10) $\dfrac{\partial E_\mathrm{c}}{\partial \beta} = P_2 \ln\left(\dfrac{2856\mathrm{K}}{T_\mathrm{d}}\right) \dfrac{c_y \cdot c_\mathrm{R}}{2G_\mathrm{r}} \cdot L_\mathrm{f} \cdot S_\mathrm{L} \cdot T_\mathrm{S} \cdot S_\mathrm{SL} \cdot \gamma_\mathrm{P}$

11) $\dfrac{\partial E_\mathrm{c}}{\partial c_y} = \dfrac{E_\mathrm{c}}{c_y}$ 12) $\dfrac{\partial E_\mathrm{c}}{\partial G_\mathrm{r}} = \dfrac{-E_\mathrm{c}}{G_\mathrm{r}}$ 13) $\dfrac{\partial E_\mathrm{c}}{\partial c_\mathrm{R}} = \dfrac{E_\mathrm{c}}{c_\mathrm{R}}$

14) $\dfrac{\partial E_\mathrm{c}}{\partial L_\mathrm{f}} = \dfrac{E_\mathrm{c}}{L_\mathrm{f}}$ 15) $\dfrac{\partial E_\mathrm{c}}{\partial S_\mathrm{L}} = \dfrac{E_\mathrm{c}}{S_\mathrm{L}}$ 16) $\dfrac{\partial E_\mathrm{c}}{\partial T_\mathrm{S}} = \dfrac{E_\mathrm{c}}{T_\mathrm{S}}$

17) $\dfrac{\partial E_\mathrm{c}}{\partial S_\mathrm{SL}} = \dfrac{E_\mathrm{c}}{S_\mathrm{SL}}$ 18) $\dfrac{\partial E_\mathrm{c}}{\partial \gamma_\mathrm{P}} = \dfrac{E_\mathrm{c}}{\gamma_\mathrm{P}}$

Sensitivity coefficients for Table 12

$$R_\mathrm{s} = \frac{(y_\mathrm{ext} - y_d) \cdot c_y \cdot \rho}{G_\mathrm{r} \cdot E_\mathrm{C} \cdot k_\mathrm{a} \cdot A} \cdot T_\mathrm{w} \cdot T_\mathrm{S} \cdot M_{\mathrm{f_e}} \cdot S_{\mathrm{f_e}} \cdot S_\mathrm{SL}$$

1) $\dfrac{\partial R_\mathrm{S}}{\partial y_\mathrm{ext}} = \dfrac{R_\mathrm{S}}{(y_\mathrm{ext} - y_\mathrm{d})}$ 2) $\dfrac{\partial R_\mathrm{S}}{\partial y_\mathrm{ext}} = \dfrac{-R_\mathrm{S}}{(y_\mathrm{ext} - y_\mathrm{d})}$ 3) $\dfrac{\partial R_\mathrm{S}}{\partial c_y} = \dfrac{R_\mathrm{S}}{c_y}$

4) $\dfrac{\partial R_\mathrm{S}}{\partial \rho} = \dfrac{R_\mathrm{S}}{\rho}$ 5) $\dfrac{\partial R_\mathrm{S}}{\partial G_\mathrm{r}} = \dfrac{-R_\mathrm{S}}{G_\mathrm{r}}$ 6) $\dfrac{\partial R_\mathrm{S}}{\partial E_\mathrm{c}} = \dfrac{-R_\mathrm{S}}{E_c}$

7) $\dfrac{\partial R_\mathrm{S}}{\partial k_\mathrm{a}} = \dfrac{-R_\mathrm{S}}{k_\mathrm{a}}$ 8) $\dfrac{\partial R_\mathrm{S}}{\partial A} = \dfrac{-R_\mathrm{S}}{A}$ 9) $\dfrac{\partial R_\mathrm{S}}{\partial T_\mathrm{w}} = \dfrac{R_\mathrm{S}}{T_\mathrm{w}}$

10) $\dfrac{\partial R_\mathrm{S}}{\partial T_\mathrm{S}} = \dfrac{R_\mathrm{S}}{T_\mathrm{S}}$ 11) $\dfrac{\partial R_\mathrm{S}}{\partial M_{\mathrm{f_e}}} = \dfrac{R_\mathrm{S}}{M_{\mathrm{f_e}}}$ 12) $\dfrac{\partial R_\mathrm{S}}{\partial S_{\mathrm{f_e}}} = \dfrac{R_\mathrm{S}}{S_{\mathrm{f_e}}}$

13) $\dfrac{\partial R_\mathrm{S}}{\partial S_\mathrm{SL}} = \dfrac{R_\mathrm{S}}{S_\mathrm{SL}}$

Sensitivity coefficients for Table 13

$$\Phi_{\text{test}} = \frac{(y - y_{\text{d}}) \cdot c_y}{G_{\text{f}} \cdot R_{\text{s}}} \cdot \left(\frac{U \cdot c_U}{J_0 \cdot R}\right)^{m_{\text{J}}} \left(\frac{U_{\text{L}}}{U_0}\right)^{m_{\text{U}}} T_{\text{w}} \cdot T_{\text{S}} \cdot M_{\text{f}_{\text{i}}} \cdot S_{\text{f}_{\text{i}}} \cdot S_{\text{SL}}$$

1) $\dfrac{\partial \Phi_{\text{test}}}{\partial y} = \dfrac{\Phi_{\text{test}}}{(y - y_{\text{d}})}$ 2) $\dfrac{\partial \Phi_{\text{test}}}{\partial y_{\text{d}}} = \dfrac{-\Phi_{\text{test}}}{(y - y_{\text{d}})}$ 3) $\dfrac{\partial \Phi_{\text{test}}}{\partial c_y} = \dfrac{\Phi_{\text{test}}}{c_y}$

4) $\dfrac{\partial \Phi_{\text{test}}}{\partial R_{\text{s}}} = \dfrac{-\Phi_{\text{test}}}{R_{\text{s}}}$ 5) $\dfrac{\partial \Phi_{\text{test}}}{\partial G_{\text{f}}} = \dfrac{-\Phi_{\text{test}}}{G_{\text{f}}}$ 6) $\dfrac{\partial \Phi_{\text{test}}}{\partial U} = \dfrac{m_{\text{J}}\Phi_{\text{test}}}{U}$

7) $\dfrac{\partial \Phi_{\text{test}}}{\partial c_{\text{U}}} = \dfrac{m_{\text{J}}\Phi_{\text{test}}}{c_{\text{U}}}$ 8) $\dfrac{\partial \Phi_{\text{test}}}{\partial R} = \dfrac{-m_{\text{J}}\Phi_{\text{test}}}{R}$

9) $\dfrac{\partial \Phi_{\text{test}}}{\partial m_{\text{J}}} = \Phi_{\text{test}} \ln\left(\dfrac{U \cdot c_U}{J_0 \cdot R}\right)$ 10) $\dfrac{\partial \Phi_{\text{test}}}{\partial U_{\text{L}}} = \dfrac{m_{\text{U}}\Phi_{\text{test}}}{U_{\text{L}}}$

11) $\dfrac{\partial \Phi_{\text{test}}}{\partial m_{\text{U}}} = \Phi_{\text{test}} \ln\left(\dfrac{U_{\text{L}}}{U_0}\right)$ 12) $\dfrac{\partial \Phi_{\text{test}}}{\partial T_{\text{w}}} = \dfrac{\Phi_{\text{test}}}{T_{\text{w}}}$ 13) $\dfrac{\partial \Phi_{\text{test}}}{\partial T_{\text{S}}} = \dfrac{\Phi_{\text{test}}}{T_{\text{S}}}$

14) $\dfrac{\partial \Phi_{\text{test}}}{\partial M_{\text{f}_{\text{i}}}} = \dfrac{\Phi_{\text{test}}}{M_{\text{f}_{\text{i}}}}$ 15) $\dfrac{\partial \Phi_{\text{test}}}{\partial S_{\text{f}_{\text{i}}}} = \dfrac{\Phi_{\text{test}}}{S_{\text{f}_{\text{i}}}}$ 16) $\dfrac{\partial \Phi_{\text{test}}}{\partial S_{\text{SL}}} = \dfrac{\Phi_{\text{test}}}{S_{\text{SL}}}$

Sensitivity coefficients for Table 14

$$\Phi_{\text{test}} = \frac{(y - y_{\text{d}}) \cdot c_y}{G_{\text{f}} \cdot R_{\text{s}}} \cdot \left(\frac{J_{\text{L}}}{J_0}\right)^{m_{\text{J}}} \left(\frac{U_{\text{L}}}{U_0}\right)^{m_{\text{U}}} T_{\text{L}} \cdot B_{\text{R}} \cdot N_{\text{F}} \cdot T_{\text{w}} \cdot T_{\text{S}} \cdot M_{\text{f}_{\text{i}}} \cdot S_{\text{f}_{\text{i}}} \cdot S_{\text{SL}}$$

1) $\dfrac{\partial \Phi_{\text{test}}}{\partial y} = \dfrac{\Phi_{\text{test}}}{(y - y_{\text{d}})}$ 2) $\dfrac{\partial \Phi_{\text{test}}}{\partial y_{\text{d}}} = \dfrac{-\Phi_{\text{test}}}{(y - y_{\text{d}})}$ 3) $\dfrac{\partial \Phi_{\text{test}}}{\partial c_y} = \dfrac{\Phi_{\text{test}}}{c_y}$

4) $\dfrac{\partial \Phi_{\text{test}}}{\partial R_{\text{s}}} = \dfrac{-\Phi_{\text{test}}}{R_{\text{s}}}$ 5) $\dfrac{\partial \Phi_{\text{test}}}{\partial G_{\text{f}}} = \dfrac{-\Phi_{\text{test}}}{G_{\text{f}}}$ 6) $\dfrac{\partial \Phi_{\text{test}}}{\partial J_{\text{L}}} = \dfrac{m_{\text{J}}\Phi_{\text{test}}}{J_{\text{L}}}$

7) $\dfrac{\partial \Phi_{\text{test}}}{\partial m_{\text{J}}} = \Phi_{\text{test}} \ln\left(\dfrac{J_{\text{L}}}{J_0}\right)$ 8) $\dfrac{\partial \Phi_{\text{test}}}{\partial U_{\text{L}}} = \dfrac{m_{\text{U}}\Phi_{\text{test}}}{U_{\text{L}}}$ 9) $\dfrac{\partial \Phi_{\text{test}}}{\partial m_{\text{U}}} = \Phi_{\text{test}} \ln\left(\dfrac{U_{\text{L}}}{U_0}\right)$

10) $\dfrac{\partial \Phi_{\text{test}}}{\partial T_{\text{L}}} = \dfrac{\Phi_{\text{test}}}{T_{\text{L}}}$ 11) $\dfrac{\partial \Phi_{\text{test}}}{\partial T_{\text{L}}} = \dfrac{\Phi_{\text{test}}}{T_{\text{L}}}$ 12) $\dfrac{\partial \Phi_{\text{test}}}{\partial B_{\text{R}}} = \dfrac{\Phi_{\text{test}}}{B_{\text{R}}}$

13) $\dfrac{\partial \Phi_{\text{test}}}{\partial N_{\text{F}}} = \dfrac{\Phi_{\text{test}}}{N_{\text{F}}}$ 14) $\dfrac{\partial \Phi_{\text{test}}}{\partial T_{\text{w}}} = \dfrac{\Phi_{\text{test}}}{T_{\text{w}}}$ 15) $\dfrac{\partial \Phi_{\text{test}}}{\partial T_{\text{S}}} = \dfrac{\Phi_{\text{test}}}{T_{\text{S}}}$

16) $\dfrac{\partial \Phi_{\text{test}}}{\partial M_{\text{f}_\text{i}}} = \dfrac{\Phi_{\text{test}}}{M_{\text{f}_\text{i}}}$ 17) $\dfrac{\partial \Phi_{\text{test}}}{\partial S_{\text{f}_\text{i}}} = \dfrac{\Phi_{\text{test}}}{S_{\text{f}_\text{i}}}$ 18) $\dfrac{\partial \Phi_{\text{test}}}{\partial S_{\text{SL}}} = \dfrac{\Phi_{\text{test}}}{S_{\text{SL}}}$

Sensitivity coefficients for Table 16

$$L = k \cdot \frac{(y - y_{\text{d}})c_y \cdot d^2}{G_{\text{f}} \cdot R_{\text{v,i}} \cdot A} \cdot S_{\text{L}} \cdot L_{\text{f}} \cdot M_{\text{f}} \cdot S_{\text{SL}} \cdot \gamma_{\text{P}} \cdot \gamma_{\text{S}}$$

1) $\dfrac{\partial L}{\partial y} = \dfrac{L}{(y - y_{\text{d}})}$ 2) $\dfrac{\partial L}{\partial y_{\text{d}}} = \dfrac{-L}{(y - y_{\text{d}})}$ 3) $\dfrac{\partial L}{\partial c_y} = \dfrac{L}{c_y}$

4) $\dfrac{\partial L}{\partial G_{\text{f}}} = \dfrac{-L}{G_{\text{f}}}$ 5) $\dfrac{\partial L}{\partial R_{\text{v,i}}} = \dfrac{-L}{R_{\text{v,i}}}$ 6) $\dfrac{\partial L}{\partial d} = \dfrac{2L}{d}$

7) $\dfrac{\partial L}{\partial A} = \dfrac{L}{A}$ 8) $\dfrac{\partial L}{\partial S_{\text{L}}} = \dfrac{L}{S_{\text{L}}}$ 9) $\dfrac{\partial L}{\partial L_{\text{f}}} = \dfrac{L}{L_{\text{f}}}$

10) $\dfrac{\partial L}{\partial M_{\text{f}}} = \dfrac{L}{M_{\text{f}}}$ 11) $\dfrac{\partial L}{\partial S_{\text{SL}}} = \dfrac{L}{S_{\text{SL}}}$ 12) $\dfrac{\partial L}{\partial \gamma_{\text{P}}} = \dfrac{L}{\gamma_{\text{P}}}$

13) $\dfrac{\partial L}{\partial \gamma_{\text{S}}} = \dfrac{L}{\gamma_{\text{S}}}$

Sensitivity coefficients for Table 19

$$R_{\text{f}} = \frac{(Y - Y_{\text{d}}) \cdot G_{\text{r}} \cdot R_{\text{v,L}}}{(y - y_{\text{d}}) \cdot c_y} \cdot L_{\text{U}} \cdot S_{\text{L}} \cdot H_{\text{f}} \cdot H_{\text{r}} \cdot L_{\text{f}} \cdot M_{\text{f}} \cdot S_{\text{SL}}$$

1) $\dfrac{\partial R_{\text{f}}}{\partial Y} = \dfrac{R_{\text{f}}}{(Y - Y_{\text{d}})}$ 2) $\dfrac{\partial R_{\text{f}}}{\partial Y_{\text{d}}} = \dfrac{-R_{\text{f}}}{(Y - Y_{\text{d}})}$ 3) $\dfrac{\partial R_{\text{f}}}{\partial c_y} = \dfrac{-R_{\text{f}}}{c_y}$

4) $\dfrac{\partial R_{\text{f}}}{\partial G_{\text{r}}} = \dfrac{R_{\text{f}}}{G_{\text{r}}}$ 5) $\dfrac{\partial R_{\text{f}}}{\partial R_{\text{v,L}}} = \dfrac{R_{\text{f}}}{R_{\text{v,L}}}$ 6) $\dfrac{\partial R_{\text{f}}}{\partial y} = \dfrac{-R_{\text{f}}}{(y - y_{\text{d}})}$

7) $\dfrac{\partial R_{\text{f}}}{\partial y_{\text{d}}} = \dfrac{R_{\text{f}}}{(y - y_{\text{d}})}$ 8) $\dfrac{\partial R_{\text{f}}}{\partial L_{\text{U}}} = \dfrac{R_{\text{f}}}{L_{\text{U}}}$ 9) $\dfrac{\partial R_{\text{f}}}{\partial S_{\text{L}}} = \dfrac{R_{\text{f}}}{S_{\text{L}}}$

10) $\dfrac{\partial R_\mathrm{f}}{\partial H_\mathrm{f}} = \dfrac{R_\mathrm{f}}{H_\mathrm{f}}$ 11) $\dfrac{\partial R_\mathrm{f}}{\partial H_\mathrm{r}} = \dfrac{R_\mathrm{f}}{H_\mathrm{r}}$ 12) $\dfrac{\partial R_\mathrm{f}}{\partial L_\mathrm{f}} = \dfrac{R_\mathrm{f}}{L_\mathrm{f}}$

13) $\dfrac{\partial R_\mathrm{f}}{\partial M_\mathrm{f}} = \dfrac{R_\mathrm{f}}{M_\mathrm{f}}$ 14) $\dfrac{\partial R_\mathrm{f}}{\partial S_\mathrm{SL}} = \dfrac{R_\mathrm{f}}{S_\mathrm{SL}}$

Sensitivity coefficients for Table 19

$$q_0 = \frac{(y_1 - y_{\mathrm{d},1}) \cdot c_y \cdot G_\mathrm{r} \cdot d^2}{(y_0 - y_{\mathrm{d},0}) \cdot A \cdot \Omega_0} \cdot E_\mathrm{U} \cdot S_\mathrm{L} \cdot T_\mathrm{S} \cdot T_\mathrm{O} \cdot M_{\mathrm{f},0} \cdot M_{\mathrm{f},1} \cdot \gamma_{\mathrm{P}_0} \cdot \gamma_{\mathrm{P}_1} \cdot \gamma_\mathrm{O} \cdot I_\mathrm{S} \cdot S_\mathrm{SL}$$

1) $\dfrac{\partial q_0}{\partial y_0} = \dfrac{-q_0}{(y_0 - y_{\mathrm{d},0})}$ 2) $\dfrac{\partial q_0}{\partial y_{\mathrm{d},0}} = \dfrac{q_0}{(y_0 - y_{\mathrm{d},0})}$ 3) $\dfrac{\partial q_0}{\partial c_y} = \dfrac{q_0}{c_y}$

4) $\dfrac{\partial q_0}{\partial G_\mathrm{r}} = \dfrac{q_0}{G_\mathrm{r}}$ 5) $\dfrac{\partial q_0}{\partial d} = \dfrac{2q_0}{d}$ 6) $\dfrac{\partial q_0}{\partial A} = \dfrac{q_0}{A}$

7) $\dfrac{\partial q_0}{\partial y_1} = \dfrac{q_0}{(y_1 - y_{\mathrm{d},1})}$ 8) $\dfrac{\partial q_0}{\partial y_{\mathrm{d},1}} = \dfrac{-q_0}{(y_1 - y_{\mathrm{d},1})}$ 9) $\dfrac{\partial q_0}{\partial E_\mathrm{U}} = \dfrac{q_0}{E_\mathrm{U}}$

10) $\dfrac{\partial q_0}{\partial S_\mathrm{L}} = \dfrac{q_0}{S_\mathrm{L}}$ 11) $\dfrac{\partial q_0}{\partial T_\mathrm{S}} = \dfrac{q_0}{T_\mathrm{S}}$ 12) $\dfrac{\partial q_0}{\partial T_\mathrm{O}} = \dfrac{q_0}{T_\mathrm{O}}$

13) $\dfrac{\partial q_0}{\partial M_{\mathrm{f},0}} = \dfrac{q_0}{M_{\mathrm{f},0}}$ 14) $\dfrac{\partial q_0}{\partial M_{\mathrm{f},1}} = \dfrac{q_0}{M_{\mathrm{f},1}}$ 15) $\dfrac{\partial q_0}{\partial \gamma_{\mathrm{P}_0}} = \dfrac{q_0}{\gamma_{\mathrm{P}_0}}$

16) $\dfrac{\partial q_0}{\partial \gamma_{\mathrm{P}_1}} = \dfrac{q_0}{\gamma_{\mathrm{P}_1}}$ 17) $\dfrac{\partial q_0}{\partial \gamma_\mathrm{O}} = \dfrac{q_0}{\gamma_\mathrm{O}}$ 18) $\dfrac{\partial q_0}{\partial I_\mathrm{S}} = \dfrac{q_0}{I_\mathrm{S}}$

19) $\dfrac{\partial q_0}{\partial S_\mathrm{SL}} = \dfrac{q_0}{S_\mathrm{SL}}$

Sensitivity coefficients for Table 23

$$O_{\mathrm{T}} = (F_{\mathrm{S}} - S)\left(\frac{U \cdot c_{\mathrm{U}}}{J_0 \cdot R}\right)^{m_{\mathrm{T}}} \left(\frac{V}{V_0}\right)^{m_{\mathrm{V}}} + L_{\mathrm{f}} + D + \phi_{\mathrm{L}}$$

1) $$\frac{\partial O_{\mathrm{T}}}{\partial F_S} = \left(\frac{U \cdot c_{\mathrm{U}}}{J_0 \cdot R}\right)^{m_{\mathrm{T}}} \left(\frac{V}{V_0}\right)^{m_{\mathrm{V}}}$$

2) $$\frac{\partial O_{\mathrm{T}}}{\partial S} = -\left(\frac{U \cdot c_{\mathrm{U}}}{J_0 \cdot R}\right)^{m_{\mathrm{T}}} \left(\frac{V}{V_0}\right)^{m_{\mathrm{V}}}$$

3) $$\frac{\partial O_{\mathrm{T}}}{\partial L_{\mathrm{f}}} = 1$$

4) $$\frac{\partial O_{\mathrm{T}}}{\partial D} = 1$$

5) $$\frac{\partial O_{\mathrm{T}}}{\partial \phi_{\mathrm{L}}} = 1$$

6) $$\frac{\partial O_{\mathrm{T}}}{\partial U} = \frac{m_{\mathrm{T}}}{U}(F_{\mathrm{S}} - S)\left(\frac{U \cdot c_{\mathrm{U}}}{J_0 \cdot R}\right)^{m_{\mathrm{T}}} \left(\frac{V}{V_0}\right)^{m_{\mathrm{V}}}$$

7) $$\frac{\partial O_{\mathrm{T}}}{\partial c_{\mathrm{U}}} = \frac{m_{\mathrm{T}}}{c_{\mathrm{U}}}(F_{\mathrm{S}} - S)\left(\frac{U \cdot c_{\mathrm{U}}}{J_0 \cdot R}\right)^{m_{\mathrm{T}}} \left(\frac{V}{V_0}\right)^{m_{\mathrm{V}}}$$

8) $$\frac{\partial O_{\mathrm{T}}}{\partial R} = \frac{m_{\mathrm{T}}}{R}(F_{\mathrm{S}} - S)\left(\frac{U \cdot c_{\mathrm{U}}}{J_0 \cdot R}\right)^{m_{\mathrm{T}}} \left(\frac{V}{V_0}\right)^{m_{\mathrm{V}}}$$

9) $$\frac{\partial O_{\mathrm{T}}}{\partial m_{\mathrm{T}}} = (F_{\mathrm{S}} - S)\left(\frac{U \cdot c_{\mathrm{U}}}{J_0 \cdot R}\right)^{m_{\mathrm{T}}} \left(\frac{V}{V_0}\right)^{m_{\mathrm{V}}} \ln\left(\frac{U \cdot c_{\mathrm{U}}}{J_0 \cdot R}\right)$$

10) $$\frac{\partial O_{\mathrm{T}}}{\partial V} = \frac{m_{\mathrm{V}}}{V}(F_{\mathrm{S}} - S)\left(\frac{U \cdot c_{\mathrm{U}}}{J_0 \cdot R}\right)^{m_{\mathrm{T}}} \left(\frac{V}{V_0}\right)^{m_{\mathrm{V}}}$$

11) $$\frac{\partial O_{\mathrm{T}}}{\partial m_{\mathrm{V}}} = (F_{\mathrm{S}} - S)\left(\frac{U \cdot c_{\mathrm{U}}}{J_0 \cdot R}\right)^{m_{\mathrm{T}}} \left(\frac{V}{V_0}\right)^{m_{\mathrm{V}}} \ln\left(\frac{V}{V_0}\right)$$

Appendix C: Samples of calibration reports

Appendix C.1 – Luminous Intensity and Color Temperature Standard Lamp 37010C

REPORT OF CALIBRATION

Luminous Intensity and Color Temperature Standard Lamp 37010C
Designation No. NIST20001

Supplied to:

Company ABC
Attn.: Mr. John Doe
100 1st Avenue
Hometown, MD 10000

(See your Purchase Order No. XXXXXX, dated xx xx, 2015)

1. Calibration Item

One 1000 watt, T6 modified FEL type quartz halogen lamp with a tungsten coiled-coil filament has been calibrated for 2856 K color temperature, calibrated for luminous intensity at 2856 K and supplied to the customer. The lamp, manufactured by Osram Sylvania Inc., was potted onto a medium bi-post base and seasoned for 24 h at 8.4 A DC and then 72 h at 7.2 A DC prior to the calibration. The lamp designation, NIST20001, is printed on an identification plate affixed on the lamp base.

2. Description of the Calibration

The luminous intensity measurement is based on the NIST detector-based candela scale realized in 2015 and, therefore, on the international definition of candela in effect since 1979. The color temperature measurement is based on the international temperature scale of 1990 (ITS-90). The details of the NIST luminous intensity unit and the color temperature scale are described in Section 3.1 and 7.2 of reference [1].

The height of the test lamp was aligned so that the optical axis was 9.5 cm (3.75 inches) above the bottom of the posts. The distance origin of the lamp was the center of the lamp posts. The operating current of the test lamp was first determined so that the lamp operated at a color temperature of 2856 K. The color temperature value is calculated based on the definition of correlated color temperature and the calculation procedures given in reference [2].

After determining the lamp current, the luminous intensity of the lamp was measured for three burnings at 2856 K to check its reproducibility, and the average values were reported. The total operating time of the lamp was approximately 80 minutes. The room temperature was 24 °C and relative humidity was 43 % at the time of calibration. The equipment and the details of the calibration procedures of the luminous intensity and color temperature measurements are described in Section 3 and Section 7 of reference [1].

3. Results of the Calibration

The results of the calibration are shown in Table 1. The relative expanded uncertainty (with coverage factor k=2) of the luminous intensity value is 0.57 %. The uncertainty budget analysis is shown in Table 2 based on the following model,

$$I_{\mathrm{v}} = \frac{(y - y_{\mathrm{d}}) \cdot c_y \cdot d^2}{G_{\mathrm{f}} \cdot R_{\mathrm{v,i}} \cdot \Omega_0} \cdot \left(\frac{U_J \cdot c_U}{J_0 \cdot R_{\mathrm{S}}} \right)^{m_{\mathrm{J}}} \left(\frac{U_{\mathrm{L}}}{U_0} \right)^{m_{\mathrm{U}}} \cdot T_{\mathrm{S}} \cdot L_{\mathrm{f}} \cdot F^* \cdot S_{\mathrm{SL}} \cdot \gamma_{\mathrm{P}} \cdot \gamma_{\mathrm{L}} \cdot I_{\mathrm{S}}$$

where $R_{\mathrm{v,i}}$ is the photometric responsivity of the photometer, Ω_0 is the unit steradian, y is the photometer signal, y_{d} is the photometer dark signal, G_{f} is the gain factor, d is the distance between the lamp reference plane and the photometer reference plane, U is the voltage measured across the shunt resistor for the measurement of current, J_0 is the calibrated current for the lamp, R_{S} is the resistance of the shunt resistor, U_{L} is the measured voltage which is only a small deviation from the calibrated voltage, U_0, and m_{U} is the voltage dependent coefficient. The remaining terms are corrections factors: T_{S} is for the temperature correction of the photometer during the time of calibration, L_{f} is the long-term stability of the NIST standard photometers, F^* is the SMCF, S_{SL} is for the stray light in the NIST photometric bench. The angular alignment of the photometer is corrected by γ_{P} and the angular alignment of the lamp is corrected by γ_{L}. The deviation for the inverse square law of the lamp under test is captured in the correction factor I_{S}. The expanded uncertainty (k=2) of the color temperature value is 8 K. The NIST policy on uncertainty statements is described in reference [3].

Table 1. Results of Calibration

Lamp No.	Current DC [A]	Voltage* DC [V]	Color Temperature [K]	Luminous Intensity [cd]
NIST20001	7.213	84.5	2856	1089

*Voltage is for reference only.

4. General Information

The lamp should be carefully aligned in accordance with the procedures described above. The lamp should be operated on DC power at the reported current and at the prescribed polarity. Photometric measurements should be made at least 10 minutes after turning on. The uncertainty value is valid only for distances larger than 2 m. The luminous intensity value may change slightly at shorter distances due to change in filament shadowing and offset of filament position.

The customer should take the uncertainty associated with the aging of the lamp and the calibration cycle into account. This type of lamp typically exhibits decrease of luminous intensity by about 0.4 % per 24 hours of use at a color temperature of 2856 K.

The Calibration Report shall not be reproduced except in full, without the written approval of NIST.

Prepared by:

Maria E. Nadal
Sensor Science Division
Physical Measurement Laboratory
(301) 975-5949

Approved by:

C. Cameron Miller
For the Director,
National Institute of Standards and Technology
(301) 975-4713

References:

[1] Y. Ohno, NIST Special Publication 250-37 "Photometric Calibration" (1997).
[2] CIE Publication No.15:2006, Colorimetry – Third Edition (2006).
[3] B. N. Taylor and C. E. Kuyatt, "Guidelines for Evaluating and Expressing the Uncertainty of NIST Measurement Results," NIST Technical Note 1297 (1994).

Table 2. **Uncertainty budget for this luminous intensity calibration**

	Symbol	Value x_i	Standard Uncertainty $u(x_i)$	Unit	Type of evaluation	Degree of freedom ν_i	Sensitivity Coefficient c_i	Uncertainty Contribution $u_i(y)$
1	y	0.82819	0.00011	V	A	19	1314.6	0.1446
2	y_d	-0.00005	6.1×10^{-7}	V	A	19	-1314.6	-0.0008
3	c_y	1.00000	0.00004		B	∞	1088.8	0.0437
4	d	3.65000	0.00107	m	B	∞	596.6	0.6384
5	G_f	0.09999	0.00002	V/V	B	∞	-10889	-0.2178
6	$R_\mathrm{v,i}$	0.10118	0.00019	V/lx	B	∞	-10761	-2.0124
7	U_J	0.72130	1.0×10^{-6}	V	A	19	1509.5	0.0015
8	c_U	1.00000	0.00004		B	∞	1088.8	0.0390
9	R_S	0.100006	1.3×10^{-6}	Ω	B (cert)	∞	-10888	-0.0142
10	m_J	7.0	0.5		B	∞	0.5443	0.2721
11	U_L	84.500	0.012	V	A	3	12.89	0.1524
12	m_U	3.65	0.5		B	∞	0.1524	0.0762
13	T_S	0.99874	0.00050		B	∞	1090.2	0.5451
14	L_f	1.00000	0.00150		B	∞	1088.8	1.6332
15	M_f	1.00000	0.00030		B	∞	1088.8	0.3266
16	S_SL	1.00000	0.00050		B	∞	1088.8	0.5444
17	γ_P	1.00000	0.00002		B	∞	1088.8	0.0218
18	γ_L	1.00000	0.00050		B	∞	1088.8	0.5444
19	I_S	1.00000	0.00100		B	∞	1088.8	1.0888
	I_v	**1088.8**	**6.2 (*k*=2)**	**cd**		>100		**3.079**

Appendix C.2 – Total Luminous Flux of a Submitted Lamp 37060S

REPORT OF CALIBRATION

Special Test for Total Luminous Flux of Submitted Lamps 37060S

for

One 32W/T8 linear fluorescent lamp Model FO32/741
with S/N: NIST22001

Submitted by:

Company ABC
Attn.: Mr. John Doe
100 1st Avenue
Hometown, MD 10000

(See your Purchase Order No. XXXXX, dated xx xx, 2015)

1. Calibration Item

One 32W/T8, rapid-start type linear fluorescent lamp Model FO32/741 with designation number, NIST22001, was calibrated for total luminous flux. The lamp designation is engraved on the lamp near one of the two lamp bases.

2. Description of the Calibration

2.1 NIST luminous flux unit and measurement facility

This total luminous flux measurement is based on the NIST luminous flux scale realized in 2015 which has been derived from the NIST detector-based candela scale and therefore, based on the international definition of candela in effect since 1979. [1]

The test lamp was calibrated in the NIST 2.5 m integrating sphere by using the detector-based absolute integrating method [2]. The test lamp was mounted horizontally at the center of the integrating sphere, and its axis was aligned to be in line with the photometer and the 10 cm sphere baffle. The details for the electrical and photometric measurements of fluorescent lamps are described in the reference 3.

Prior to the luminous flux calibration, the spectral power distribution of each lamp was measured in the 2.5 m integrating sphere using an array spectroradiometer to determine the SMCF of the 2.5 m sphere system for the luminous flux calibration. The test lamp was stabilized for 15 minutes before the calibration took place with the lamp's ambient temperature (defined in reference 3) maintained to be approximately 25 °C. The lamp current, the arc voltage, the arc power, and the photometer output signal were recorded together with the data on the environmental conditions. Corrections were applied for the dark reading, the self-absorption effect (automatically corrected), and the spectral mismatch to calculate the total luminous flux of the test lamp, as described in section 5.4 of reference 1 and section 4 of reference 2. The total luminous flux measurements were made for three lightings of each test lamp. The mean value of the three lightings is reported. The variation of the total luminous flux values of the three lightings is included in the uncertainty budget of the calibration.

The room temperature was 24 °C and relative humidity was 18 % at the time of calibration.

2.2. Operation of the test lamp

The operating circuit diagram for this calibration is shown in Figure 1, which is in accordance with the ANSI standard [see section 6.1 of reference 4] for a 32 W, 48-inch, T8, rapid-start type fluorescent lamp. The circuit consists of a regulated variable ac power supply (set to 60 Hz), a step-up transformer, a reference ballast composed of an adjustable linear reactor and an adjustable resistor, a cathode heating transformer, a 2-channel ac power meter, and the test fluorescent lamp. The 2-channel ac power meter has an RMS measurement capability within a 10 kHz bandwidth. It has been confirmed that the input impedance of this instrument does not affect the circuit conditions. Both the step-up transformer and cathode heating transformer were connected to the variable ac power supply to synchronize the frequency and the phase.

The hot pin X is marked on one of the two bases of the test lamp which is adjacent to the engraved lamp designation. The test lamp was connected to the lamp-holder in such a way that the hot pin X was connected to the hot terminal X at the lamp-holder. For this calibration, the cathode heating power was switched off. The lamp current I_L, the arc voltage V_L, the arc power were measured at CH A of the 2-channel ac power meter. The lamp operating current was specified by the customer, and was set by manually adjusting the output voltage of the ac power supply.

Prior to the calibration, the reference ballast was adjusted (and fixed for all test lamps) with the test lamp shortened in the circuit to meet the required reference ballast's specifications (910 Ω impedance [see p. 33 of reference 5] and 0.075 power factor [6]):

Input voltage:	241.2 V
Short circuit current:	0.265 A
Ballast watt loss:	4.8 W

All AC values given in this report are in RMS values.

3. Results of Calibration

The results of the calibration are shown in Table 1. The relative expanded uncertainty (coverage factor k=2) of the reported luminous flux values is 1.5 %. The uncertainty budget analysis is shown in Table 2 based on the following model,

$$\Phi_{\text{test}} = \frac{(y - y_{\text{d}}) \cdot c_y}{G_{\text{f}} \cdot R_{\text{s}}} \cdot \left(\frac{J_{\text{L}}}{J_0}\right)^{m_{\text{J}}} \left(\frac{U_{\text{L}}}{U_0}\right)^{m_{\text{U}}} T_L \cdot B_{\text{R}} \cdot N_{\text{F}} \cdot T_{\text{w}} \cdot T_{\text{S}} \cdot F^* \cdot S_{\text{f}_\text{i}} \cdot S_{\text{SL}}$$

where y is the sphere photometer signal, y_{d} is the sphere photometer dark signal, R_{s} is the photometric responsivity of the sphere photometer system, G_{f} is the gain factor, J_{L} is the measurement of lamp current, J_0 is the calibrated current for the lamp, and m_{J} is the exponential dependence of the lamp luminous flux with respect to the operating current. The remaining terms are corrections factors; T_{L} is a correction factor due to the ambient temperature of the lamp, B_{R} is the correction factor based on the reference ballast settings, N_{F} is the correction factor for near field absorption losses, T_{W} is the temperature dependence of the sphere wall, T_{S} is the temperature dependence of the sphere photometer, F^* is the internal source sphere photometer system SMCF, $S_{\text{f,i}}$ is the internal source spatial non-uniformity correction factor, S_{SL} is the stray light correction, and c_y is the digital voltmeter calibration. The NIST policy on uncertainty statements is described in reference 7.

Table 1. Results of this calibration for total luminous flux

Lamp Designation	Lamp Current (A)	Arc Voltage* (V)	Arc Power* (W)	Lamp Ambient Temperature** (°C)	Total Luminous Flux (lm)
NIST22025	0.2650	141.7	32.17	25	2760

* The arc voltage and the arc power are for reference only.
** The lamp ambient temperature was measured on the photometer side of the 10 cm baffle of the NIST 2.5 m integrating sphere with a standard uncertainty of 1 °C.

4. General Information

Photometric measurements should be made at 15 minutes after turning on the fluorescent lamp.

The uncertainty due to the aging of the test lamp should be taken into account by the customer depending on the calibration cycle and the uncertainty required. The uncertainty related to the size of the integrating sphere (related to the difference in lamp's thermal conditions) should also be taken into account by the customer.

The Calibration Report shall not be reproduced except in full, without the written approval of NIST.

Prepared by:

Yuqin Zong
Sensor Science Division
Physical Measurement Laboratory
(301) 975-2332

Approved by:

C. Cameron Miller
For the Director,
National Institute of Standards and Technology
(301) 975-4713

References:

[1] Y. Ohno, NIST Special Publication 250-37 Photometric Calibrations (1997).
[2] Y. Ohno and Y. Zong: Detector-Based Integrating Sphere Photometry, CIE Proceedings, 24 Session – Warsaw, pp. 155–160 (1999).
[3] IES LM-9-1999, IES Approved Method for the Electrical and Photometric Measurements of Fluorescent Lamps.
[4] ANSI C78.375-2004, Fluorescent Lamps – Guide for Electrical Measurements.
[5] ANSI_IEC C78.81-2005, Double-Capped Fluorescent Lamps - Dimensional and Electrical Characteristics.
[6] ANSI C82.3-2002, Reference Ballasts for Fluorescent Lamps.
[7] B. N. Taylor and C. E. Kuyatt, "Guidelines for Evaluating and Expressing the Uncertainty of NIST Measurement Results," NIST Technical Note 1297 (1994).

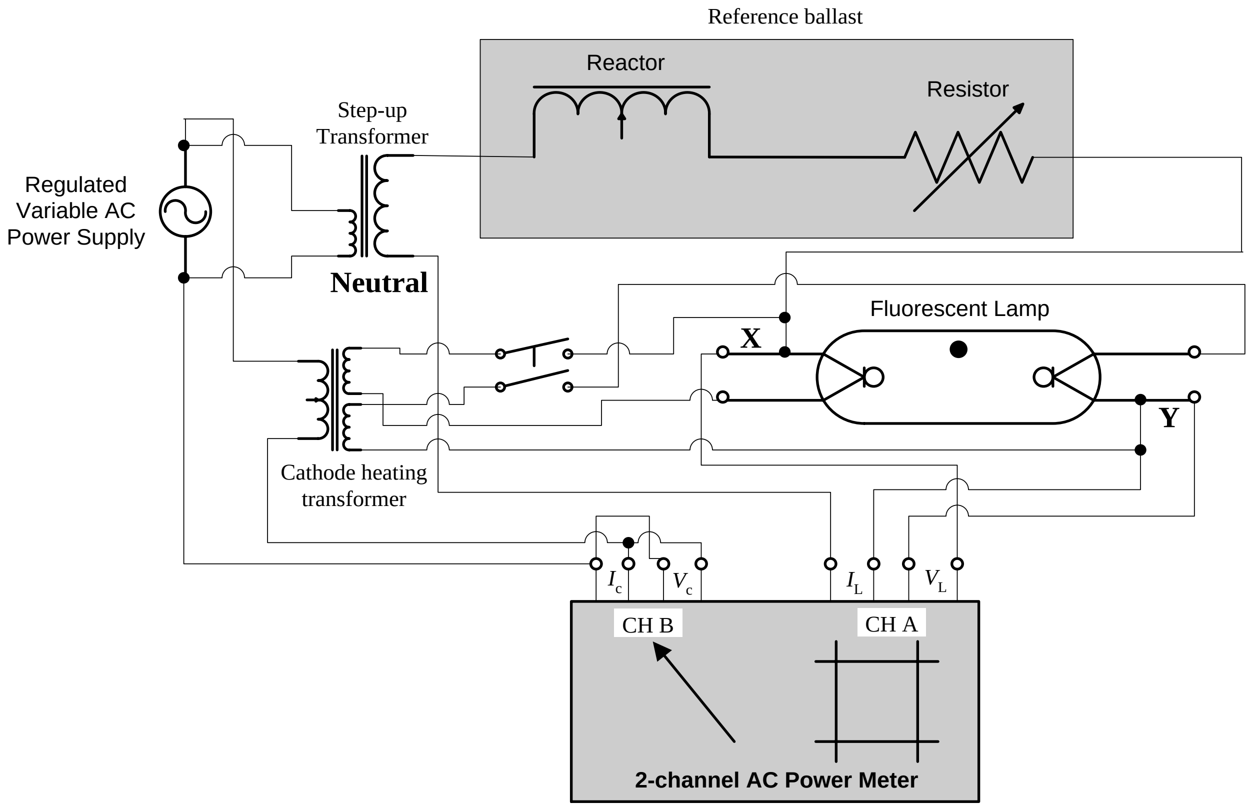

Figure 1 – Measurement circuit for the test fluorescent lamps

Table 2. **Uncertainty budget for the typical total luminous flux calibration of fluorescent lamps**

	Symbol	Value x_i	Standard Uncertainty $u(x_i)$	Unit	Type of evaluation	Degree of freedom ν_i	Sensitivity Coefficient c_i	Uncertainty Contribution $u_i(y)$
1	y	6.3427	0.0025	V	A	19	435.2	1.09
2	y_d	0.0009	0.0003	V	A	19	-435.2	-0.13
3	c_y	1.0000	0.00008		B	∞	2760	0.22
4	R_s	2.296×10^{-6}	5.1×10^{-9}	V/lm	B	∞	-1.2×10^{9}	-6.11
5	G_f	1000	0.20	V/V	B	∞	-2.760	-0.55
6	J_L	0.2650	0.0007	A	A	19	10416	6.91
7	m_J	1.00	0.20		A	19	3.12	0.62
8	U_L	141.7	0.6500	V	A	3	19.48	12.66
9	m_U	1.0000	0.200		B	∞	0.1076	0.02
10	T_L	1.0000	0.0040		B	∞	2760	11.10
11	B_R	1.0000	0.0002		B	∞	2760	0.55
12	N_F	1.0000	0.0010		B	∞	2760	2.76
13	T_w	1.0000	0.0003		B	∞	2760	0.83
14	T_S	1.0000	0.0005		B	∞	2760	1.38
15	M_{fi}	1.0000	0.0015		B	∞	2760	4.14
16	S_{fi}	0.9995	0.0012		B	∞	2762	3.31
17	S_{SL}	1.0000	0.0005		B	∞	2760	1.38
	Φ_{test}	**2760**	**41 (*k*=2)**			>100		20.3

Appendix C.3 – Calibration of a Luminance Source 37080S

REPORT OF CALIBRATION

Special Test for Calibration of Submitted Luminance Source 37080S

for

An integrating sphere source (Company, Inc.)
composed of a sphere source (Model XXXX, S/N 00000001)
and a controller (Model XXXX, S/N 00000001)

submitted by

Company ABC
Attn.: Mr. John Doe
100 1st Avenue
Hometown, MD 10000

(See your Purchase Order No. XXXXXX, dated xx xx, 2015)

1. Calibration Item

An integrating sphere source (Company, Inc.) composed of a sphere source (Model XXXX, S/N 00000001) and a controller (Model XXXX, S/N 00000001) has been calibrated for correlated color temperature and luminance.

2. Description of the Calibration

This luminance measurement is based on the NIST luminance scale that has been derived from the NIST detector-based candela scale [1] and therefore based on the international definition of candela in effect since 1979.

The test item was calibrated for luminance (cd/m^2), using a NIST reference luminance meter that is calibrated against the NIST luminance scale realized on a reference sphere source operated at 2856 K [1]. The test source was aligned, so that the center of the exit port of the source was on the optical axis, and the front surface around the exit port was normal to the optical axis. The reference luminance meter was placed on the optical axis, and the luminance of the source was measured with a measurement angle of 1° at a distance of 1.0 m. The average luminance area measured was 18 mm in diameter at the center of the exit port.

The test source was turned on and stabilized for 60 min before measurements. The operating current of the test source was determined so that the correlated color temperature of the exit port was 2856 K, with the variable aperture setting that gave a luminance reading of 2450 cd/m^2 on the instrument display. The color temperature was measured using a spectroradiometer, by comparison with two 2856 K color temperature standard lamps that were calibrated in the NIST Facility for Automated Spectroradiometric Calibrations (FASCAL) described in reference [2]. The color temperature was calculated as a correlated color temperature from the measured relative spectral irradiance.

The test source was calibrated at the amplifier range of 5000 with the variable aperture position that produced luminance readings of 2450 cd/m^2 on the instrument display. While the luminance of the test source was measured with the NIST reference luminance meter, the readings of the luminance displayed on the controller of the test source were recorded and compared. The test source had a dark reading of 0.000.

The room temperature was 23 °C, the ambient sphere temperature was 23 °C, and the room humidity was 46 % at the calibration.

3. Results of Calibration

The results of the calibration are shown in Table 1. The relative expanded uncertainty (coverage factor $k=2$) of this calibration is 0.77 %. The uncertainty budget analysis is shown in Table 2 based on the following model,

$$R_{\mathrm{f}} = \frac{(L - L_{\mathrm{d}}) \cdot G_{\mathrm{r}} \cdot R_{\mathrm{v,L}}}{(y - y_{\mathrm{d}}) \cdot c_y} \cdot S_{\mathrm{L}} \cdot L_{\mathrm{f}} \cdot O_{\mathrm{S}} \cdot F^* \cdot S_{\mathrm{SL}}$$

where $R_{\mathrm{v,L}}$ is the responsivity of the NIST reference luminance photometer, L is the displayed luminance, L_{d} is the displayed zero for the luminance source under test, y is the reference luminance photometer reading and y_{d} is the dark reading, c_y is the digital voltmeter calibration, and G_{r} is the gain. The remaining terms are corrections factors, S_{L} is for the stability of the luminance source during the calibration, L_{f} is the long-term stability of the NIST reference luminance photometer, O_{s} is the out-of-field sensitivity of the NIST reference luminance photometer, F^* is the SMCF, and S_{SL} is for the stray light in the NIST photometric bench. The expanded uncertainty (coverage factor $k=2$) of the color temperature measurement is 8 K. The NIST policy on uncertainty statement is described in reference [3].

Table 1. Result of the calibration for Sphere Source, Model XXXX, S/N 00000001 and the Controller, Model XXXX, S/N 00000001

Current [A]	Correlated Color temp. [K]	NIST Luminance Scale [cd/m^2]	Test Source Luminance Display [cd/m^2]	Ratio*
5.207	2856	2445	2450	1.0022

*The luminance display of test source divided by the NIST luminance scale.

4. General information

This calibration is valid only under the settings of the test instruments described above. The color temperature may be different for the variable aperture positions other than the ones used in this calibration.

The test source must be stabilized for at least 60 min at the ambient temperature stated above to reproduce the results of this calibration.

The color temperature of the source is subject to change by operating time of the source. The responsivity of the monitor photometer head may also be subject to long-term drift. Periodical calibration is recommended.

The Calibration Report shall not be reproduced except in full, without the written approval of NIST.

Prepared by:

Maria E. Nadal
Sensor Science Division
Physical Measurement Laboratory
(301) 975-5949

Approved by:

C. Cameron Miller
For the Director,
National Institute of Standards and Technology
(301) 975-4713

References:

[1] Y. Ohno, "Photometric Calibrations," NIST Special Publication 250-37 (1997).
[2] J. H. Walker, R. D. Saunders, J. K. Jackson, and D.A. McSparron, Spectral Irradiance Calibrations, NBS Special Publication 250-20 (1987).
[3] B. N. Taylor and C.E. Kuyatt, "Guidelines for Evaluating and Expressing the Uncertainty of NIST Measurement Results," NIST Technical Note 1297 (1994).

Table 2. **Uncertainty budget for this luminance source calibration**

	Symbol	Value x_i	Standard Uncertainty $u(x_i)$	Unit	Type of evaluation	Degree of freedom v_i	Sensitivity Coefficient c_i	Uncertainty Contribution $u_i(y)$
1	L	2450	0.577	cd/m^2	A	19	4.09×10^{-4}	2.36×10^{-4}
2	L_d	0	0.577	cd/m^2	A	19	-4.09×10^{-4}	-2.36×10^{-4}
3	c_y	1.00000	0.00018		B	∞	-1.0022	-1.79×10^{-4}
4	G_r	0.01004	1.50×10^{-5}	V/V	B	∞	99.8	1.50×10^{-3}
5	$R_{v,L}$	0.14968	0.00044	V/[cd/m^2]	B	∞	6.696	2.94×10^{-3}
6	y	3.6737	0.00011	V	A	19	-0.2728	-3.00×10^{-5}
7	y_d	0.00003	4.10×10^{-7}	V	A	19	0.2728	1.12×10^{-7}
8	S_L	1.00000	0.00100		B	∞	1.0022	1.00×10^{-3}
9	O_s	1.00000	0.00050		B	∞	1.0022	5.01×10^{-4}
10	L_f	1.00000	0.00150		B	∞	1.0022	1.50×10^{-3}
11	M_f	1.00000	0.00050		B	∞	1.0022	5.01×10^{-4}
12	S_{SL}	1.00000	0.00050		B	∞	1.0022	5.01×10^{-4}
	R_f	**1.0022**	**0.0078 (*k*=2)**			>100		3.88×10^{-3}

Appendix C.4 – Illuminance responsivity calibration for submitted photometer 37090S

REPORT OF CALIBRATION

Special Test of Illuminance Responsivity Calibration 37090S

for

NIST Photometer X000

submitted by:

Company ABC
Attn.: Mr. John Doe
100 1st Avenue
Hometown, MD 10000

(See your Purchase Order No. XXXXX, dated xx xx, 2015)

1. Calibration Item

One photometer, NIST X000, with a temperature controller (Company Corp., Model XXX) was calibrated for illuminance responsivity. The photometer is a temperature-controlled, V(λ)-matched, silicon photodiode with a built-in amplifier. The constants for the temperature controller are C1=1.035, C2=2.490, and C3=0.

2. Description of Calibration

This illuminance measurement is based on the NIST detector-based candela [1] realized in 2007 and, therefore, on the international definition of candela in effect since 1979.

The photometer, temperature regulated by the temperature controller, was stabilized at 25.0 °C for more than one hour prior to the calibration. The test photometer was calibrated by direct comparison with the NIST standard photometers, which maintain the NIST illuminance unit as described in reference [1]. The calibration was performed on the NIST photometry bench using a 1000 W clear FEL type quartz halogen lamp, operating at approximately 2856 K, at two illuminance levels, 80 lx and 185 lx. The distances were approximately 3.65 m and 2.4 m for the two illuminance levels, respectively. The illuminance was measured using three of the NIST standard photometers, and the output current of the test photometers was measured using a calibrated current-to-voltage converter with a gain setting of 10^7 [V/A]. The dark readings were taken by closing a shutter between the lamp and the photometer head and were subtracted from the signal readings. The reference plane of the test photometer is defined to be the front surface of the aperture, which for photometer NIST X000 is 12.4 mm from the front surface of the photometer.

The room temperature during the calibration was 23 °C, the photometer ambient temperature was 24 °C and the room humidity was 31 %.

3. Results of Calibration

The results of the calibration are shown in Table 1. The relative expanded uncertainty (coverage factor k=2) of this calibration is 0.56 %. The uncertainty budget analysis is shown in Table 2 based on the following model,

$$R_{\mathrm{v}} = \frac{(y - y_{\mathrm{d}}) \cdot G_{\mathrm{f,r}} \cdot c_{\mathrm{r}} \cdot R_{\mathrm{v,i}}}{(y_{\mathrm{r}} - y_{\mathrm{d,r}}) \cdot G_{\mathrm{f}}} \cdot C_{\mathrm{d}} \cdot E_{\mathrm{U}} \cdot S_{\mathrm{L}} \cdot T_{\mathrm{S}} \cdot L_{\mathrm{f}} \cdot F^{*} \cdot S_{\mathrm{SL}} \cdot \gamma_{\mathrm{P}} \cdot \gamma_{\mathrm{P,r}} \cdot I_{\mathrm{S}}$$

where R_{v} is the illuminance responsivity of the photometer under test, y is the photometer signal and y_{d} is the photometer dark signal, y_{r} is the photometer signal and $y_{\mathrm{d,r}}$ is the dark photometer signal for the NIST standard photometer, c_{r} is the digital voltmeter calibration for a ratio measurement, G_{f} is the gain factor for the photometer under test, $G_{\mathrm{f,r}}$ is the gain factor for the NIST standard photometer, and $R_{\mathrm{v,i}}$ is the illuminance responsivity of the NIST standard photometers. The remaining terms are corrections factors: C_{d} is a correction factor for the distance between the NIST standard photometer reference plane and the photometer under test reference plane, E_{U} is a correction factor for the differences in the illuminance uniformity at the reference plane, S_{L} is a correction factor for the stability of the transfer lamp, T_{S} is for the temperature correction of the NIST standard photometer during the time of calibration, L_{f} is the long term stability of the NIST standard photometers, F^{*} is the SMCF, S_{SL} is for the stray light in the NIST photometric bench. The angular alignment of the photometer under test is corrected by γ_{P} and the angular alignment of the NIST standard photometer is corrected by $\gamma_{\mathrm{P,r}}$. The deviation from the inverse square law of the photometer under test is captured in the correction factor I_{S}. The NIST policy on uncertainty statements is described in reference [2].

Table 1. Results of this calibration for illuminance responsivity

Photometer	Set Illuminance [lx]	Illuminance Responsivity [A/lx]
X000	81.9	3.22×10^{-8}
	185	3.22×10^{-8}
	Average	**3.22×10^{-8}**

4. General Information

This calibration is valid only for the measurement of incandescent or Planckian sources with color temperatures of approximately 2856 K. The responsivity of the photometers may change at a temperature different from that reported above.

The photometers may be subject to long-term drift. Periodic calibration is recommended.

This Calibration Report shall not be reproduced except in full, without the written approval of NIST.

Prepared by:

Maria E. Nadal
Sensor Science Division
Physical Measurement Laboratory
(301) 975-5949

Approved by:

C. Cameron Miller
For the Director,
National Institute of Standards and Technology
(301) 975-4713

References:

[1] Y. Ohno, NIST Special Publication 250-37 "Photometric Calibration" (1997).
[2] B. N. Taylor and C. E. Kuyatt, "Guidelines for Evaluating and Expressing the Uncertainty of NIST Measurement Results," NIST Technical Note 1297 (1994).

Table 2. **Uncertainty budget for this illuminance responsivity calibration**

	Symbol	Value x_i	Standard Uncertainty $u(x_i)$	Unit	Type of evaluation	Degree of freedom ν_i	Sensitivity Coefficient c_i	Uncertainty Contribution $u_i(y)$
1	y	2.6384	0.00035	V	A	19	1.22×10^{-8}	4.27×10^{-12}
2	y_d	0.00011	5.20×10^{-7}	V	A	19	-1.22×10^{-8}	-6.34×10^{-15}
3	c_r	1.00000	0.00008		B	∞	3.22×10^{-8}	2.57×10^{-12}
4	$G_{f,r}$	0.09999	0.00002	V/V	B	∞	6.44×10^{-7}	1.29×10^{-11}
5	$R_{v,i}$	0.10118	0.00019	V/lx	B	∞	-3.18×10^{-7}	-6.04×10^{-11}
6	y_r	0.82819	0.00011	V	A	19	-1.22×10^{-8}	-1.34×10^{-12}
7	$y_{d,r}$	-0.00005	6.10×10^{-7}	V	A	19	1.22×10^{-8}	7.44×10^{-15}
8	G_f	1.00×10^{6}	200	V/A	B	∞	3.22×10^{-14}	6.44×10^{-11}
9	C_d	1.00000	0.00100		B	∞	3.22×10^{-8}	3.22×10^{-11}
10	E_U	1.00000	0.00025		B	∞	3.22×10^{-8}	8.05×10^{-12}
11	S_L	1.00000	0.00015		B	∞	3.22×10^{-8}	4.83×10^{-12}
12	T_S	0.99874	0.00050		B	∞	3.22×10^{-8}	1.61×10^{-11}
13	L_f	1.00000	0.00150		B	∞	3.22×10^{-8}	4.83×10^{-11}
14	M_f	1.00000	0.00030		B	∞	3.22×10^{-8}	9.65×10^{-12}
15	S_{SL}	1.00000	0.00050		B	∞	3.22×10^{-8}	1.59×10^{-11}
16	γ_P	1.00000	0.00020		B	∞	3.22×10^{-8}	6.44×10^{-12}
17	$\gamma_{P,r}$	1.00000	0.00002		B	∞	3.22×10^{-8}	6.44×10^{-13}
18	I_S	1.00000	0.00100		B	∞	3.22×10^{-8}	3.22×10^{-11}
	R_v	**3.22×10^{-8}**	**1.8×10^{-10} (k=2)**	**A/lx**		>100		8.94×10^{-11}